Copernicus Marine Service

QUALITY INFORMATION DOCUMENT

Mediterranean Sea Production Centre
MEDSEA_MULTIYEAR_BGC_006_008

Issue: 3.2

Contributors: A. Teruzzi, V. Di Biagio, L. Feudale, G. Bolzon, P. Lazzari, S. Salon, G. Coidessa, G. Cossarini

Approval date by the CMEMS product quality coordination team: 12/07/2022

CHANGE RECORD

When the quality of the products changes, the QuID is updated and a row is added to this table. The third column specifies which sections or sub-sections have been updated. The fourth column should mention the version of the product to which the change applies.

Issue	Date	§	Description of Change	Author	Validated By
1.0	26/01/2016	all	First version of document at CMEMS V2	G. Cossarini, S. Salon, G. Bolzon, A. Teruzzi, P. Lazzari, E. Clementi	E. Clementi
1.1	04/04/2016	IV	Revised version after Acceptance Review Report and with assimilation of the updated V2 ESA-CCI data set	G. Cossarini, S. Salon, G. Bolzon, A. Teruzzi, P. Lazzari, E. Clementi	E. Clementi
2.0	18/01/2017	all	Version of document at CMEMS V3	G. Cossarini, S. Salon, G. Bolzon, A. Teruzzi, P. Lazzari	
2.1	07/02/2017	all	Updates of the version of document at CMEMS V3	G. Cossarini, S. Salon, G. Bolzon, A. Teruzzi, P. Lazzari	
2.2	16/02/2018	all	Updates of the version of document at CMEMS V4	G. Cossarini, S. Salon, G. Bolzon, A. Teruzzi, P. Lazzari, L. Feudale	Mercator Ocean
2.3	21/01/2019	all	Updates of the version of document for temporal extension Q1 2019	A. Teruzzi, G. Cossarini, S. Salon, G. Bolzon, P. Lazzari, L. Feudale	
2.4	03/09/2019	all	Updates of the version of document for temporal extension Q4 2019	A. Teruzzi, G. Cossarini, S. Salon, G. Bolzon, P. Lazzari, L. Feudale	
3.0	15/01/2021	all	New version of the document for the new reanalysis at horizontal resolution equal to 1/24°	A. Teruzzi, V. Di Biagio, L. Feudale, G. Bolzon, P. Lazzari, S. Salon, G. Coidessa, G. Cossarini	Emanuela Clementi

Issue	Date	§	Description of Change	Author	Validated By
3.1	03/09/2021		Updated document including INTERIM dataset	A. Teruzzi, V. Di Biagio, L. Feudale, G. Bolzon, P. Lazzari, S. Salon, G. Coidessa, G. Cossarini	Emanuela Clementi
3.2	14/06/2022		Updated document for substitution of 2016-2020 timeseries and extension till June2021	A. Teruzzi, V. Di Biagio, L. Feudale, G. Bolzon, P. Lazzari, S. Salon, G. Coidessa, G. Cossarini	Anna Chiara Goglio (PQ Leader)

TABLE OF CONTENTS

Summary

I EXECUTIVE SUMMARY

I.1 Products covered by this document

This document describes the quality of the product MEDSEA_MULTIYEAR_BGC_006_008, the multi-year product of the biogeochemical state of the Mediterranean Sea for the period 1999-2019. The MED Biogeochemistry reanalysis product includes 3D daily and monthly fields at 1/24° horizontal resolution (which for the Mediterranean basin is about 4 km) of 12 variables grouped in 5 datasets:

PFTC: chlorophyll and phytoplankton carbon biomass;

NUTR: phosphate, nitrate and ammonium;

BIOL: oxygen and primary production;

CARB: pH (reported on Total Scale), dissolved inorganic carbon and alkalinity;

CO2F: surface partial pressure of CO2 and surface CO2 flux (2D fields at surface).

The Reanalysis dataset is extended to six-months before present by means of an INTERIM production. The biogeochemical INTERIM dataset is initialized with the last available day of reanalysis, uses the same reanalysis biogeochemical model system and is forced by the interim physical dynamics.

This CMEMS product can be acknowledged using the following citations:

Reanalysis dataset:

Teruzzi, A., Di Biagio, V., Feudale, L., Bolzon, G., Lazzari, P., Salon, S., Coidessa, G., & Cossarini, G. (2021). Mediterranean Sea Biogeochemical Reanalysis (CMEMS MED-Biogeochemistry, MedBFM3 system) (Version 1) [Data set]. Copernicus Monitoring Environment Marine Service (CMEMS). https://doi.org/10.25423/CMCC/MEDSEA_MULTIYEAR_BGC_006_008_MEDBFM3

Cossarini, G., Feudale, L., Teruzzi, A., Bolzon, G., Coidessa, G., Solidoro C., Amadio, C., Lazzari, P., Brosich, A., Di Biagio, V., and Salon, S., 2021. High-resolution reanalysis of the Mediterranean Sea biogeochemistry (1999-2019). Frontiers in Marine Science. https://www.frontiersin.org/articles/10.3389/fmars.2021.741486/full.

Interim dataset:

Teruzzi, A., Feudale, L., Bolzon, G., Lazzari, P., Salon, S., Di Biagio, V., Coidessa, G., & Cossarini, G. (2021). Mediterranean Sea Biogeochemical Reanalysis INTERIM (CMEMS MED-Biogeochemistry, MedBFM3i system) (Version 1) [Data set]. Copernicus Monitoring Environment Marine Service (CMEMS). https://doi.org/10.25423/CMCC/MEDSEA_MULTIYEAR_BGC_006_008_MEDBFM3I

I.2 Summary of the results

The validation of the reanalysis consists of three levels of skill performance metrics that depend on the availability of observations:

(1) model capability to reproduce basin-wide spatial gradients, mean annual values in sub-basins and average vertical profiles based on GODAE Class1 metrics (level-1);

(2) model capability to reproduce the variability due to mesoscale and daily dynamics based on GODAE Class4 metrics (level-2; Hernandez et al., 2018);
(3) model capability to reproduce key biogeochemical processes based on specific metrics (level-3; Salon et al., 2019).

Thus, the validation analysis provides a “degree of confirmation” (Oreskes et al., 1994) with respect to the different scales of variability derived from the available observations. In the following table the key messages of the quality of the Mediterranean reanalysis are reported considering the level of validation that can be achieved for each of the 12 variables.

Estimate accuracy numbers of 11 variables are computed for the 1999-2021 reanalysis timeseries and for the interim production (test simulation of year 2020) only for satellite and BGC-Argo based metrics.

Variable	Level 1	Level 2	Level 3
Chlorophyll	Good agreement with climatological satellite map.	High level of accuracy thanks to data assimilation. High variability associated with higher uncertainty: higher errors in winter than summer; in coastal areas than off-shore; in subsurface layer than at surface.	Very good performance for vertical chlorophyll process-based metrics with RMSDs of 0.07 mg/m^3 for chlorophyll in euphotic layer, of 16 m (32 m) for DCM depth (WBL thickness).
Phytoplankton biomass		Accuracy ranging between 1 and 2 mgC/m^3 with lowest RMSD at the bottom of the euphotic layer, but lack of full maturity of the optical measurements to biomass conversion prevents a robust assessment of spatial patterns.	
Primary production	Good agreement with mean annual basin and sub-basin estimations.		
Phosphate	Very good agreement with horizontal and vertical patterns at basin-wide scale.	Uncertainty in predicting daily mesoscale dynamics is higher than in reproducing mean annual values. Underestimation of mesopelagic values in western sub-basins.	
Nitrate	Good agreement with horizontal and vertical patterns at basin-wide scale.	Uncertainty in predicting daily mesoscale dynamics is higher than in reproducing mean annual values. Underestimation of mesopelagic values in western sub-basins.	Very good skill statistics for vertical nitrate process-based metrics: RMSDs of 1 mmol/m^3 for nitrate in euphotic layer, and of 49 m for nitracline depth.
Oxygen	Good agreement with horizontal and vertical patterns at basin-wide scale	Mesoscale dynamics and daily surface values very well reproduced. Higher uncertainty in the mesopelagic zone of the water column.	Very good skill statistics for vertical oxygen process-based metrics: RMSDs of 15 mmol/m^3 for oxygen in euphotic depth, and of 33 m for maximum oxygen depth.

Variable	Level 1	Level 2	Level 3
Ammonium	Order of magnitude captured, but patterns not always well reproduced (accuracy affected by very limited data availability).	Typical vertical profiles and spatial gradient of ammonium are only partially reproduced.	
pH	Good agreement with horizontal and vertical patterns at basin-wide scale.	pH daily values reproduced with an error of 0.03-0.04 in all vertical layers.	
Alkalinity	Good agreement with horizontal and vertical patterns at basin-wide scale.	Higher uncertainty in the surface layer than deeper layers.	
DIC	Good agreement with horizontal and vertical patterns at basin-wide scale.	Higher uncertainty in the surface layer than deeper layers.	
pCO2 at surface	Good agreement with horizontal patterns at basin-wide scale.	Mesoscale and daily variability reproduced with nearly 40 ppm accuracy.	
Flux of CO2 at the air-sea interface	Mean annual map consistent with previous estimations.		

I.3 Estimated Accuracy Numbers

Chlorophyll [mg/m^3]								
	RMSD				BIAS			
	MEDREA24		INTERIM		MEDREA24		INTERIM	
OPEN SEA	**win**	**sum**	**win**	**sum**	**win**	**sum**	**win**	**sum**
Mod-Sat	0.04	0.01	0.04	0.01	0.02	0.00	0.02	0.00
log_{10}(Mod)-log_{10}(Sat)	0.13	0.05	0.12	0.05	0.07	0.00	0.08	0.00
COASTAL AREAS								
Mod-Sat	0.26	0.22	0.26	0.24	-0.06	-0.06	-0.08	-0.07
log_{10}(Mod)-log_{10}(Sat)	0.19	0.17	0.20	0.19	0.01	-0.07	-0.01	-0.07

Table I.1. Mean RMSD and BIAS (model minus satellite) of surface chlorophyll [mg/m^3] over the open sea and coastal areas of the Mediterranean Sea for the Jan1999-Jun2021 reanalysis. Winter corresponds to January to April, summer corresponds to June to September. INTERIM product (green cells) has been evaluated with a test simulation between 1 January – 31 December 2020 using the same metrics.

	Units	RMSD						
Layers (m)		**0-30**	**30-60**	**60-100**	**100-150**	**150-300**	**300-600**	**600-1000**
Phosphate	**[mmol/m^3]**	0.03	0.04	0.05	0.06	0.06	0.08	0.08
Nitrate	**[mmol/m^3]**	0.71	0.96	1.18	1.29	1.53	1.86	1.69
Oxygen	**[mmol/m^3]**	10.1	12.9	12.7	14.9	16.8	21.8	20.2
Ammonium	**[mmol/m^3]**	0.24	0.25	0.34	0.36	0.34	0.34	0.32
pH	**total scale**	0.034	0.032	0.037	0.037	0.042	0.039	0.033
Alkalinity	**[µmol/kg]**	47.7	41.1	35.2	30.3	29.5	20.9	18.6
Dissolved inorganic carbon	**[µmol/kg]**	46.7	38.3	30.3	30.5	26.0	21.3	17.6
Surface partial pressure of CO_2	**[ppm]**	38.4	-	-	-	-	-	-

Table I.2. Mean RMSD of phosphate, nitrate, oxygen, ammonium, pH, alkalinity, dissolved inorganic carbon and surface partial pressure of CO_2 estimated by comparing the reanalysis and in-situ 1999-2017 observations. Skill performance statistics are computed based on EMODnet2018_int dataset, that consists in the integration of the Aggregated EMODnet data collections (Buga et al., 2018) and the datasets listed in Lazzari et al. (2016) and Cossarini et al. (2015).

		RMSD							
Variables		**0-10m**	**10-30m**	**30-60m**	**60-100m**	**100-150m**	**150-300m**	**300-600m**	**600-1000m**
		BGC-Argo floats available since 2013							
Chlorophyll [mg/m^3]	**MEDREA24**	0.09	0.09	0.13	0.11	0.07	-	-	-
	INTERIM	0.07	0.07	0.10	0.10	0.08	-	-	-
Phytoplankton biomass [mg/m^3]	**MEDREA24**	1.83	1.57	1.77	1.78	1.21	-	-	-
NITRATE [mmol/m^3]	**MEDREA24**	0.57	0.51	0.46	0.75	1.21	1.31	1.42	2.11
	INTERIM	0.58	0.56	0.61	0.92	1.34	1.09	1.64	2.02
OXYGEN [mmol/m^3]	**MEDREA24**	6.9	9.3	11.7	14.3	17.3	23.5	32.6	31.9
	INTERIM	4.7	6.0	8.6	14.5	19.5	28.1	34.3	32.4
SSOCAT dataset larger than EMODnet2018_int									
Surface partial pressure of CO_2 [ppm]	**MEDREA24**	38.7	-	-	-	-	-	-	-

Table I.3. Basin-scale mean RMSD at different layers of chlorophyll, phytoplankton biomass, nitrate, oxygen and surface partial pressure of CO_2 estimated by comparing the reanalysis with datasets other than EMODnet2018_int or satellite observations using class4 metrics. INTERIM product (green cells) has been evaluated with a test simulation between 1 January – 31 December 2020 using the same metric.

II PRODUCTION SYSTEM DESCRIPTION

II.1 Production centre details

Production centre name: MED-MFC

Production system name: Mediterranean Sea Biogeochemistry Reanalysis (CMEMS name: MEDSEA_MULTIYEAR_BGC_006_008)

Production Unit: Med-BIO; Istituto Nazionale di Oceanografia e di Geofisica Sperimentale – OGS (Italy)

Description

The Mediterranean Sea biogeochemical reanalysis at 1/24° of horizontal resolution (approximately 4 km) covers the period January 1999 – June 2021 and is produced by means of the MedBFM3.2 model system. MedBFM3.2, which is run by OGS (IT), includes the transport model OGSTMv4.3 coupled with the biogeochemical flux model BFMv5.1 and the variational data assimilation module 3DVAR-BIO v3.3 for surface chlorophyll. MedBFM3.2 is offline coupled with the physical reanalysis (MEDSEA_MULTIYEAR_PHY_006_004 product run by CMCC) that provides daily forcing fields (i.e., currents, temperature, salinity, diffusivities, wind and solar radiation). The ESA-CCI database of surface chlorophyll concentration (CMEMS-OCTAC REP product) is assimilated with a weekly frequency.

II.2 Description of the MedBFM3.2 model system

The biogeochemical component of the Mediterranean reanalysis at 1/24° horizontal resolution (Med-BIO) is produced by means of the MedBFM model system which is off-line coupled with the NEMO3.6-WW3-Oceanvar hydrodynamic model (Med-PHY component).

MedBFM version 3.2 includes the transport model OGSTMv4.3 coupled with the Biogeochemical Flux Model BFMv5.1 and the data assimilation 3DVAR-BIOv3.3 scheme (Salon et al., 2019). The data assimilation is performed weekly using the satellite chlorophyll (i.e., a composite average of 7 days) from CMEMS OC product. The off-line physical-biogeochemical coupling consists in a daily update of the 2D/3D field physical output (i.e., velocity, temperature, salinity, vertical eddy diffusivity, sea surface height, and solar radiation and wind at surface from the physical reanalysis) that forces the transport processes, the biogeochemical model (e.g., kinetic rates of chemical reactions depend on temperature) and the energy and matter fluxes at the air-sea interface (e.g., photosynthetic available radiation (PAR) depends on incoming solar radiation, CO2 and O2 gas exchanges depend on wind and surface water conditions).

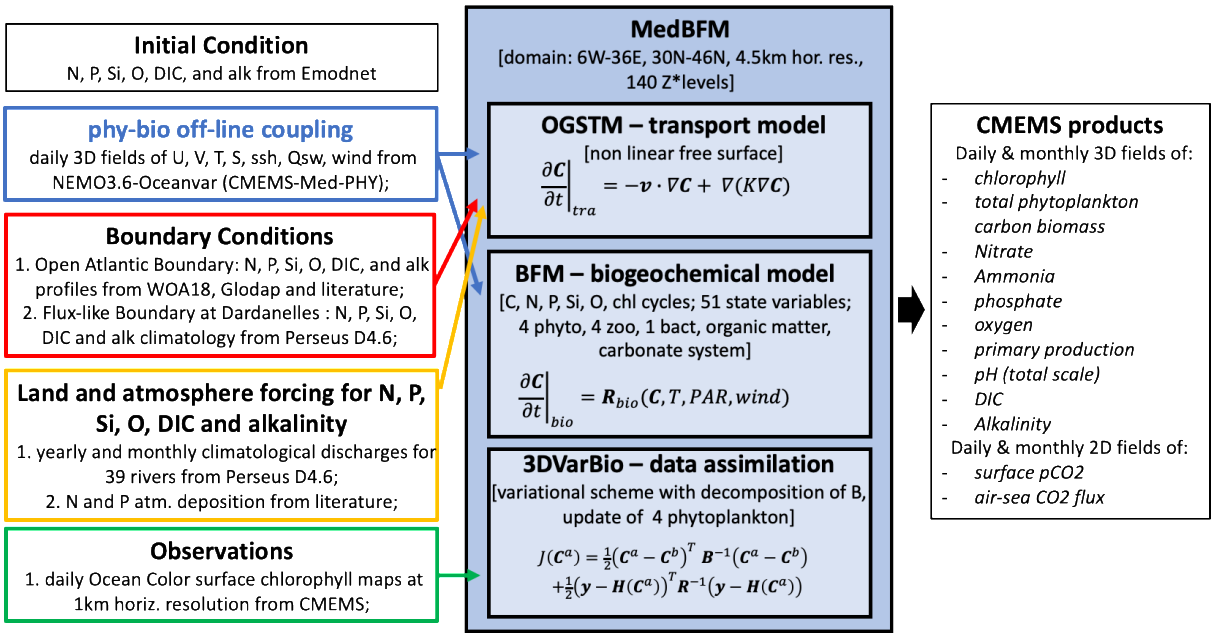

Figure II.2. The Med-BIO model system and interfaces with other CMEMS system. Components.

The OGSTMv4.3 transport model is a modified version of the OPA 8.1 transport model (Foujols et al., 2000), which resolves the advection, the vertical diffusion and the sinking terms of the tracers (biogeochemical variables). The OGSTM resolves the free surface and variable volume layer effects on the transport of tracers being fully consistent with NEMO3.6_vvl output provided by Med-PHY. The horizontal meshgrid is based on 1/24° longitudinal scale factor and on 1/24°cos(ϕ) latitudinal scale factor. The vertical discretization accounts for 141 vertical z-levels, with 125 active in the Mediterranean Sea domain: 35 in the first 200 m depth, 60 between 200 and 2000 m, 30 below 2000 m. The temporal scheme of OGSTM is an explicit forward time scheme for the advection and horizontal diffusion terms, whereas an implicit time step is adopted for the vertical diffusion.

The sinking term is a vertical flux, which acts on a sub-set of the biogeochemical variables (particulate matter and phytoplankton groups). Sinking velocity is fixed for particulate matter and dependent on nutrients for two phytoplankton groups (diatoms and dinoflagellates).

The daily mean physical dynamics are off-line coupled with the transport-biogeochemical processes, and are pre-computed by the Med-PHY reanalysis model system, which supplies the temporal evolution of the fields of horizontal and vertical current velocities, vertical eddy diffusivity, potential temperature, salinity, sea surface height in addition to surface data for solar shortwave irradiance and wind stress (see section on upstream data and boundary conditions for further details).

The features of the biogeochemical reactor BFM (Biogeochemical Flux Model) have been chosen to target the energy and material fluxes through both “classical food chain” and “microbial food web” pathways (Thingstad and Rassoulzadegan, 1995), and to take into account co-occurring effects of multi-nutrient interactions. Both of these factors are very important in the Mediterranean Sea, wherein microbial activity fuels the trophodynamics of a large part of the system for much of the year and both phosphorus and nitrogen can play limiting roles (Béthoux et al., 1998; Krom et al., 1991).

BFMv5.1 model (i.e., the official version released by www.bfm-community.eu) describes the biogeochemical cycles of 4 chemical compounds: carbon, nitrogen, phosphorus and silicon through the dissolved inorganic, living organic and non-living organic compartments (Figure II.3). The model

includes nine plankton functional types (PFTs). Phytoplankton PFTs are diatoms, flagellates, picophytoplankton and dinoflagellates. Heterotrophic PFTs consist of carnivorous and omnivorous mesozooplankton, bacteria, heterotrophic nanoflagellates and microzooplankton. Nitrate and ammonium are considered for the dissolved inorganic nitrogen. The non-living compartment consists of 3 groups: labile, semilabile and refractory organic matter. The first two are described in terms of carbon, nitrogen, phosphorus and silicon contents. The model is fully described in Lazzari et al. (2012, 2016), where it was corroborated for chlorophyll, primary production and nutrients in the Mediterranean Sea for a 1998-2004 simulation. The BFM model is also coupled to a carbonate system model (Cossarini et al., 2015; Melaku Canu et al., 2015), which consists of three prognostic state variables: alkalinity (ALK) and dissolved inorganic carbon (DIC) and particulate inorganic carbon (PIC) which are driven by biological processes (i.e. photosynthesis, respiration, precipitation and dissolution of CaCO3, nitrification, denitrification, and uptake and release of nitrate, ammonium and phosphate by plankton cells) and physical processes (exchanges at air-sea interface and dilution-concentration due to evaporation minus precipitation process). In particular, PIC precipitation occurs in correspondence of phytoplankton mortality and grazing by zooplankton (Orr et al., 2017). Dissolution of PIC occurs for oversaturated calcite conditions according to Berner and Morse (1974). pCO2 and pH (expressed in total scale) are calculated at the in-situ temperature and pressure conditions using Mehrbach et al. (1973) refit by Lueker et al. (2000). Formulations for the kinetic constants of thermodynamic equilibrium of carbon acid dissociation as prescribed in Orr and Epitalon (2015). CO2 air-sea gas exchange formulation is computed according to updates provided by Wanninkhof (2014).

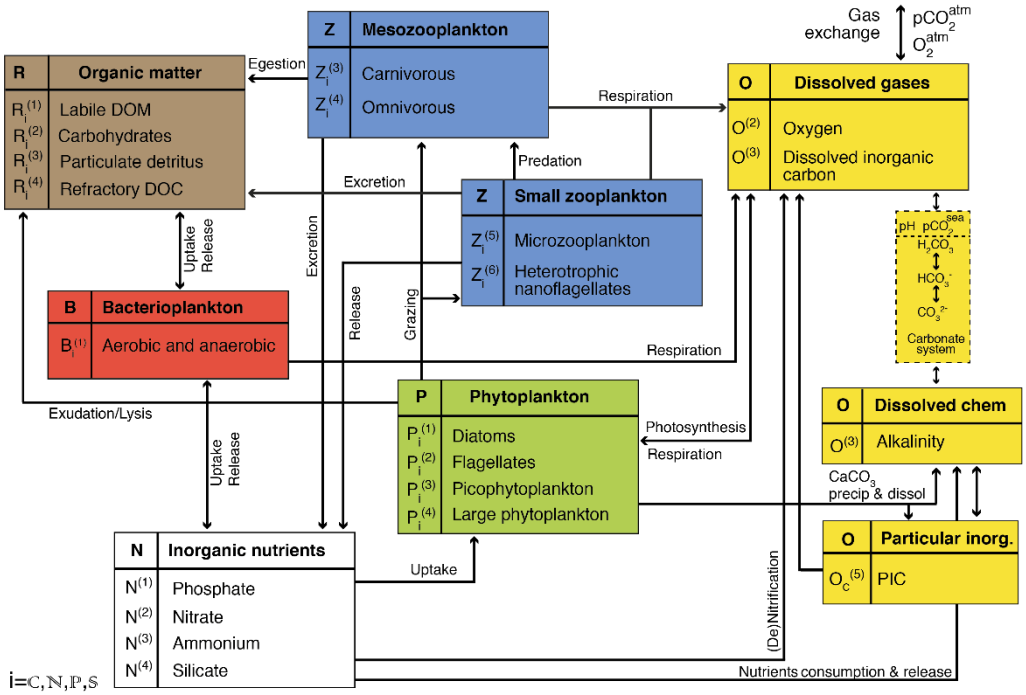

Figure II.3. Scheme of the state variables and significant processes of the upgraded Biogeochemical Flux Model (BFM) version 5.

II.3 Description of Data Assimilation scheme

The data assimilation of surface chlorophyll concentration is performed once a week during the reanalysis run through a variational scheme (3DVarBio, see details in Teruzzi et al., 2019, 2018, 2014). The surface chlorophyll concentrations consist of satellite observations produced by OCTAC based on the ESA-CCI data. The present version of 3DVarBio assimilates chlorophyll concentration over the whole domain including both the open sea and the coastal areas. The data assimilation corrects the four phytoplankton functional groups (17 state variables including carbon, chlorophyll, nitrogen phosphorus and silicon internal quotas) of the BFM. The 3DVarBio scheme decomposes the background error covariance matrix using a sequence of different operators that account separately for the vertical covariance (Vv), the horizontal covariance (Vh) and the covariance among biogeochemical variables (Vb). Vv is defined by a set of synthetic profiles that are evaluated by means of an Empirical Orthogonal Function (EOF) decomposition applied to a validated ten-year run (Teruzzi et al., 2018). EOFs are computed for 12 months and 30 coastal and open sea sub-regions in order to account for the variability of 3D chlorophyll and nitrate anomaly fields. Vh is built using a Gaussian filter whose correlation radius modulates the smoothing intensity. A non-uniform and direction-dependent correlation radius has been implemented (Teruzzi et al., 2018). Vb operator maintains the ratio among the phytoplankton groups and preserves the physiological status of the phytoplankton cells (i.e. preserve optimal values for the internal chlorophyll and carbon nutrients quota).

The assimilation scheme updates the initial conditions every week during the simulation run according to the following steps:

1. a 7-day [from T-3 to T+3] average map of satellite chlorophyll is computed and spatially interpolated on the model grid;
2. the misfit is evaluated as the difference between the satellite chlorophyll and the simulated sum of the four phytoplankton type chlorophylls at 12 noon (12.00pm) of the central day of the 7-day period [T0];
3. the 3D-VAR provides the increment for the four phytoplankton group variables;
4. the new initial conditions (analysis) are produced, and the setup for the simulation of the next seven days is prepared;
5. a new 7-day period is simulated [from T0 to T+7] using the updated initial conditions, plus the physical and boundary conditions.

II.4 Upstream data and boundary conditions

The CMEMS–Med-MFC-Biogeochemistry system uses the following upstream data:

1. Initial conditions of biogeochemical variables are set as 16 sub-basin (Fig. III.1) climatological profiles. A spin-up period (2 years of hindcast simulation) is carried out to reach the start date of the simulation (1/1/1999). Climatological profiles for nitrate, phosphate, silicate, ammonium, oxygen, DIC and alkalinity are computed from a dataset that integrates the in-situ EMODnet data collections (Buga et al., 2018) and the datasets listed in Lazzari et al. (2016) and Cossarini et al. (2015) by averaging available profiles in the period 1997-2007. If the number of profiles per sub-basin is less than 5, profiles of the entire 1997-2015 period are used instead. Initial conditions for the other BFM variables are set equal to values of the standard BFM initialization (Vichi et al., 2015).

2. The daily physical forcing fields (current, temperature, salinity, vertical eddy diffusivity, SSH) and atmospheric (short wave radiation and wind stress) are provided by the MEDSEA_MULTIYEAR_PHY_006_004 produced by Med-PHY. The physical-biogeochemical off-line coupling includes the same number and position of rivers, the same setup for the boundaries (i.e., closed boundary at Dardanelles and open in the Atlantic even if at different longitude) and the same setup/formulation for the free surface dynamics and volume vertical layers.
3. The Jan1999-Jun2021 daily surface chlorophyll and weekly K_d datasets at 1 km horizontal resolution is extracted from the CMEMS multi-sensor (MERIS, MODIS-AQUA, SeaWiFS and VIIRS data) satellite product OCEANCOLOUR_MED_CHL_L3_REP_OBSERVATIONS_009_073. Daily satellite maps of chlorophyll are checked for spikes and outliners considering the sum of a daily climatology and 2 times its daily standard deviation. Climatology and standard deviation are computed for each pixel and each day using available observations in a time window of ± 7 days for the period 1999-2021.
4. The biogeochemical open boundary conditions in the Atlantic Ocean at the longitude of 9°W are provided through a Dirichlet-type scheme. Climatological profiles of phosphate, nitrate, silicate, dissolved oxygen are computed averaging the World Ocean Atlas 2018 data (Garcia et al., 2019; data from https://www.nodc.noaa.gov/OC5/woa18) for the area: Lon=8°W-9°W and Lat=34°N-37°N. Nitrate and phosphate profiles are revised to preserve the N:P ratio values of 5 and 17 in the surface and subsurface layers, respectively. The oxygen profile unit was converted in mmol m^{-3} by using the seawater density profile computed from temperature and salinity data provided by the World Ocean Atlas 2018. Climatological profiles of DIC and Alkalinity are derived from the GLODAP v2 dataset (Olsen et al., 2019, 2016; data from https://www.nodc.noaa.gov/ocads/oceans/GLODAPv2_2019/) by averaging the available in situ observations in the area: Lon=8°W-10°W, Lat=34°N-37°N. A nudging scheme is applied in the 9°W-7°W area using the same profiles to avoid numerical instability.
5. Terrestrial inputs of N, P, Si, O, Alkalinity and DIC take into account the 39 rivers showed in Fig. III.1 (river names are Nile, Vjosë, Seman, Buna/Bojana, Piave, Tagliamento, Soca/Isonzo, Livenza, Brenta-Bacchiglione, Adige, Lika, Reno, Krka, Arno, Nerveta, Aude, Trebisjnica, Tevere/Tiber, Mati, Volturno, Shkumbini, Struma/Strymonas, Meric/Evros/Maritsa, Axios/Vadar, Arachtos, Pinios, Acheloos, Gediz, Buyuk Menderes, Kopru, Manavgat, Seyhan, Ceyhan, Gosku, Medjerda, Asi/Orontes). Monthly N, P and Si discharges are derived from the 1999-2018 annual values (PERSEUS FP7-287600 dataset, Deliverable D4.6) multiplied by climatological monthly river run-off. Monthly alkalinity and DIC discharges are derived multiplying their *typical concentrations* per fresh water mass in macro coastal areas of the Mediterranean Sea (Copin-Montégut, 1993; Kempe et al., 1991; Meybeck and Ragu, 1997) by the river water runoff from the PERSEUS dataset (Deliverable D4.6). Oxygen *typical concentration* in freshwater is set equal to the saturation value at 15°C and 5 PSU.
6. The biogeochemical boundary conditions at the Dardanelles Strait are provided through a Neumann-type scheme. The climatological annual value of the net exchange fluxes (positive toward the Mediterranean Sea) of nitrate, phosphate, silicate is derived from PERSEUS dataset. Annual net exchange fluxes of alkalinity and DIC are derived as in Cossarini et al. (2015)
7. Atmospheric deposition rates of inorganic nitrogen and phosphorus were set according to the synthesis proposed by Ribera d'Alcalà et al. (2003) and based on measurements of field data (Bergametti et al., 1992; Cornell et al., 1995; Guerzoni et al., 1999; Herut and Krom, 1996; Loÿe-Pilot et al., 1990). Atmospheric deposition rates of nitrate and phosphate were assumed to be constant in time during the simulation year, but with different values for the western (580 Kt N yr^{-1} and 16 Kt P yr^{-1}) and eastern (558 Kt N yr^{-1} and 21 Kt P yr^{-1}) sub-basins. The rates

were calculated by averaging the “low” and “high” estimates reported by Ribera d’Alcalà et al. (2003).

8. Atmospheric pCO2 concentration is set equal to the annual averages measured at the Lampedusa station (Artuso et al., 2009) between 1999 and 2018 (data from http://cdiac.ess-dive.lbl.gov/ftp/trends/co2/lampedus.co2). Values for years after 2018 are linearly extrapolated.
9. Surface evaporation-precipitation effects on dilution and concentration of tracers at surface are directly computed by OGSTM through the non-linear free-surface z*-coordinate configuration and using directly the sea surface anomaly evolution provided by the NEMO3.6 output.

II.5 Reanalysis *INTERIM* production

The operational INTERIM reanalysis, which covers the most recent period of the multi-year biogeochemical product (i.e., from July 2021 to 1 month before present) is provided by means of the same biogeochemical reanalysis model system (Medeaf 3.2), the same assimilation scheme and setup and the same biogeochemical model setup (section II.4). The only differences are that the INTERIM is forced by the physical INTERIM production dynamics (see QUID of MEDSEA_MULTIYEAR_PHY_006_004 product) and the ECMWF ERA5/ERA5T atmospheric forcing fields and the assimilated observations are from the delay mode NRT L3 Ocean Color product (MED_CHL_L3_NRT_OBSERVATIONS_009_040). The INTERIM dataset is initialized with the last available day of the reanalysis. The present document reports the INTERIM validation based on a test simulation covering Jan – Dec 2020.

III VALIDATION FRAMEWORK

The Med-BIO reanalysis products are chlorophyll, net primary production, phosphate, nitrate, ammonium, oxygen, pH, pCO2, DIC, alkalinity and CO2 air-sea flux. Three different levels of validation are presented for the model variables:

1. model capability to reproduce basin wide spatial gradients, mean annual values in sub-basin and average vertical profiles based on GODAE Class1 metrics (level-1);
2. model capability to reproduce the variability due to mesoscale and daily dynamics based on GODAE Class4 metrics (level-2; Hernandez et al., 2018);
3. model capability to reproduce key biogeochemical processes based on specific metrics (level-3; Salon et la., 2019).

Data availability represents an important constrain in biogeochemical model validation (Salon et al., 2019): depending on the variables, different uncertainty levels can be provided on the basis of the availability of reference data. Thus, the validation analysis provides a “degree of confirmation” (Oreskes et al., 1994) with respect to the different scales of variability derived from the available observations.

All of the variables are validated with GODAE class1 metrics using a reference climatology computed from the available in situ data (i.e., reference mean annual vertical profiles for the 16 sub-basins, Appendix A) or literature reviews (level-1). For most of the variables, the validation analysis is based on a model-observations comparison (level-2) and metrics are calculated and reported considering 16 sub-basins (Fig. III.1) and 8 vertical layers (Tab. III.1).

The validation refers primarily to the open sea areas (i.e., areas whose depth is greater than 200m; grey line in Fig. III.1). The accuracy of the reanalysis in the coastal areas can be assessed only for surface chlorophyll using CMEMS satellite product, and for some variables and few sub-basins when in situ data are available.

Applied skill performance metrics are the BIAS and the Root Mean Square of the differences between model output and observations (RMSD) and correlation between timeseries or spatial distributions of model output and observations. The reference in situ and satellite datasets are: EMODnet integrated dataset (EMODnet2018_int) with additional oceanographic cruises (Cossarini et al., 2015; Lazzari et al., 2016), CMEMS ocean colour and SOCAT. Further, a quality checked BGC-Argo float dataset has been used to evaluate specific metrics for chlorophyll, oxygen and nutrient vertical dynamics (Salon et al., 2019).

Model chlorophyll is validated using both satellite and in situ observations. Besides comparison of mean climatological maps (level-1), multi-sensor satellite chlorophyll data from CMEMS (MED_CHL_L3_REP_OBSERVATIONS_009_073) are used to compute the differences between satellite and model mean maps of each week between two assimilation steps (a semi-independent skill metric) (level-2). The metrics (BIAS and RMSD) are evaluated at sub-basin scale and provided as timeseries to show the uncertainty of the chlorophyll w.r.t the weekly dynamics and the mesoscale. BGC-Argo floats data (Fig. III.4) from Coriolis/Ifremer datacentre (Schmechtig et al., 2015) are used to compute BIAS, RMSD, correlation (level-2 metrics) along with level-3 novel metrics (e.g., deep chlorophyll maximum depth, integral values and thickness of the layer of the winter bloom) considering the model output at the time and location of the in-situ profile. This validation provides insights of model capability to reproduce the vertical chlorophyll dynamics at the daily scale and at mesoscale. Validation metrics, which cover only a limited period of the reanalysis (i.e., 2013-2019) are reported as time series for selected layers and sub-basins (Fig. III.1) and as average statistics computed from all the matching pairs of model and observation profiles for each sub-basin (Table III.1).

Model net primary production data are compared with literature data based on multi-annual simulations (Lazzari et al., 2012), satellite (Bosc et al., 2004; Colella, 2006), in situ estimates (Siokou-Frangou et al., 2010). Consistency in annual and seasonal values and basin-wide gradients (level-1) is the maximum degree of confirmation reachable for this variable.

Model phytoplankton biomass expressed as carbon is compared with BGC-Argo floats data of particulate backscattering coefficient at 700nm (bbp700) from Coriolis/Ifremer datacentre (Schmechtig et al., 2018). Data of bbp700 are converted to carbon biomass using the relationship proposed by Bellacicco et al. (2019). Given the scarce and sparse availability of this optical measurements only an indicative value can be provided by the level-2 validation framework.

Model phosphate, nitrate, ammonium, dissolved oxygen, pH in total scale, pCO2, alkalinity and DIC are compared with a dataset of in situ observations from EMODnet and other scientific cruises (EMODnet2018_int) listed in Cossarini et al. (2015) and Lazzari et al. (2016). The dataset spans the period 1997-2016; for the time period considered in the reanalysis (1999-2019) it consists of 12257 observations for nitrate, 17323 for phosphate and 104910 for dissolved oxygen, and about 3500 and 4200 for DIC and alkalinity, respectively, covering the Mediterranean Sea as shown in Figs. III.3-5. Data of pH in total scale and pCO2 are partly real observations (about 30%) and partly reconstructed (70%) using CO2sys software (Lewis and Wallace, 1998) with available DIC, ALK and other regulatory information (i.e., temperature, salinity and concentration of phosphate and silicate), and the same carbonate system specification used by BFM. A measure of the goodness of such a calculation (Álvarez et al., 2014) shows that residuals of the reconstructed pH values have mean value and standard deviation equal to -0.001 ± 0.005. Given the sparse and uneven distribution in time and space of the data, two levels of validation are performed for both nutrients and carbonate variables. Firstly, the consistency with the vertical climatological profiles for each sub-basin and with reference values at different layers provides the model validation at the basin-wide scale (level-1). Secondly, the class 4 metrics (level-2) based on the model-observation match-up, which are shown in the density plot and synthetized as the sub-basin and layers accuracy numbers, represent the accuracy at the scale of variability of the daily and mesoscale dynamics.

Nitrate and dissolved oxygen BGC-Argo float profiles (Fig. III.4) from Coriolis/Ifremer datacentre (Johnson et al., 2018; Thierry et al., 2018) are also used to compute the BIAS, RMSD (level-2), correlation and level-3 novel metrics (integrated vertical values and depth of nutricline) considering the model output at the time and location of the in-situ profile. This validation provides insights of model capability to reproduce vertical nitrate and oxygen dynamics at daily scale and at mesoscale. Validation metrics, which cover only a limited period of the reanalysis (i.e., 2013-2019) are reported as time series for selected layers and sub-basins (Fig. III.1) and as average statistics computed from all the matching pairs of model and observation profiles for each sub-basin (Table III.1).

Model pCO2 has been validated also considering another dataset: the SOCAT data collection (Bakker et al., 2016; 2020 release, https://www.socat.info/index.php/data-access/). SOCAT dataset consists of surface ocean fugacity (fCO2) measurements (up to 6500 observations in the Mediterranean Sea) covering the period 1998-2018 (Fig. III.5). Fugacity measurements are converted to partial pressure measurements using standard formula.

Model surface flux of CO2 has been validated by evaluating the consistency of the model results with those published in the Ocean State Report (Schuckmann et al., 2018).

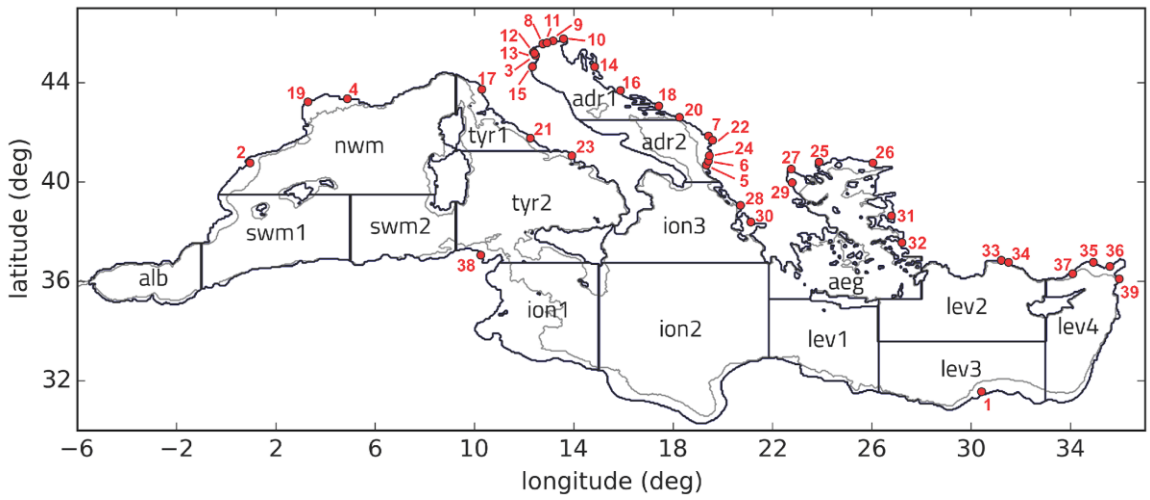

Figure III.1. Subdivision of the model domain in sub-basins used for the validation of the qualification run. According to data availability and to ensure consistency and robustness of the metrics, different subsets of the sub-basins or some combinations among them can be used for the different metrics: lev = lev1+lev2+lev3+lev4; ion = ion1+ion2+ion3; tyr = tyr1+tyr2; adr = adr1+adr2; swm = swm1+swm2. The grey line defines the bathymetric contour at 200 m. Red dots with numbers correspond to main river mouth positions: Nile (1), Ebro (2), Po (3), Rhone (4), Vjosë (5), Seman (6), Buna/Bojana (7), Piave (8), Tagliamento (9), Soca/Isonzo (10), Livenza (11), Brenta-Bacchiglione (12), Adige (13), Lika (14), Reno (15), Krka (16), Arno (17), Nerveta (18), Aude (19), Trebisjnica (20), Tevere (21), Mati (22), Volturno (23), Shkumbini (24), Struma/Strymonas (25), Meric/Evros/Maritsa (26), Axios/Vadar (27), Arachtos (28), Pinios (29), Acheloos (30), Gediz (31), Buyuk Menderes (32), Kopru (33), Manavgat (34), Seyhan (35), Ceyhan (36), Gosku (37), Medjerda (38), Asi/Orontes (39).

Layer 1	Layer 2	Layer 3	Layer 4	Layer 5	Layer 6	Layer 7	Layer 8
0-10	10-30	30-60	60-100	100-150	150-300	300-600	600-1000

Table III.1. Vertical layers (in m) considered for the validation of the qualification run products.

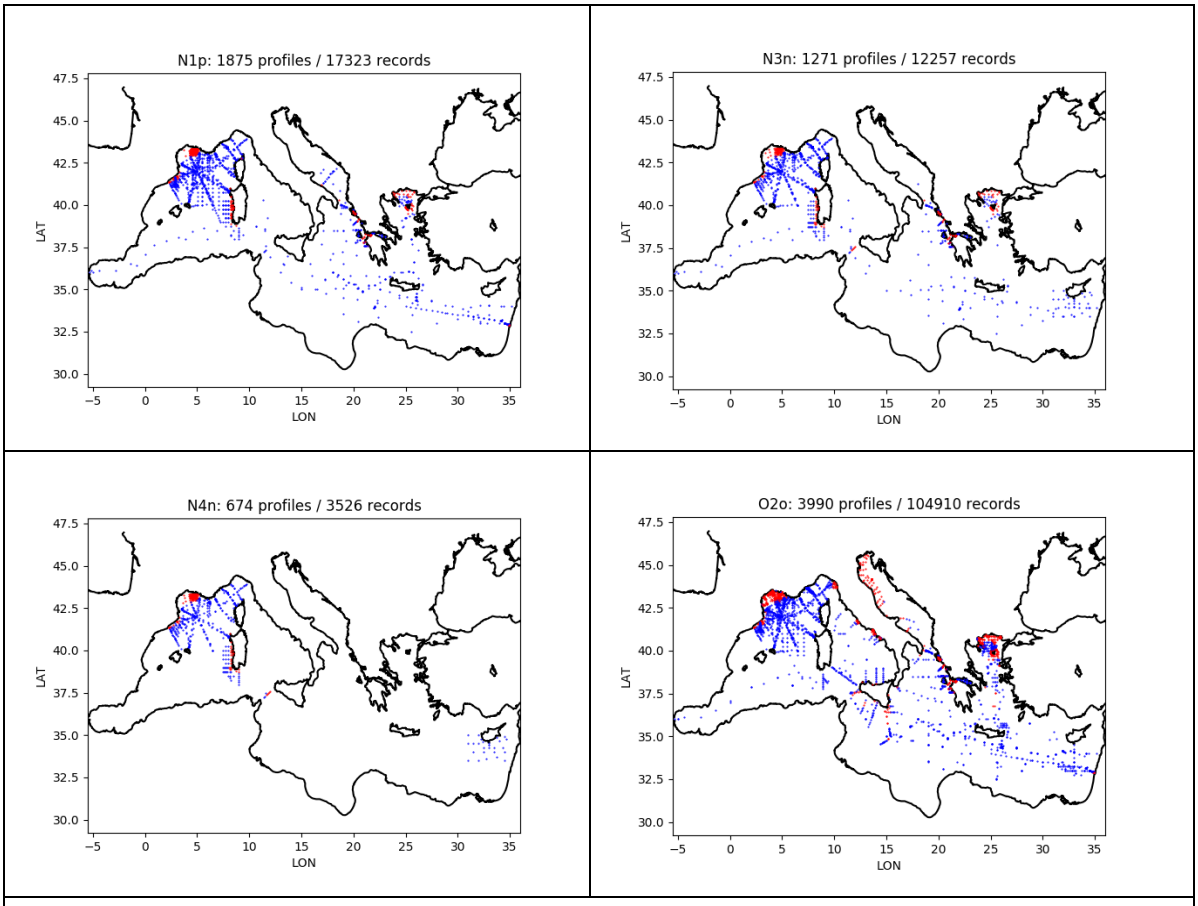

Figure III.2. Map of in situ observations of the EMODnet2018_int dataset, i.e., integration of the aggregated EMODnet data collections (Buga et al., 2018) and the datasets listed in Lazzari et al. (2016) for nutrients and oxygen variables. Top row: phosphate and nitrate; bottom row: ammonium and oxygen. Blue and red dots indicates open sea and coastal areas location respectively.

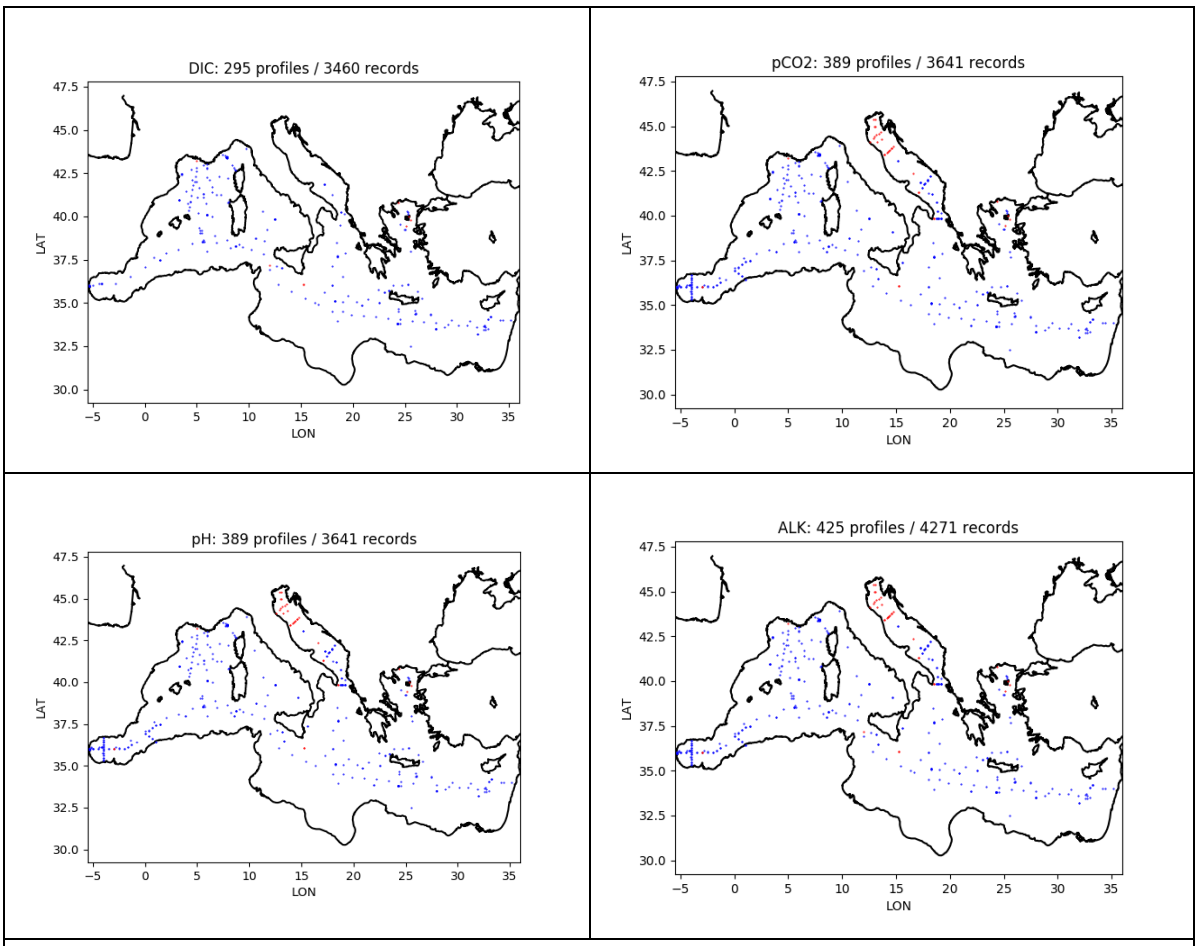

Figure III.3. Map of in situ observations of the EMODnet2018_int dataset, i.e., integration of the Aggregated EMODnet data collections (Buga et al., 2018) and the datasets listed in Cossarini et al. (2015) for carbonate system variables. Top row: DIC and pCO2; bottom row: pH and alkalinity. Blue and red dots indicates open sea and coastal areas location respectively.

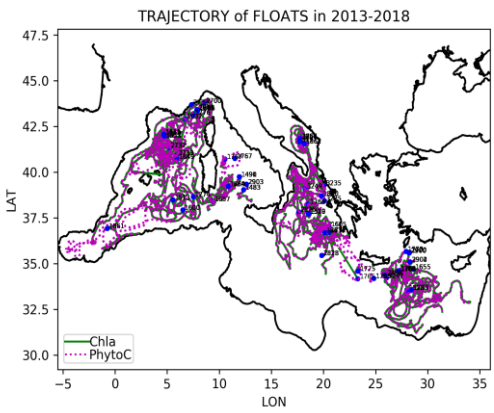

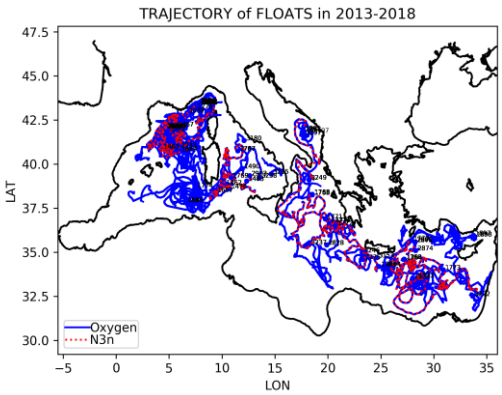

Figure III.4. Trajectories of 80 BGC-Argo floats in 2013-2019. Left panel: observations of chlorophyll (53) and phytoplankton biomass (54). Right panel: oxygen (53) and nitrate (23).

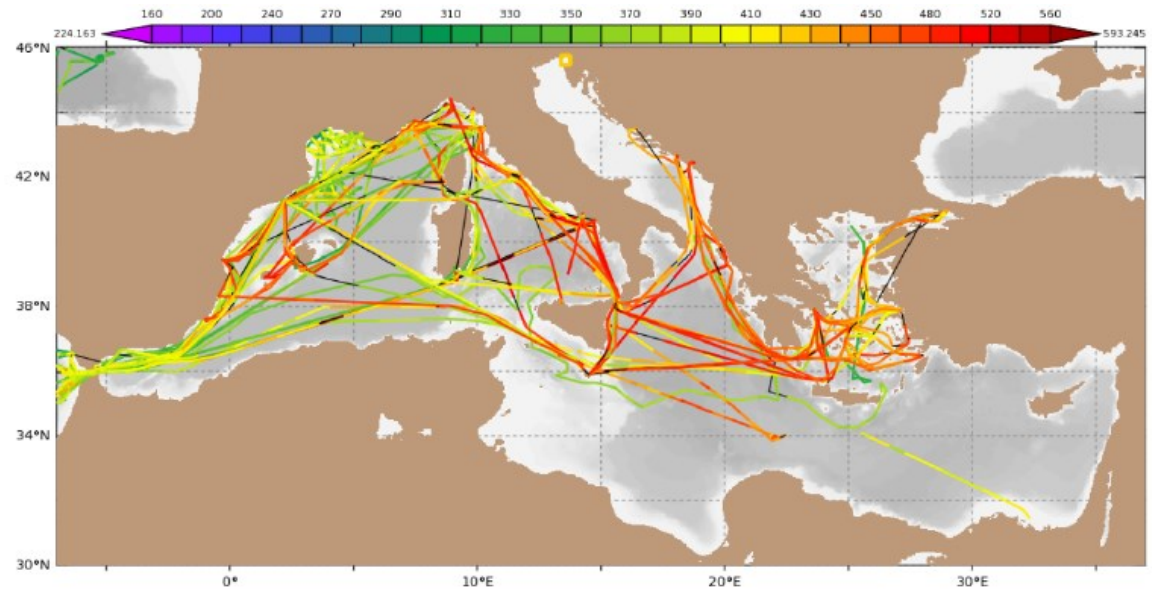

Figure III.5. Map of surface fCO2 observations from the SOCAT dataset for the period 1998-2016.

IV VALIDATION RESULTS

IV.1 Chlorophyll

The accuracy of the reanalysis chlorophyll is evaluated by three quality assessment levels. Class1 validation metrics (level 1) consist in the comparison between model average surface map and the reference climatological map (Figure IV.1.1) and between model and satellite time series of weekly surface mean values in the 16 sub-basins (Figure IV.1.2).

Class4 validation (level 2) consists of skill performance metrics computed using satellite and in situ BGC-Argo observations. In particular, the 1999-2021 time series of RMSD between surface model and satellite are shown in Figure IV.4.3 and statistics summarised in Tables IV.1.1-2 for 16 sub-basins and for open-sea and coastal areas, respectively. Matchups of model and BGC-Argo are shown in the Hovmoeller diagrams of Figure IV.4.4 and BIAS and RMSD statistics summarised in Table IV.1.3 for 7 aggregated sub-basins and 5 depths.

Level 3 validation consists of process-based metrics specifically developed for the comparison between model and BGC-Argo data (Salon et al., 2019). In particular, the metrics aim to assess the model capability to reproduce important ecosystem processes such as the winter surface bloom and the formation of the deep chlorophyll maximum. Process-based metrics are summarised in Table IV.1.4 for 7 aggregated sub-basins.

The results of the three validation levels show that the MedBFM reanalysis has a very good accuracy in reproducing both temporal and spatial variability of surface values and of vertical profiles. Level 1 comparison between model surface annual average map and the reference climatological map (Fig. IV.1.1) shows the good skill of the model in simulating the west-eastern basin-wide gradient, the sub-basin mean values and the coastal-off shore patterns. Modelled annual cycles and interannual variability are consistent with those of satellite observations in all sub-basins (Fig. IV.1.2). RMSD and BIAS statistics for INTERIM 2020 product are similar to those reported for the reanalysis (Fig. IV.1.2).

Skill metrics (class 4 statistics) highlight that model accuracy is higher in summer than in winter, higher in off-shore areas than coastal ones (Tables IV.1.1-2) and higher at surface than in the subsurface layers (i.e., at the depth of transition between vertical mixed layer and DCM formation in winter/spring and around the DCM depth in summer; Tables IV.1.3). In general, errors are higher when spatial and/or temporal variabilities are higher.

For the INTERIM product (year 2020), class 4 metrics are similar to those of the reanalysis both for the satellite chlorophyll (green columns in Tables IV.1.1-2) and for the BGC-Argo float profiles (green rows in Tables IV.1.3). Small differences are due to the different number of the observations available for the reanalysis and INTERIM period.

The MedBFM model has a very high skill in reproducing the vertical dynamics of the phytoplankton chlorophyll, both considering the very high spatial heterogeneity of the Mediterranean Sea and the seasonal cycle of the coupled physical-biogeochemical processes (see Hovmoeller diagram of Fig. IV.1.4). In particular, the correlation between vertical profiles of model and observations is close to or higher than 0.8 in all aggregated subbasins (Fig. IV.1.4 and Tab. IV.1.4). The deep chlorophyll maximum (DCM) depth and the winter layer bloom (WBL) thickness are characterized by a mean uncertainty of 16 m and 30 m, respectively (Tab. IV.1.4). The RMSD of the 0-200 m vertical averages is always less than 0.06 mg/m^3 in all the aggregated sub-basins except in NWM and ALB.

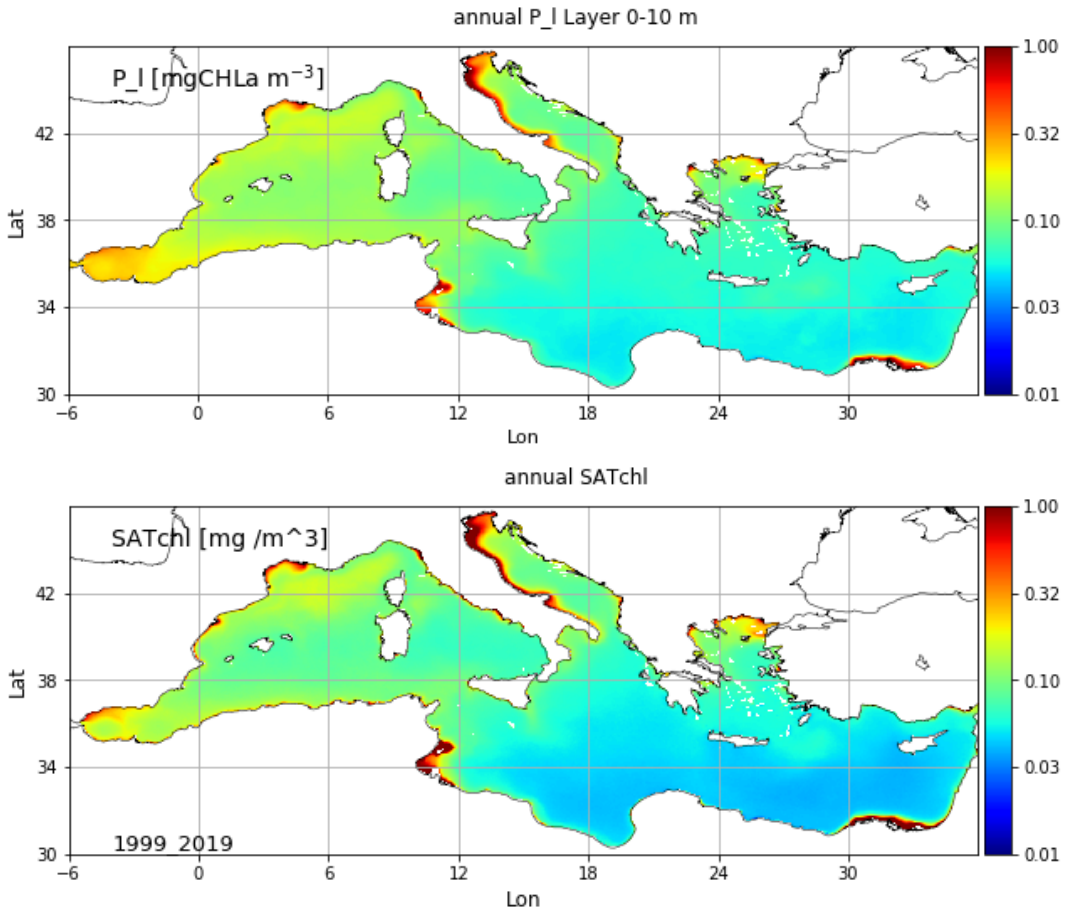

Fig. IV.1.1. Averaged annual maps of surface chlorophyll from reanalysis (top) and from REP OC-TAC product (bottom). The average is computed considering the period 1999-2019, and the layer 0-10 m for the model results.

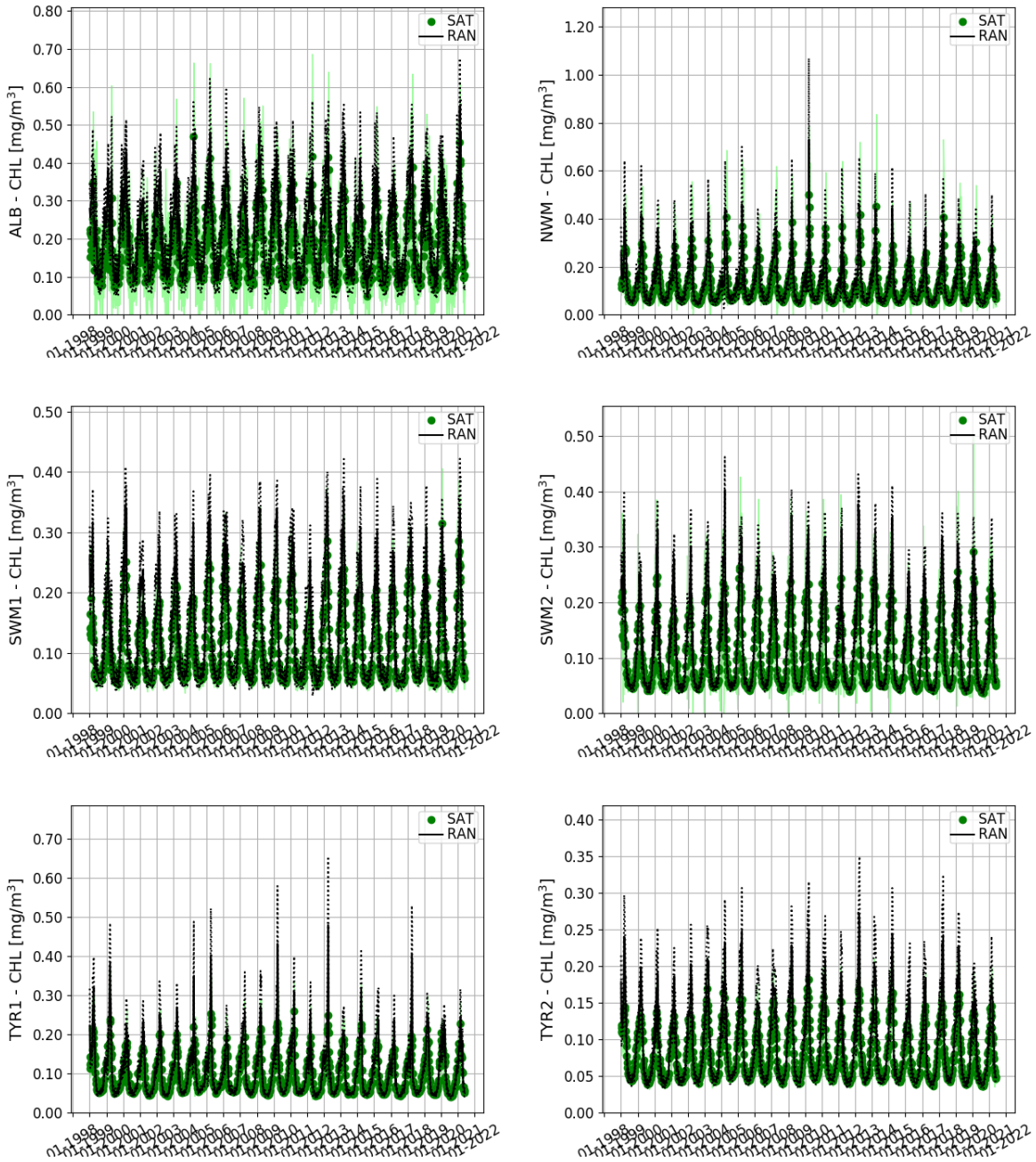

Figure IV.1.2. Jan1999-Jun2020 weekly time series of the reanalysis mean surface chlorophyll concentration (black solid line) with its spatial standard deviation (STD, dotted black line) compared with ESA-CCI satellite data set (green dots) with its STD (shaded green area) for selected sub-basins and for the Mediterranean Sea (MED). (continues overleaf).

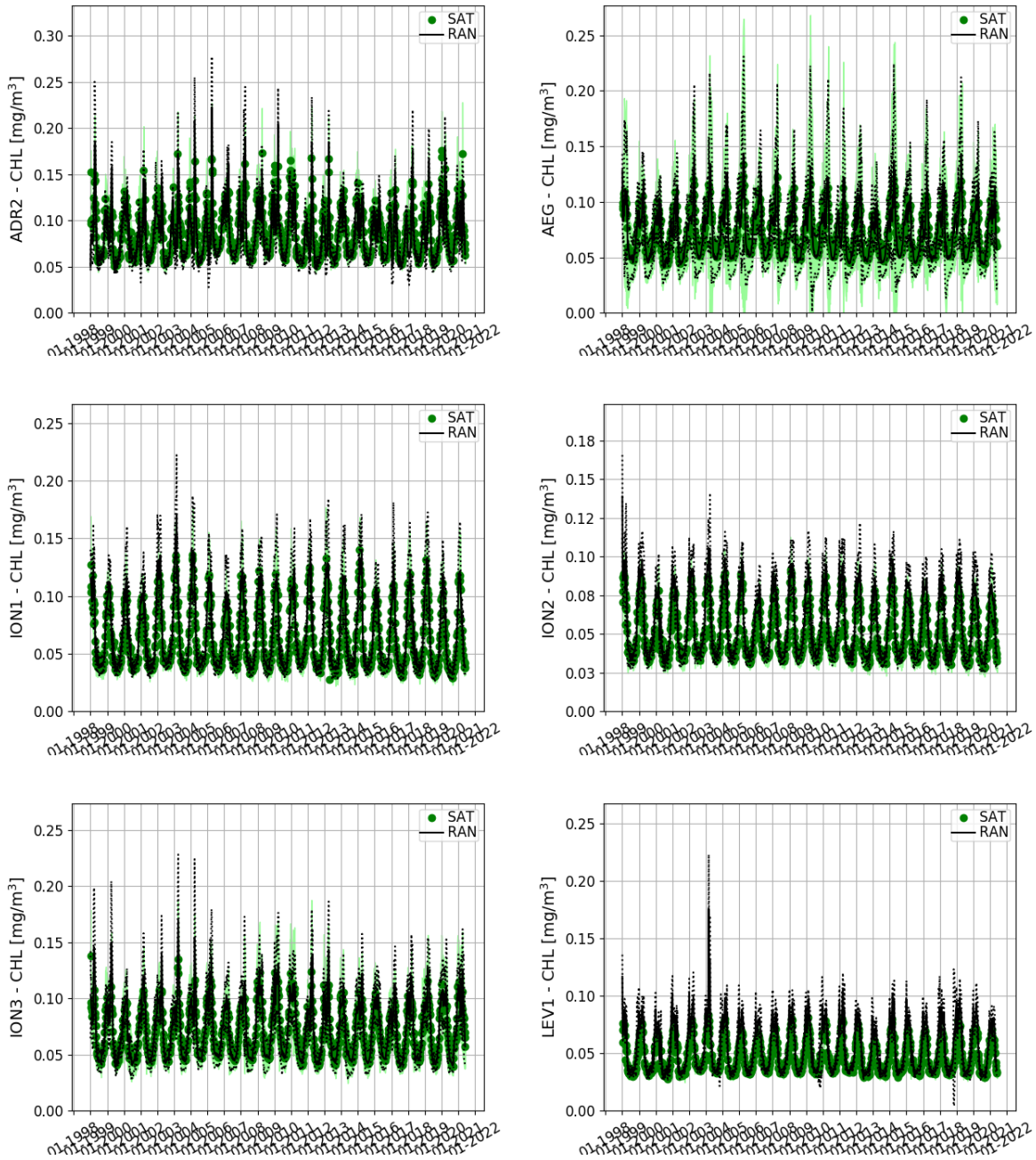

Figure IV.1.2. Same as above.

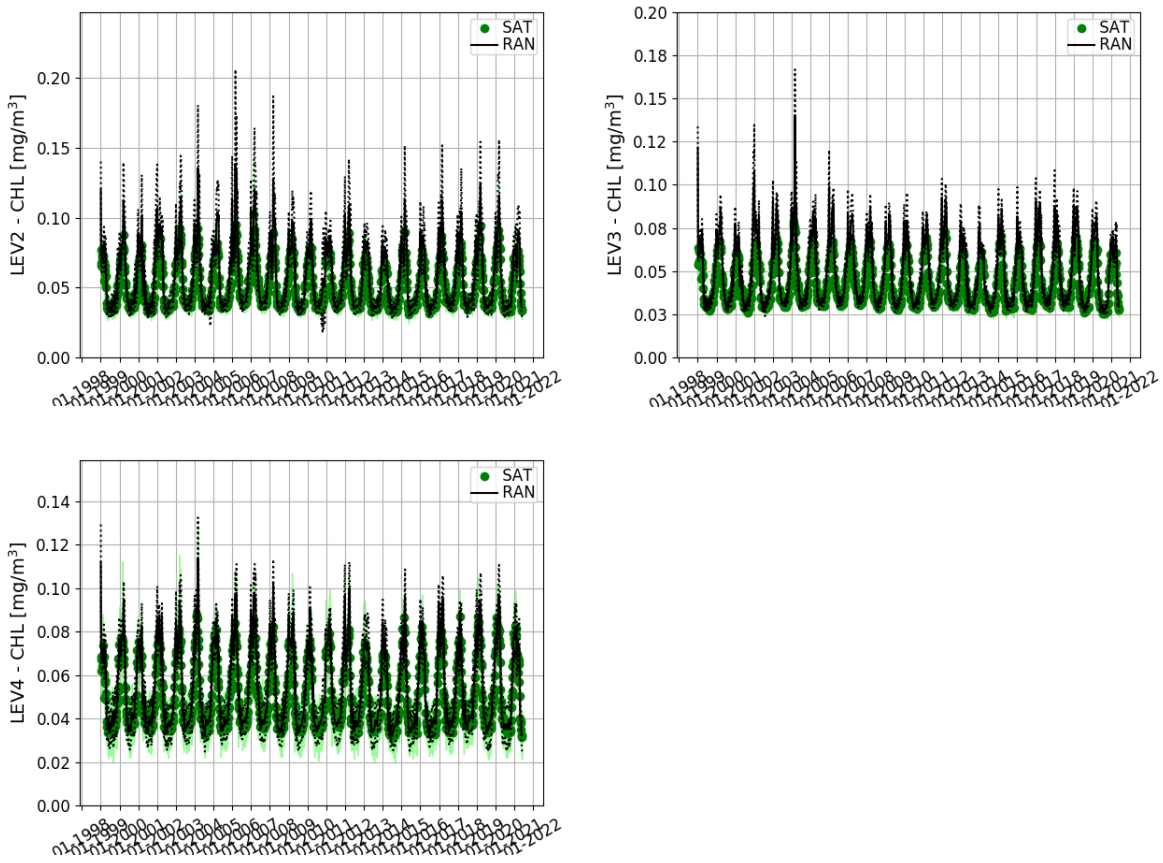

Figure IV.1.2. Same as above.

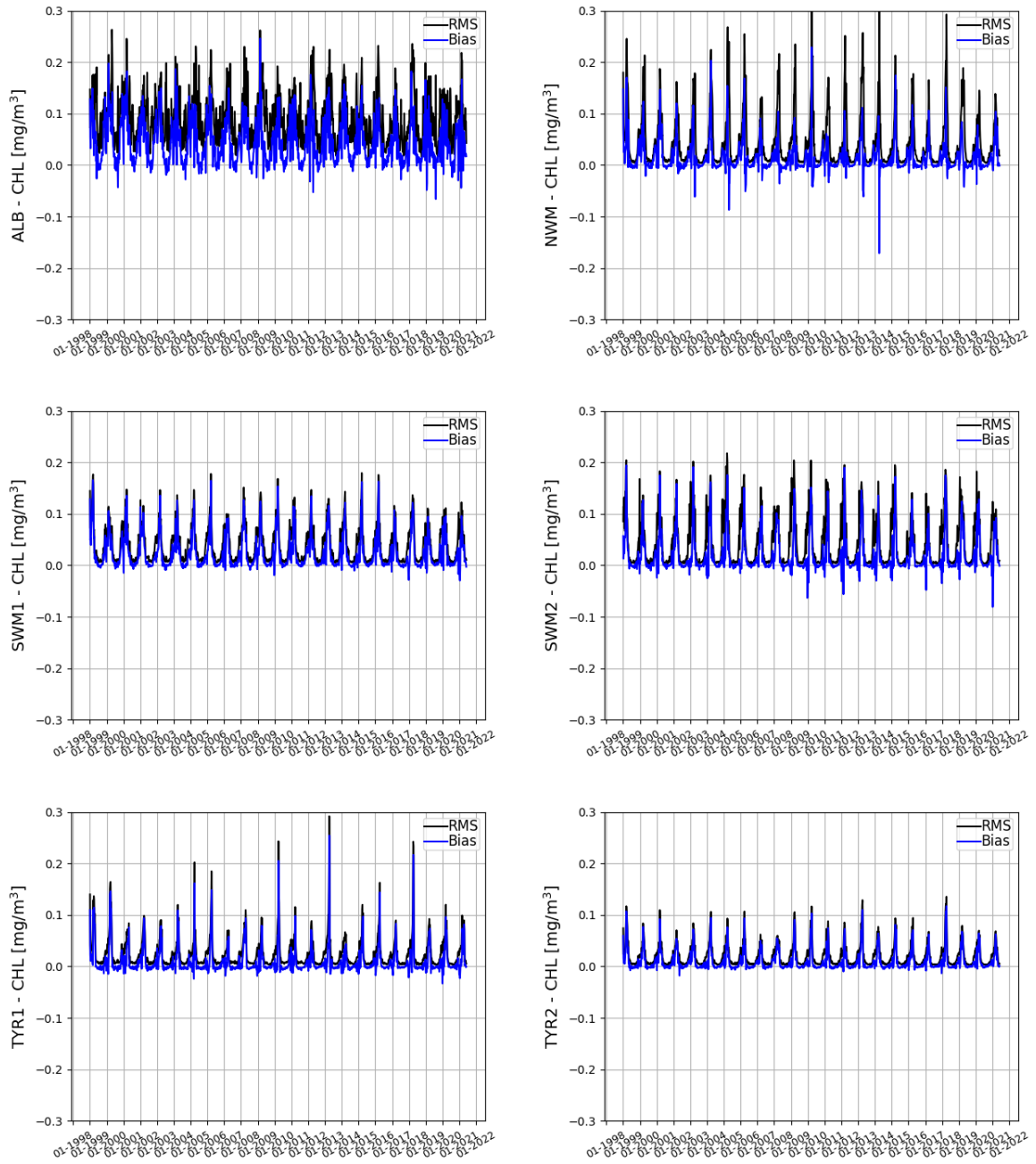

Figure IV.1.3. Jan1999-Jun2021 weekly time series of BIAS and RMSD metrics computed for selected Mediterranean sub-basins reported in Figure III.1 and for the Mediterranean Sea (MED). Computation of BIAS and RMSD are based on the reanalysis surface chlorophyll concentration referred only to offshore areas (depth deeper than 200 m) (continues overleaf).

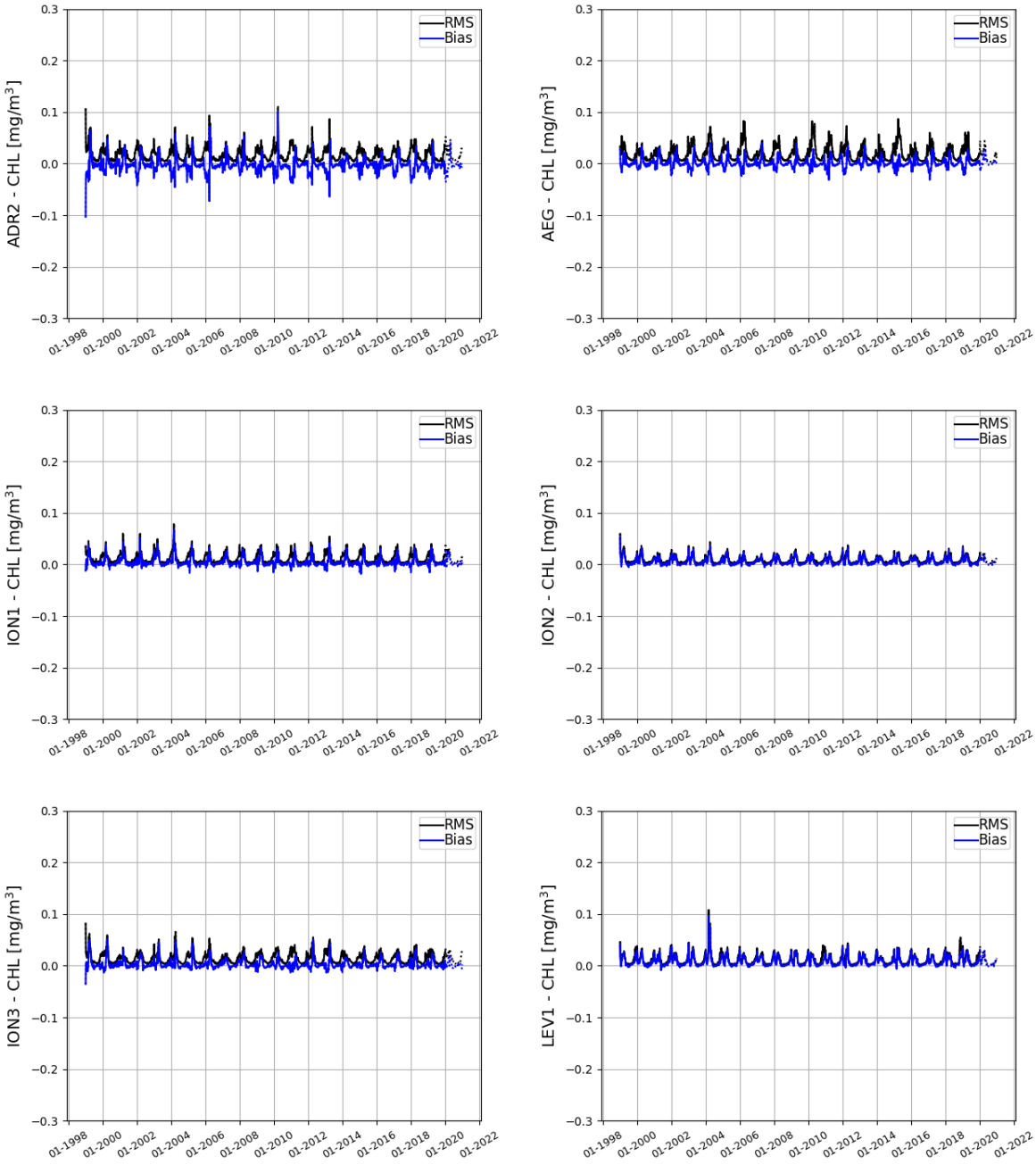

Fig. IV.1.3. Same as above.

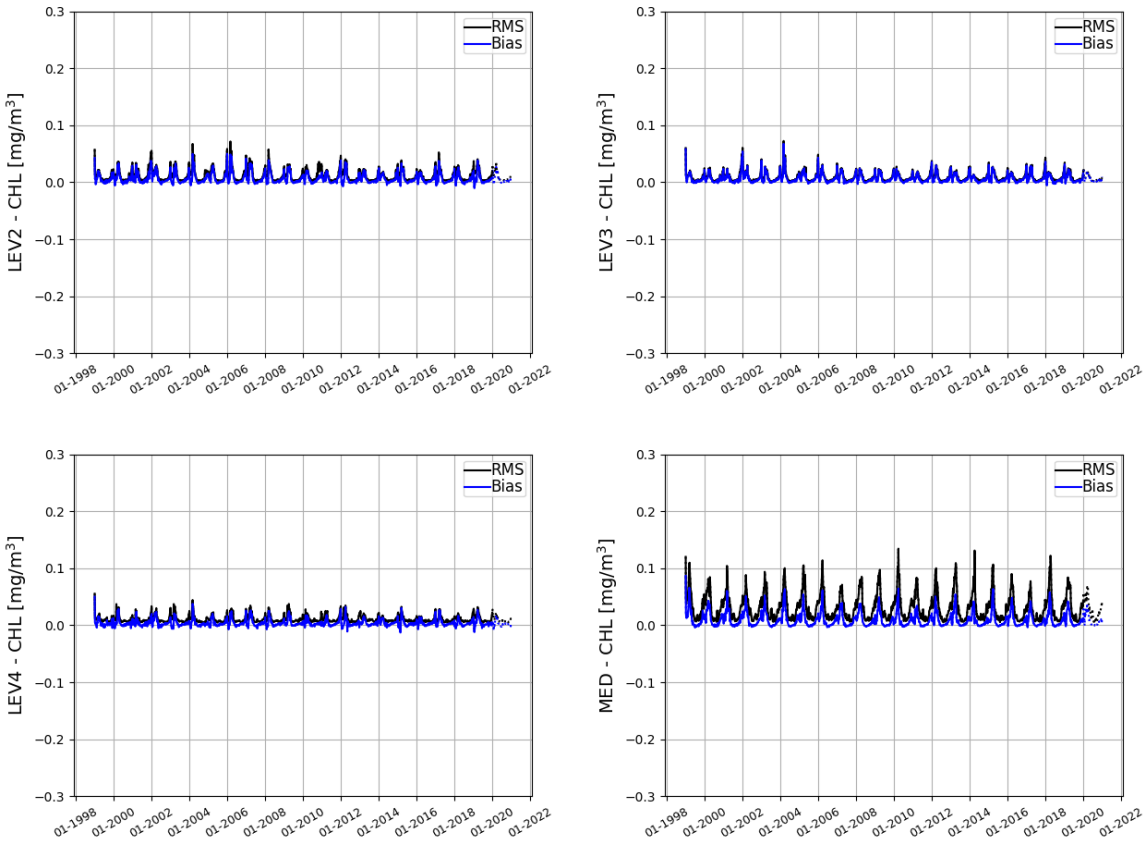

Fig. IV.1.3. Same as above.

OPEN SEA	Mod-Sat								log10(Mod)-log10(Sat)							
	RMSD				BIAS				RMSD				BIAS			
	MEDREA24		INTERIM		MEDREA24		INTERIM		MEDREA24		INTERIM		MEDREA24		INTERIM	
	win	sum	win	sum	win	sum	win	sum	win	sum	win	sum	win	Sum	win	sum
alb	0.13	0.06	0.13	0.06	0.08	0.01	0.08	0.01	0.21	0.14	0.23	0.15	0.15	0.05	0.17	0.05
swm1	0.08	0.01	0.07	0.01	0.05	0.00	0.05	0.00	0.18	0.05	0.17	0.05	0.14	0.01	0.13	0.02
swm2	0.09	0.01	0.08	0.01	0.05	0.00	0.05	0.00	0.18	0.04	0.19	0.04	0.13	-0.01	0.16	0.00
nwm	0.10	0.01	0.07	0.01	0.03	0.00	0.02	0.00	0.19	0.05	0.14	0.04	0.07	-0.01	0.07	-0.01
tyr1	0.05	0.01	0.05	0.00	0.03	0.00	0.03	0.00	0.14	0.05	0.15	0.04	0.08	-0.02	0.10	-0.01
tyr2	0.04	0.01	0.04	0.00	0.03	0.00	0.03	0.00	0.13	0.04	0.15	0.03	0.09	-0.01	0.12	0.00
adr1	0.02	0.01	0.02	0.01	0.00	-0.01	0.00	-0.01	0.08	0.05	0.06	0.05	0.00	-0.04	0.00	-0.04
adr2	0.03	0.01	0.03	0.01	0.00	0.00	0.00	0.00	0.12	0.05	0.11	0.04	-0.02	-0.03	-0.01	-0.02
aeg	0.03	0.01	0.03	0.01	0.00	0.00	0.01	0.00	0.11	0.05	0.10	0.04	0.03	-0.01	0.04	-0.01
ion1	0.02	0.00	0.02	0.00	0.01	0.00	0.01	0.00	0.09	0.05	0.10	0.05	0.06	0.01	0.07	0.01
ion2	0.02	0.00	0.02	0.00	0.01	0.00	0.01	0.00	0.09	0.04	0.09	0.04	0.07	0.01	0.07	0.01
ion3	0.03	0.01	0.02	0.01	0.01	0.00	0.01	0.00	0.10	0.04	0.09	0.04	0.04	-0.01	0.04	-0.01
lev1	0.02	0.00	0.02	0.00	0.01	0.00	0.02	0.00	0.11	0.04	0.11	0.04	0.09	0.01	0.09	0.01
lev2	0.02	0.00	0.02	0.00	0.01	0.00	0.01	0.00	0.11	0.04	0.11	0.04	0.08	0.01	0.06	0.01
lev3	0.02	0.00	0.01	0.00	0.01	0.00	0.01	0.00	0.10	0.04	0.09	0.04	0.09	0.02	0.08	0.02
lev4	0.02	0.01	0.02	0.01	0.01	0.00	0.01	0.00	0.09	0.07	0.08	0.07	0.05	0.01	0.04	0.01
med	**0.04**	**0.01**	**0.04**	**0.01**	**0.02**	**0.00**	**0.02**	**0.00**	**0.13**	**0.05**	**0.12**	**0.05**	**0.07**	**0.00**	**0.08**	**0.00**

Table IV.1.1. Mean RMSD and BIAS between surface (0-10 m) chlorophyll model maps and satellite maps referred to open sea areas (deeper than 200 m, Fig. III.1) over the whole simulation. On the right side, the skill indexes are computed on the log-transformed model and satellite chlorophyll. Winter (win) corresponds to January to April, summer (sum) corresponds to June to September. Reanalysis product (white cells) has been evaluated for the period Jan1999-Dec2020. INTERIM product (orange cells) has been evaluated with a test simulation between 1 January – 31 December 2020.

COAST	Mod-Sat								log10(Mod)-log10(Sat)							
	RMSD				BIAS				RMSD				BIAS			
	MEDREA24		INTERIM		MEDREA24		INTERIM		MEDREA24		INTERIM		MEDREA24		INTERIM	
	win	sum	win	sum	win	sum	win	sum	win	sum	win	sum	win	Sum	win	sum
alb	0.22	0.13	0.20	0.12	0.02	-0.03	0.02	-0.03	0.22	0.17	0.23	0.19	0.08	-0.04	0.09	-0.03
swm1	0.14	0.05	0.17	0.06	0.02	-0.01	-0.01	-0.01	0.19	0.11	0.19	0.13	0.10	-0.04	0.05	-0.04
swm2	0.30	0.10	0.22	0.10	-0.02	-0.01	0.01	-0.02	0.25	0.14	0.24	0.16	0.08	-0.04	0.11	-0.04
nwm	0.23	0.11	0.26	0.12	-0.03	-0.02	-0.10	-0.02	0.19	0.13	0.19	0.14	0.02	-0.04	-0.03	-0.04
tyr1	0.30	0.09	0.30	0.11	-0.09	-0.02	-0.11	-0.03	0.24	0.17	0.25	0.20	-0.04	-0.07	-0.05	-0.08
tyr2	0.23	0.11	0.20	0.12	-0.02	-0.02	-0.03	-0.02	0.21	0.14	0.23	0.16	0.04	-0.05	0.05	-0.05
adr1	0.46	0.48	0.36	0.58	-0.12	-0.14	-0.13	-0.19	0.15	0.19	0.14	0.21	-0.04	-0.11	-0.07	-0.13
adr2	0.28	0.13	0.28	0.16	-0.09	-0.04	-0.13	-0.05	0.18	0.15	0.19	0.18	-0.05	-0.09	-0.09	-0.09
aeg	0.22	0.08	0.19	0.11	-0.04	-0.02	-0.03	-0.02	0.16	0.10	0.15	0.10	0.00	-0.04	0.01	-0.04
ion1	0.43	1.06	0.46	1.10	-0.09	-0.25	-0.10	-0.25	0.17	0.26	0.18	0.26	-0.01	-0.09	-0.02	-0.09
ion2	0.03	0.04	0.05	0.06	0.00	-0.01	0.00	-0.01	0.11	0.15	0.14	0.17	0.03	-0.04	0.01	-0.04
ion3	0.11	0.07	0.14	0.06	-0.03	-0.02	-0.04	-0.02	0.16	0.13	0.17	0.14	-0.03	-0.06	-0.04	-0.07
lev1	0.02	0.02	0.02	0.02	0.01	0.00	0.01	0.00	0.11	0.13	0.12	0.15	0.07	0.00	0.06	0.00
lev2	0.06	0.02	0.09	0.02	-0.01	-0.01	-0.03	-0.01	0.16	0.13	0.19	0.14	-0.01	-0.06	-0.06	-0.07
lev3	0.70	0.70	0.72	0.65	-0.33	-0.27	-0.35	-0.26	0.26	0.31	0.24	0.32	-0.07	-0.15	-0.10	-0.16
lev4	0.40	0.40	0.51	0.43	-0.13	-0.14	-0.21	-0.17	0.28	0.32	0.33	0.35	-0.07	-0.16	-0.15	-0.19
med	**0.26**	**0.22**	**0.26**	**0.24**	**-0.06**	**-0.06**	**-0.08**	**-0.07**	**0.19**	**0.17**	**0.20**	**0.19**	**0.01**	**-0.07**	**-0.01**	**-0.07**

Table IV.1.2. Mean RMSD and BIAS between surface (0-10 m) chlorophyll model maps and satellite maps referred to coastal areas (shallower than 200 m, Fig. III.1) over the whole simulation. On the right side, the skill indexes are computed on the log-transformed model and satellite chlorophyll. Winter (win) corresponds to January to April, summer (sum) corresponds to June to September. Reanalysis product (white cells) has been evaluated for the period Jan1999-Dec2020. INTERIM product (green cells) has been evaluated with a test simulation between 1 January – 31 December 2020

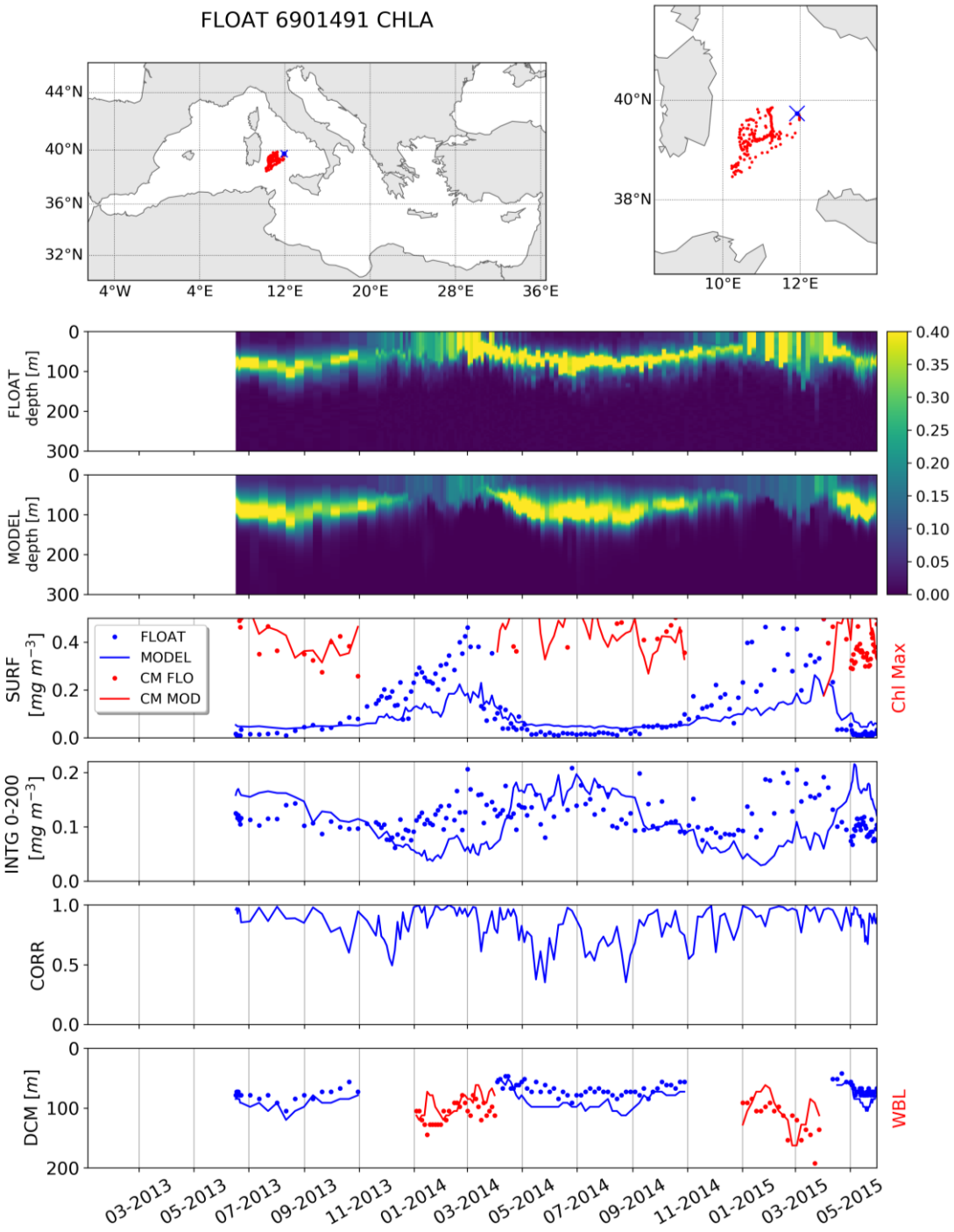

Fig. IV.1.4. Comparison between BGC-Argo floats and model (examples for three selected floats). Panels are: Trajectory of the BGC-Argo float (red dots) with deployment position (blue cross); Hovmöller diagrams of chlorophyll concentration (mg/m^3) from float data (2nd row) and model outputs (3rd row) matched-up with float position for the period of float life; selected skill indexes for model (solid line) and float data (dots): surface chlorophyll (SURF, 4th row), 0–200m vertically averaged chlorophyll (INTG, 5th row), correlation between vertical profiles (CORR, 6th row) and depth of the DCM/WBL (blue/red, 7th row) (continues overleaf).

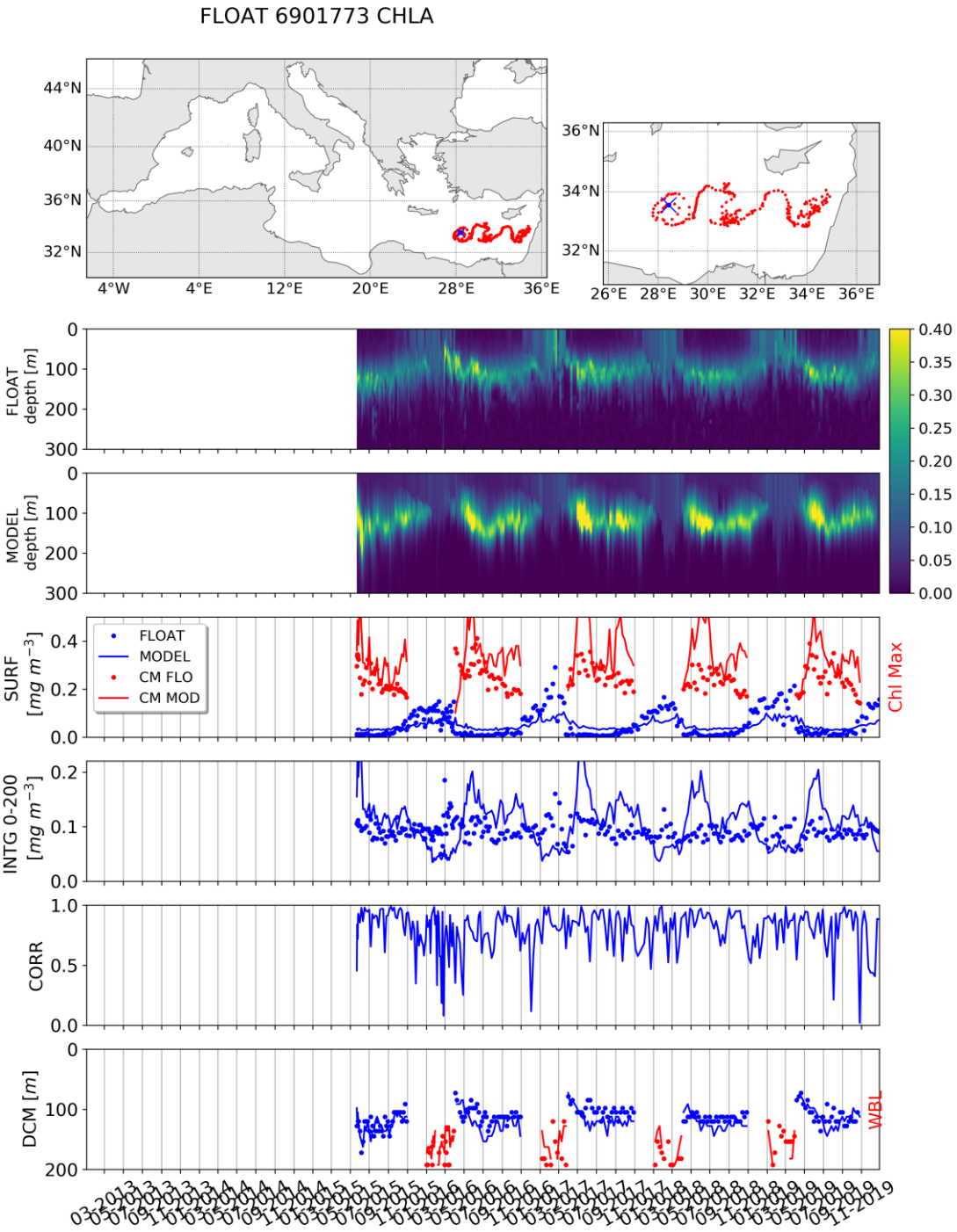

Fig. IV.1.4. Same as above.

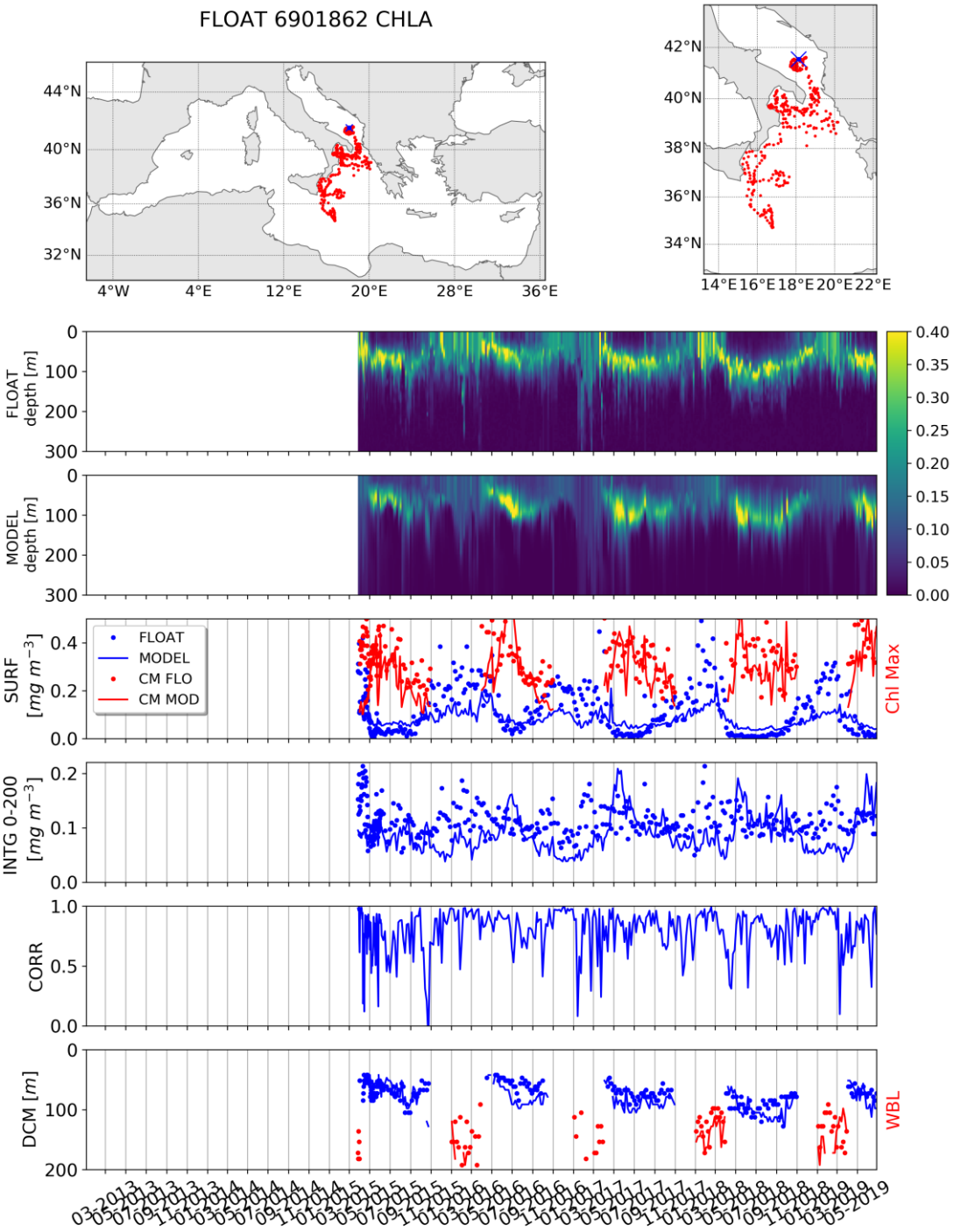

Fig. IV.1.4. Same as above

		BIAS					RMSD				
		0-10 m	10-30 m	30-60 m	60-100 m	100-150 m	0-10 m	10-30 m	30-60 m	60-100 m	100-150 m
alb	REA24	0.04	0.07	0.11	0.11	0.01	0.11	0.13	0.20	0.17	0.07
	INTERIM	-	-	-	-	-	-	-	-	-	-
swm	REA24	-0.06	-0.06	-0.07	0.03	0.03	0.10	0.10	0.13	0.11	0.06
	INTERIM	-0.03	-0.03	-0.12	-0.02	0.07	0.07	0.07	0.17	0.13	0.09
nwm	REA24	-0.12	-0.12	-0.12	-0.01	0.00	0.17	0.18	0.23	0.12	0.06
	INTERIM	-0.07	-0.08	-0.10	-0.02	0.01	0.12	0.13	0.15	0.12	0.10
tyr	REA24	-0.04	-0.04	-0.04	-0.02	0.03	0.07	0.08	0.09	0.10	0.07
	INTERIM	0.05	0.05	0.05	0.05	0.03	0.05	0.05	0.05	0.05	0.03
adr	REA24	-0.02	-0.03	-0.05	-0.09	-0.03	0.06	0.07	0.09	0.10	0.04
	INTERIM	0.07	0.07	0.08	0.14	0.04	0.07	0.07	0.08	0.14	0.04
ion	REA24	-0.03	-0.03	-0.03	-0.02	0.03	0.06	0.06	0.07	0.08	0.08
	INTERIM	0.04	0.04	0.05	0.07	0.10	0.04	0.04	0.05	0.07	0.10
lev	REA24	-0.01	-0.01	-0.01	0.00	0.04	0.05	0.05	0.07	0.09	0.10
	INTERIM	0.06	0.06	0.07	0.09	0.11	0.06	0.06	0.07	0.09	0.11

Table IV.1.3. Time averaged BIAS and RMSD of chlorophyll (mg/m^3) for selected layers and aggregated sub-basins for the period 2013-2019. Statistics are computed using the match-ups of model with BGC-Argo float data. INTERIM product (green cells) has been evaluated between 1 January – 31 December 2020 using the same metrics.

	CORR	Average 0-200 m [mg/m^3]		Depth of the deep chlorophyll maximum [m]		Depth of the vertically mixed bloom in winter [m]		Average number of available profiles per month
		BIAS	RMSD	BIAS	RMSD	BIAS	RMSD	
alb	0.77	0.03	0.12	-2	5	32	32	1
swm	0.78	-0.01	0.05	12	20	16	32	8
nwm	0.82	-0.05	0.12	9	14	9	38	23
tyr	0.86	0	0.06	11	17	1	24	7
adr	0.82	-0.03	0.05	1	15	-10	24	5
ion	0.79	0	0.06	7	17	1	28	22
lev	0.78	0.01	0.05	10	21	-14	30	22

Table IV.1.4. Time averages of the chlorophyll ecosystem indicators based on the BGC-Argo floats and model comparison 2013-2019.

IV.2 Net primary production

Net primary production (NPP) is the measure of the net uptake of carbon by phytoplankton groups (gross primary production minus fast release processes – e.g. respiration). The lack of any extensive dataset of measures of primary production prevents the computation of quantitative metrics for the assessment of the quality of this product. Thus, the product quality consists of an assessment of the consistency (i.e., class1 metrics) of the modelled NPP with previous estimations published in scientific literature (Fig. IV.2.1 and Tab. IV.2.1). Averaged NPP values in the different sub-basins are consistent with basin-wide estimations (maps of Fig. 8 in Lazzari et al., 2012 and of Fig. 13 in Bosc et al., 2004) and with published values for the reference subbasins (Tab. IV.2.1). A slight overestimation in the eastern sub-basins is observed.

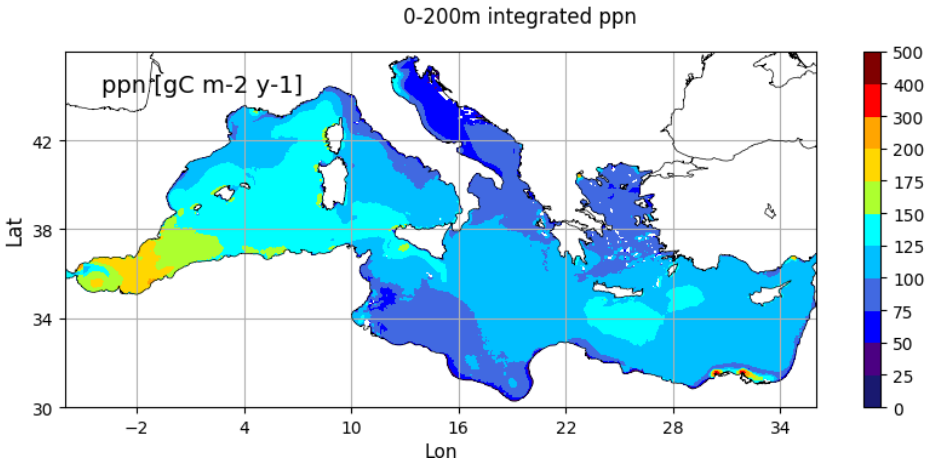

Fig. IV.2.1. Net primary production integrated in the 0-200 m depth in the period 1999-2019.

	MODEL Lazzari et al. (2012)	SATELLITE Colella (2006)	IN-SITU ESTIMATES Siokou-Frangou et al., 2010 (Reported in Table 1, only in-situ estimates)		CMEMS Reanalysis: 1999-2019
	Annual mean [gC/m²/y]	Annual mean [gC/m²/y]	Annual mean [gC/m²/y]	Short term estimates [mgC/m³/d]	Annual mean [gC/m²/y]
Mediterranean Sea (MED)	98±82	90±48			111
Alboran Sea (ALB)	274±155	179±116		353–996; May-Jun1996 142; Nov2003	171
South West Med –West (SWM1)	160±89	113±43		186–636 (avg. 440) Oct1996	148
South West Med –East (SWM2)	118±70	102±38			138
North West Med (NWM)	116±79	115±67	105.8-119.6 86-232 (only DYFAMED station) 140-170 (South Gulf of Lion)	353–996; May–Jun1996 401; Mar-Apr1998 (G. Lion) 166; Jan-Feb1999 (G. Lion) 160–760; May-Jul (Cat-Bal) 150–900; Apr1991 (Cat-Bal) 450, 700; Jun1993 (Cat-Bal) 210, 250; Oct1992 (Cat-Bal) 1000±71 Mar1999 (Cat-Bal) 404±248 Jan-Feb00 (Cat-Bal)	122
Levantine (LEV1+LEV2+LEV3+LEV4)	76±61	72±21	59 (Cretan Sea)		113
Ionian Sea (ION1+ION2+ION3)	77±58	79±23	61.8	119–419; May-June 1996 208–324; April-May 1999 186±65; August 1997-98	98
Tyrrhenian Sea (TYR1 + TYR2)	92±5	90±35		398; May–Jun1996 273; Jul2005 429; Dec2005	110

Table IV.2.1. Annual averages and short period estimates of the vertically integrated primary production for some selected sub-regions. Estimates are from multi-annual simulations (Lazzari et al., 2012), from satellite model (Colella, 2006), from in-situ estimates (Siokou-Frangou et al., 2010) and from the present CMEMS reanalysis.

IV.3 Phytoplankton biomass

In the CMEMS catalogue the unit of phytoplankton carbon biomass is [mmol m-3]. In this document, the phytoplankton carbon biomass is the content of carbon (mgC/m^3) in phytoplankton cells. The BFM model, featured by the MedBFM reanalysis system, simulated 4 phytoplankton functional groups and variable chlorophyll to carbon ratio, which depends on photoacclimatation and balance between synthesis and loss terms (Lazzari et al., 2012). Thus, phytoplankton biomass along with chlorophyll should be accounted for studying the evolution and variability of the primary producer biomass.

The accuracy of the phytoplankton biomass is assessed by class4 metrics using BGC-Argo floats optical data. Observations for biomass of phytoplankton (PhytoC) are retrieved from particulate backscattering coefficient at 700nm (bbp700) data using Bellacicco et al. (2019) relationship. Statistics

of RMSD and BIAS are summarized in Table IV.3.1 for aggregated sub-basins and 5 layers. Higher errors are depicted in surface and subsurface layers where biomass values are higher (Fig. IV.3.1). Statistics computed for the comparison of vertical profiles (Table IV.3.2) show that the shape of profiles is reproduced with a correlation always higher than 0.6 except for ADR and that the 0-200m averaged values are reproduced with an accuracy of around 2 mg/m^3 over values ranging between 2 and 3.5 mg/m^3 for the vertical averaged phytoplankton biomass. It should be noted that, given the not full maturity of the conversion relationship and of quality control for these optical measurements, the level-2 validation framework should be cautiously accounted.

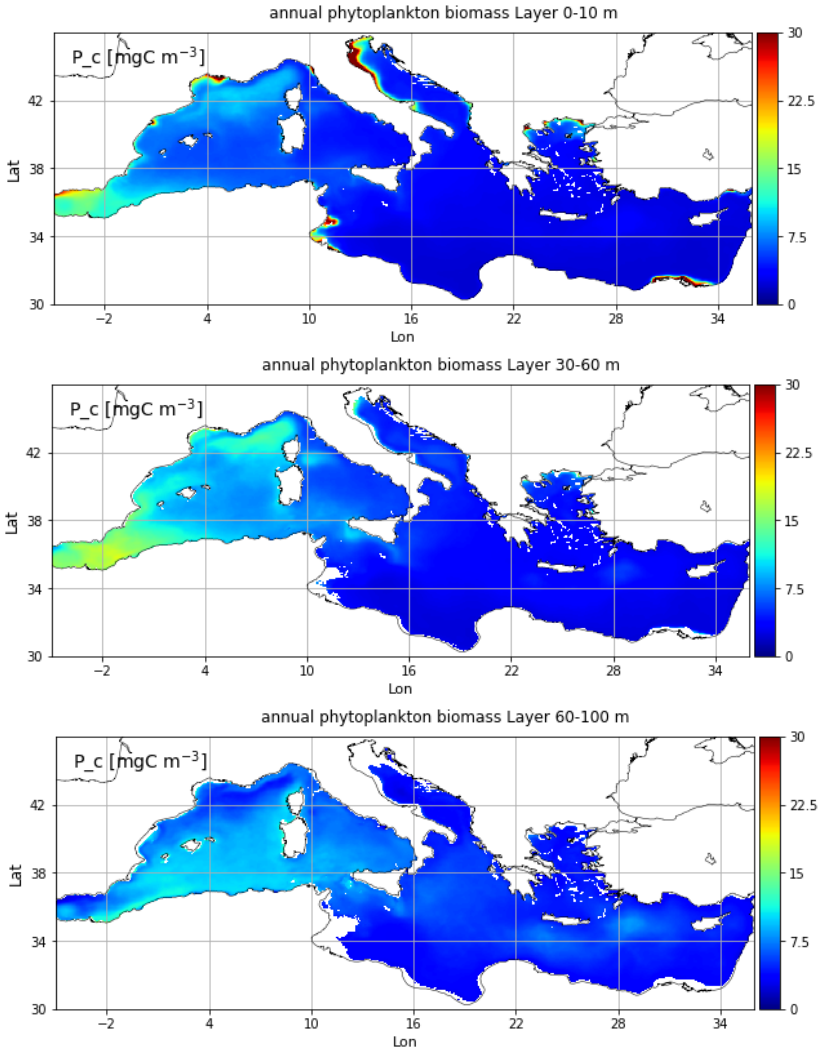

Fig. IV.3.1. Averaged mean annual map of phytoplankton biomass (mg/m^3) for three selected layers over the full simulation period (1999-2019).

	BIAS					RMSD				
	0-10 m	10-30 m	30-60 m	60-100 m	100-150 m	0-10 m	10-30 m	30-60 m	60-100 m	100-150 m
alb	3.17	1.24	2.44	2.39	-0.98	3.17	2.90	2.44	2.39	1.89
swm	0.74	0.94	1.28	0.16	-0.48	1.93	1.77	1.85	1.41	0.85
nwm	0.08	0.26	0.97	0.46	0.01	2.16	2.01	2.13	1.83	1.14
tyr	0.42	0.39	0.81	1.06	0.06	1.88	1.69	1.77	2.03	1.18
adr	-0.26	0.44	1.75	1.14	0.09	2.09	1.51	2.24	1.67	0.74
ion	-0.27	-0.20	-0.05	1.00	0.52	1.53	1.28	1.30	1.86	1.44
lev	-0.10	-0.08	0.05	0.88	0.97	1.39	1.19	1.31	1.90	1.88

Table IV.3.1. Time averaged BIAS and RMSD of phytoplankton biomass (mg/m^3) for selected layers and aggregated sub-basins for the period 2013-2019. Statistics are computed using the match-ups of model with BGC-Argo float data.

	CORR	Average 0-200 m [mg/m^3] (model on matchup positions)	Average 0-200 m [mg/m^3]		Average number of available profiles per month
			BIAS	RMSD	
alb	0.88	-	2.46	3.72	2
swm	0.89	3.53	1.26	3.02	9
nwm	0.86	3.33	1.31	3.09	26
tyr	0.8	2.57	0.16	1.04	9
adr	0.57	2.22	1.07	2	5
ion	0.68	2.54	0.8	2.04	23
lev	0.70	2.13	0.05	1.15	23

Table IV.3.2. Time averages of the phytoplankton biomass ecosystem indicators based on the BGC-Argo floats and model comparison 2013-2019.

IV.4 Phosphate

Phosphate accuracy is assessed by two validation levels. Class1 metrics (level 1) validation consists of the comparison between model average vertical profiles and the reference climatological profiles (Figures IV.13.1-16 in appendix A) and of the skill performance statistics computed using the 16 sub-basins climatological values and the corresponding model annual means (Table IV.4.1). Class4 metrics (level 2) validation consists of the density plots (Fig. IV.4.1) and profiles plots (Fig. IV.4.2) built on the space and time matchup of in situ observations and model daily output. Validation statistics of the 16 sub-basins and 8 depths for the open sea and coastal areas are then reported in Tab. IV.4.2.

The reanalysis shows good performances in reproducing basin-wide gradients and sub-basin values (Fig. IV.13.1-16, Table IV.4.1). Larger uncertainty values are for the deepest layer (Table IV.4.1). Considering class 4 metrics, the uncertainty increase with mean RMSD values is almost double than those for computed for class 1 metrics especially in the western sub-basins. As expected, predicting mesoscale dynamics (i.e., at the 1/24° horizontal resolution) and the daily variability can be achieved by the MedBFM model with a lower accuracy than that for the simulation of mean annual values and mean spatial gradients.

Modelled subsurface layers (i.e., below 300 m) show a systematic slight underestimation (Tab. IV.4.1 and Fig. IV.4.2).

Error in coastal areas are roughly 20-40% higher than in off-shore areas given the much higher variability in simulating coastal dynamics (Tab. IV.4.2).

	Phosphate		
Layer depth	**BIAS**	**RMSD**	**CORR**
0-10 m	-0.01	0.03	0.43
10-30 m	-0.01	0.02	0.36
30-60 m	-0.01	0.02	0.76
60-100 m	-0.01	0.03	0.91
100-150 m	0.02	0.04	0.90
150-300 m	0.01	0.03	0.96
300-600 m	-0.06	0.07	0.98
600-1000 m	-0.07	0.07	0.97

Table IV.4.1 Skill metrics for the comparison of phosphate with respect to climatology in open sea. Model average and climatology refers to the period covered by observations (i.e., 1999-2016).

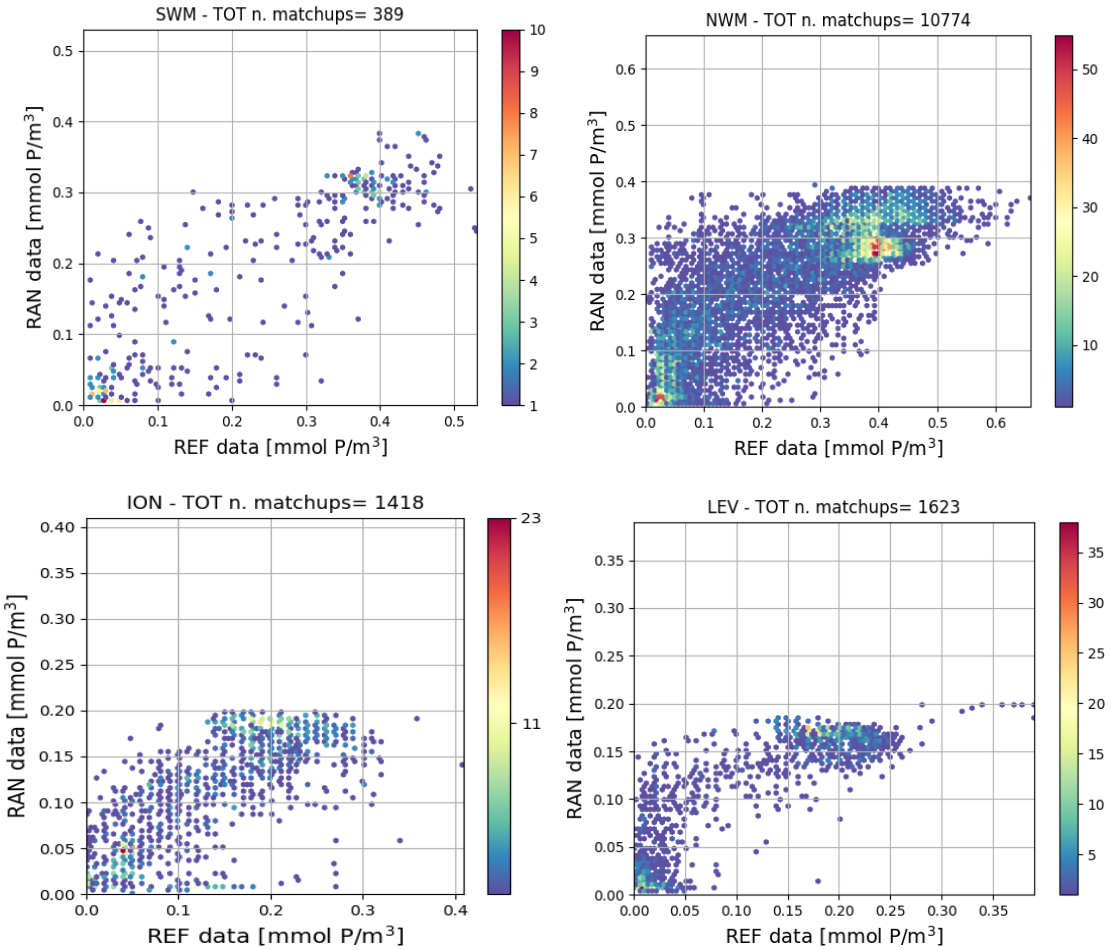

Figure IV.4.1. Density plots of model (RAN, y-axis) and reference (REF, x-axis) matchups of phosphate (mmol P/m^3) for SWM, NWM, ION and LEV.

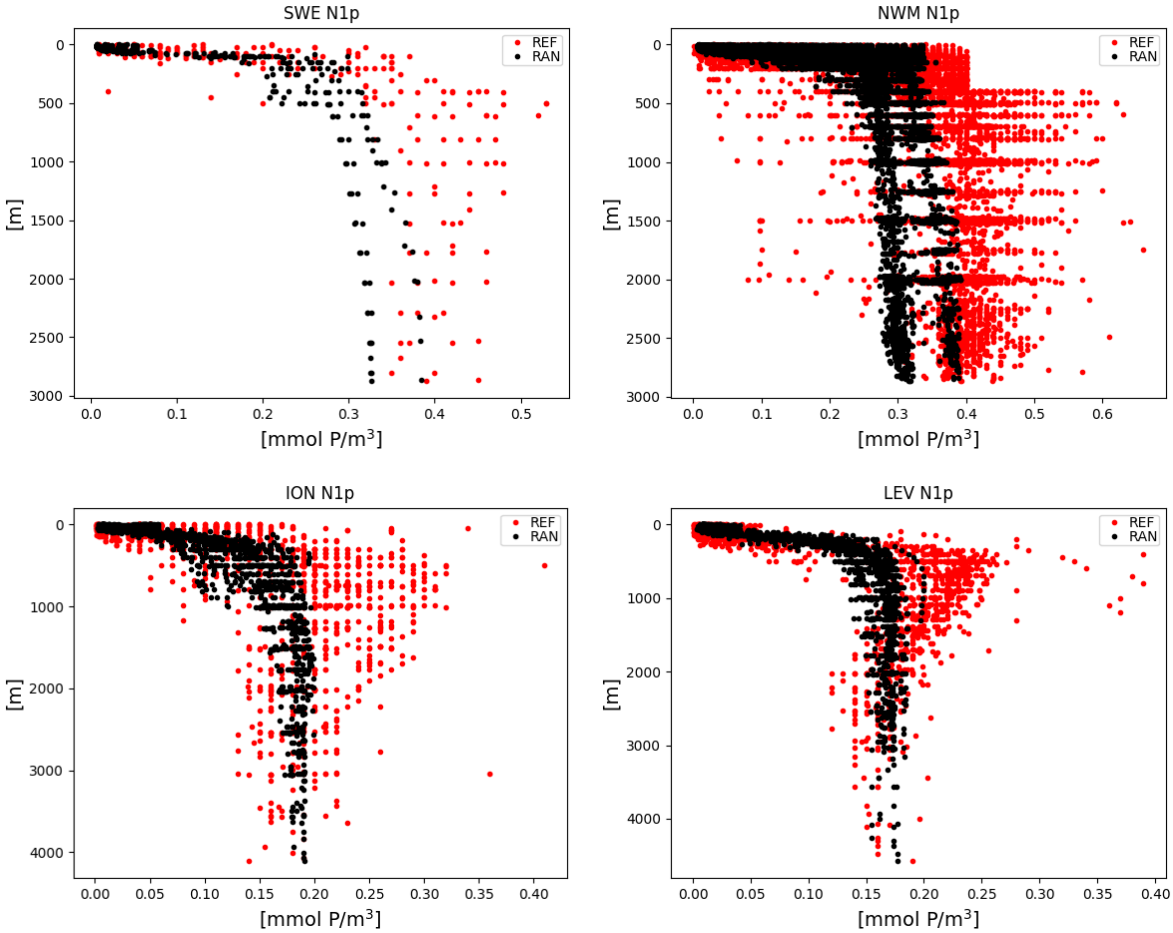

Figure IV.4.2 Vertical profiles of phosphate (mmol P/m^3) for reanalysis (RAN; black) and reference dataset (REF; red) for SWE, NWM, ION and LEV in open sea.

	Open Sea									Coast		
	RMSD							CORR	n. profiles/ matchups	RMSD		n. profiles/ matchups
Layer [m]	0-30	30-60	60-100	100-150	150-300	300-600	600-1000			0-60	60-200	
ALB	0.03	0.06	0.08	0.06	0.06	0.13	0.10	0.94	6/54	-	-	0/0
SWM1	0.01	0.09	0.11	0.10	0.08	0.10	0.10	0.83	7/69	-	-	0/0
SWM2	0.08	0.07	0.10	0.10	0.08	0.15	0.12	0.81	34/242	0.09	0.05	10/48
NWM	0.07	0.08	0.09	0.08	0.09	0.11	0.11	0.81	1051/8531	0.09	0.07	274/1428
TYR1	0.02	0.01	0.02	0.12	0.11	0.08	-	0.80	13/63	-	-	0/0
TYR2	0.03	0.04	0.05	0.06	0.08	0.08	0.05	0.88	13/123	-	-	0/0
ADR1	-	-	-	-	-	-	-	-	0/0	-	-	0/0
ADR2	0.04	0.03	0.05	0.02	0.05	0.07	0.06	0.68	22/225	0.05	-	2/7
AEG	0.02	0.02	0.02	0.03	0.04	0.04	0.05	0.77	66/503	0.03	0.02	37/175
ION1	0.02	0.02	0.02	0.04	0.04	0.07	0.06	0.91	6/70	-	-	0/0
ION2	0.02	0.02	0.03	0.05	0.05	0.06	0.06	0.88	41/360	-	-	0/0
ION3	0.07	0.09	0.08	0.03	0.05	0.08	0.09	0.59	73/652	0.09	0.09	29/141
LEV1	0.02	0.02	0.05	0.07	0.07	0.06	0.06	0.80	38/296	-	-	0/0
LEV2	0.02	0.01	0.01	0.04	0.06	0.05	0.06	0.81	19/171	-	-	0/0
LEV3	0.01	0.02	0.01	0.04	0.08	0.07	0.06	0.81	20/163	-	-	0/0
LEV4	0.02	0.02	0.02	0.03	0.05	0.07	0.06	0.91	91/565	0.02	0.02	26/101
MED average	0.03	0.04	0.05	0.06	0.06	0.08	0.07					

Table IV.4.2. Mean RMSD between phosphate model outputs and EMODnet2018_int dataset computed at the in situ observation locations. The metric is calculated for selected layers (0-30 m, 30-60 m, 60-100 m, 100-150 m, 150-300 m, 300-600 m, 600-1000 m for open sea and 0-60 m and 60-200 m for coastal areas), and averaged over the whole reanalysis period (1999-2019). The overall correlation between observations and model output is also reported (for open sea) with references of n. of profiles and matchups available for open sea and coastal areas. MED average is obtained as the mean od RMSD of all the subbasins with more than 5 profiles in open sea.

IV.5 Nitrate

Nitrate accuracy is assessed by three validation levels. Basin scale (Level 1) validation is shown in Figures IV.13.1-16 (Appendix A; comparison between model average vertical profiles and the reference climatological profiles) and summarized in statistics of Table IV.5.1. Figures IV.5.1 and IV.5.2 (density and profile plots) report the point-to-point class4 comparison that is summarized in statistics of Table IV.5.2. Additionally, the level 3 validation (Fig. IV.5.3) shows, for selected floats, the comparison of observations and model daily output and the computation of the process-based metrics (i.e., depth of nitracline as defined in Salon et al., 2019, and mean values at surface and in the euphotic layer) along the float trajectory. Considering all available BGC-Argo floats in the period 2014-2019, validation statistics of the RMSD of the observation are reported in Table IV.5.3 for selected aggregated sub-basin and layers. Validation statistics of the process-based nitrate metrics are reported in Table IV.5.4.

The reanalysis shows a good performance in surface layers: the RMSD is on average lower than 1 mmol/m^3 for the climatological (Tab. IV.5.1), the daily in situ (Tab. IV.5.2) and the float (Tab. IV.5.3) comparison in the layer between 0 to 60 m. Greater errors are shown for western sub-basins (Tab. IV.5.2) showing some model deficiency in capturing surface mesoscale and daily spatial patterns.

For the INTERIM 2020 product, statistics are in line with those calculated for the reanalysis (Tab. IV.5.2). A general improvement is seen in all basins except for Tyrrhenian and Adriatic Seas, however the low number of available BGC-Argo floats in 2020 might have affected the statistics significance.

The evolution of nitracline depth is simulated with an accuracy of 30-45 m excluding subbasins with less than 2 profiles per month (Tab. IV.5.4).

An underestimation of 1-2 mmol/m^3 in the mesopelagic layers (below 300m) of the western sub-basins affects the model accuracy both at the level of class1 validation (Tab. IV.5.1) and of the daily class4 validation (Tab. IV.5.2).

	Nitrate		
Layer depth	**BIAS**	**RMSD**	**CORR**
0-10 m	0.22	0.34	0.71
10-30 m	0.33	0.43	0.51
30-60 m	0.20	0.56	0.47
60-100 m	0.03	0.84	0.79
100-150 m	0.31	0.91	0.86
150-300 m	-0.15	0.94	0.91
300-600 m	-1.35	1.66	0.90
600-1000 m	-1.50	1.68	0.91

Table IV.5.1 Skill metrics for the comparison of nitrate with respect to climatology in open sea. Model average and climatology refers to the period covered by observations (i.e., 1999-2016).

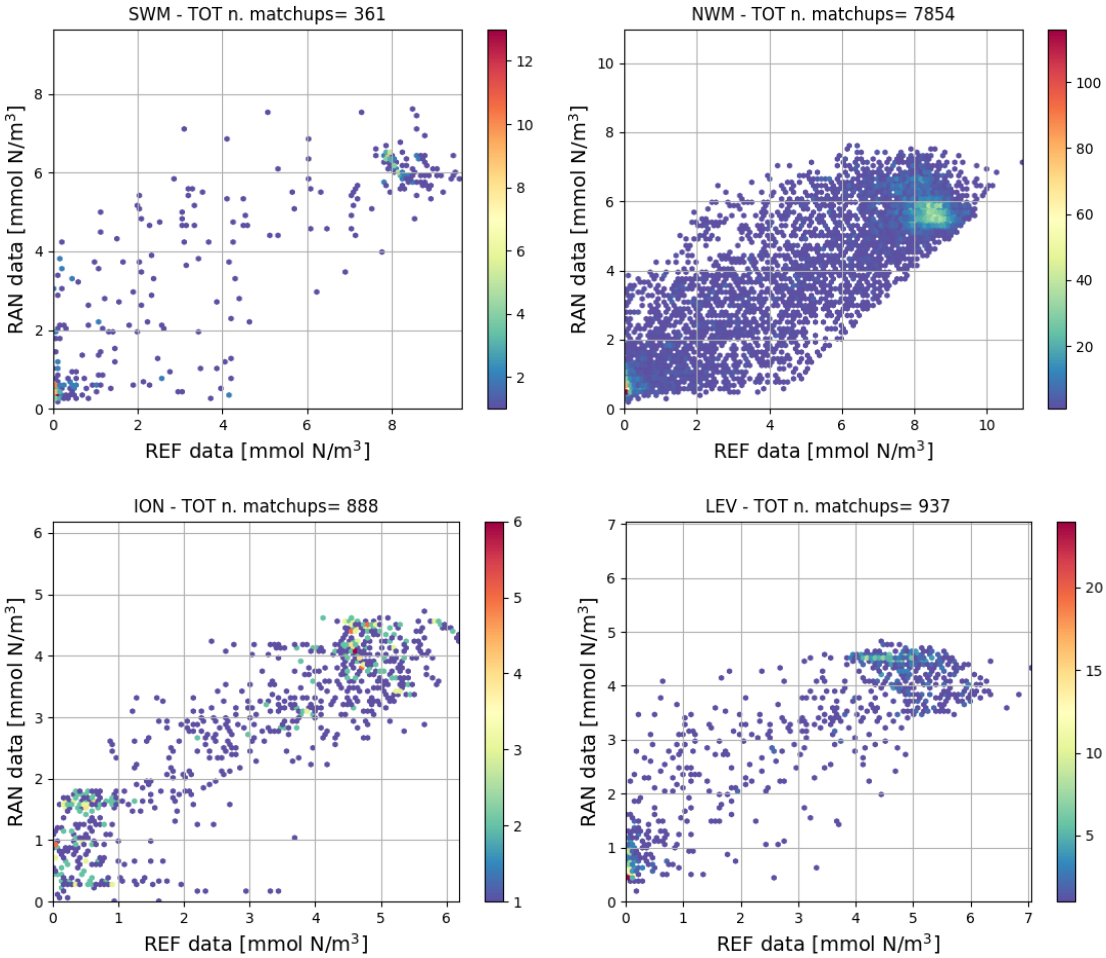

Figure IV.5.1. Density plots of model (RAN, y-axis) and reference (REF, x-axis) matchups of nitrate (mmol N/m^3) for SWM, NWM, ION and LEV.

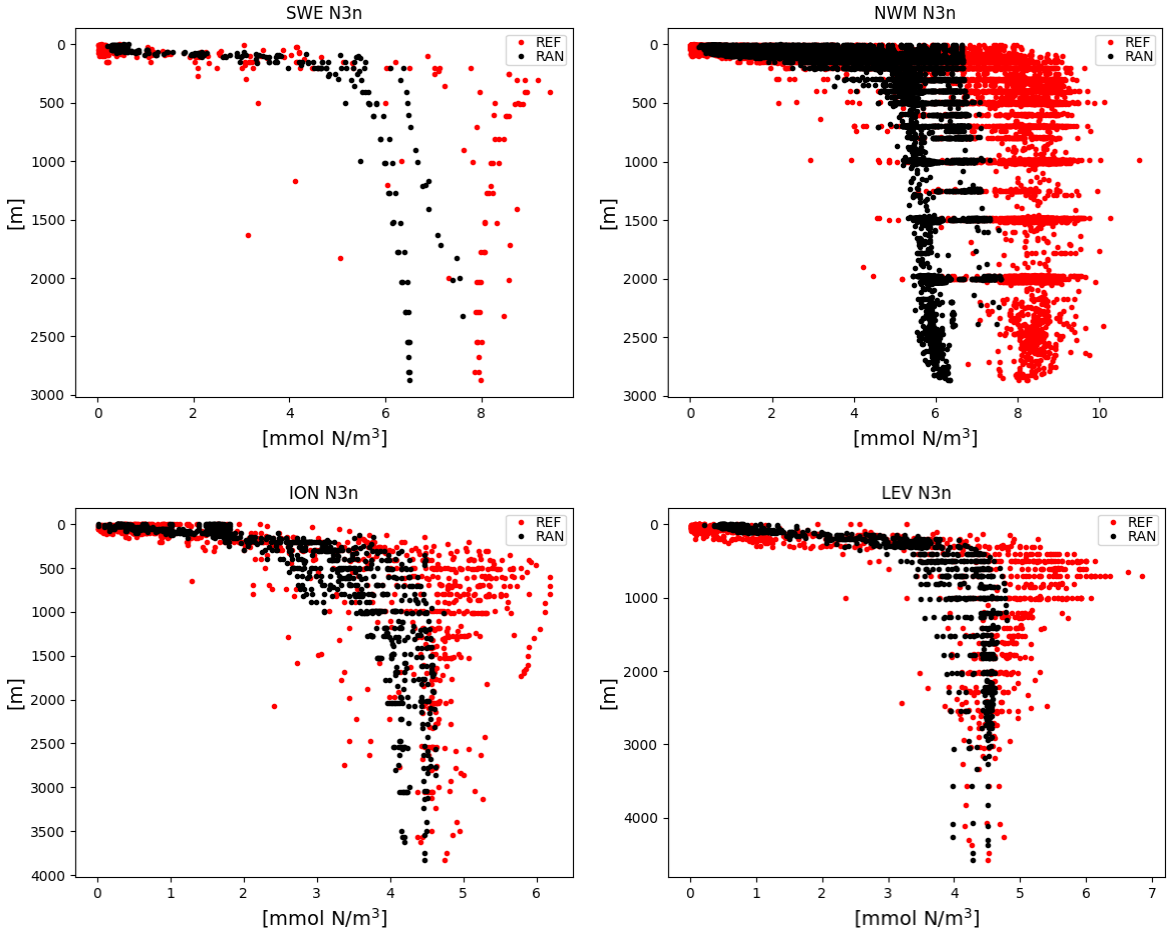

Figure IV.5.2. Vertical profiles of nitrate (mmol N/m^3) for reanalysis (RAN; black) and reference dataset (REF; red) for SWW, NWM, ION and LEV in open sea.

	Open Sea									Coast		
	RMSD							CORR	n. profiles/ matchups	RMSD		n. profiles/ matchups
Layer [m]	0-30	30-60	60-100	100-150	150-300	300-600	600-1000			0-60	60-200	
ALB	0.19	1.43	2.86	1.94	2.55	3.57	3.31	0.93	6/45	--	-	0/0
SWM1	0.35	1.80	1.43	1.64	2.26	2.77	2.56	0.90	7/74	-	-	0/0
SWM2	0.94	0.74	1.86	2.28	2.18	2.74	2.15	0.80	36/213	0.81	1.61	11/47
NWM	1.19	1.38	1.72	1.84	2.22	2.57	2.45	0.87	782/6338	2.01	1.31	146/616
TYR1	-	-	0.56	1.32	1.54	2.53	-	0.91	14/64	-	-	0/0
TYR2	0.66	1.48	1.27	1.61	1.98	1.91	1.16	0.90	12/115	1.11	1.07	5/18
ADR1	-	-	-	-	-	-	-	-	0/0	-	-	0/0
ADR2	1.00	0.96	0.90	0.84	0.68	1.27	1.96	0.74	5/52	-	-	1/1
AEG	1.04	0.70	1.10	0.77	1.06	1.06	0.69	0.71	34/258	0.96	0.89	32/178
ION1	0.10	-	0.34	-	0.64	1.41	1.38	0.98	3/34	-	-	0/0
ION2	0.41	0.74	0.67	1.01	0.94	1.18	1.25	0.94	17/178	-	-	0/0
ION3	0.96	0.96	0.95	0.70	0.69	1.35	1.16	0.84	61/482	0.98	1.21	29/138
LEV1	0.53	0.62	0.80	1.07	1.23	1.06	1.09	0.90	23/226	-	-	0/0
LEV2	0.62	0.55	0.81	0.99	1.35	1.17	1.47	0.89	26/256	-	-	0/0
LEV3	0.58	0.54	0.73	0.98	1.32	1.45	1.30	0.89	7/64	-	-	0/0
LEV4	0.72	0.65	0.90	1.02	1.46	1.45	1.42	0.89	20/176	-	-	0/0
MED average	0.71	0.96	1.18	1.29	1.53	1.86	1.69					

Table IV.5.2. Mean RMSD between nitrate model outputs and EMODnet2018_int dataset computed at the in situ observation locations. The metric is calculated for selected layers (0-30 m, 30-60 m, 60-100 m, 100-150 m, 150-300 m, 300-600 m, 600-1000 m for open sea and 0-60 m and 60-200 m for coastal areas), and averaged over the whole reanalysis period (1999-2019). The overall correlation between observations and model output is also reported (for open sea) with references of n. of profiles and matchups available for open sea and coastal areas. MED average is obtained as the mean od RMSD of all the subbasins with more than 5 profiles in open sea.

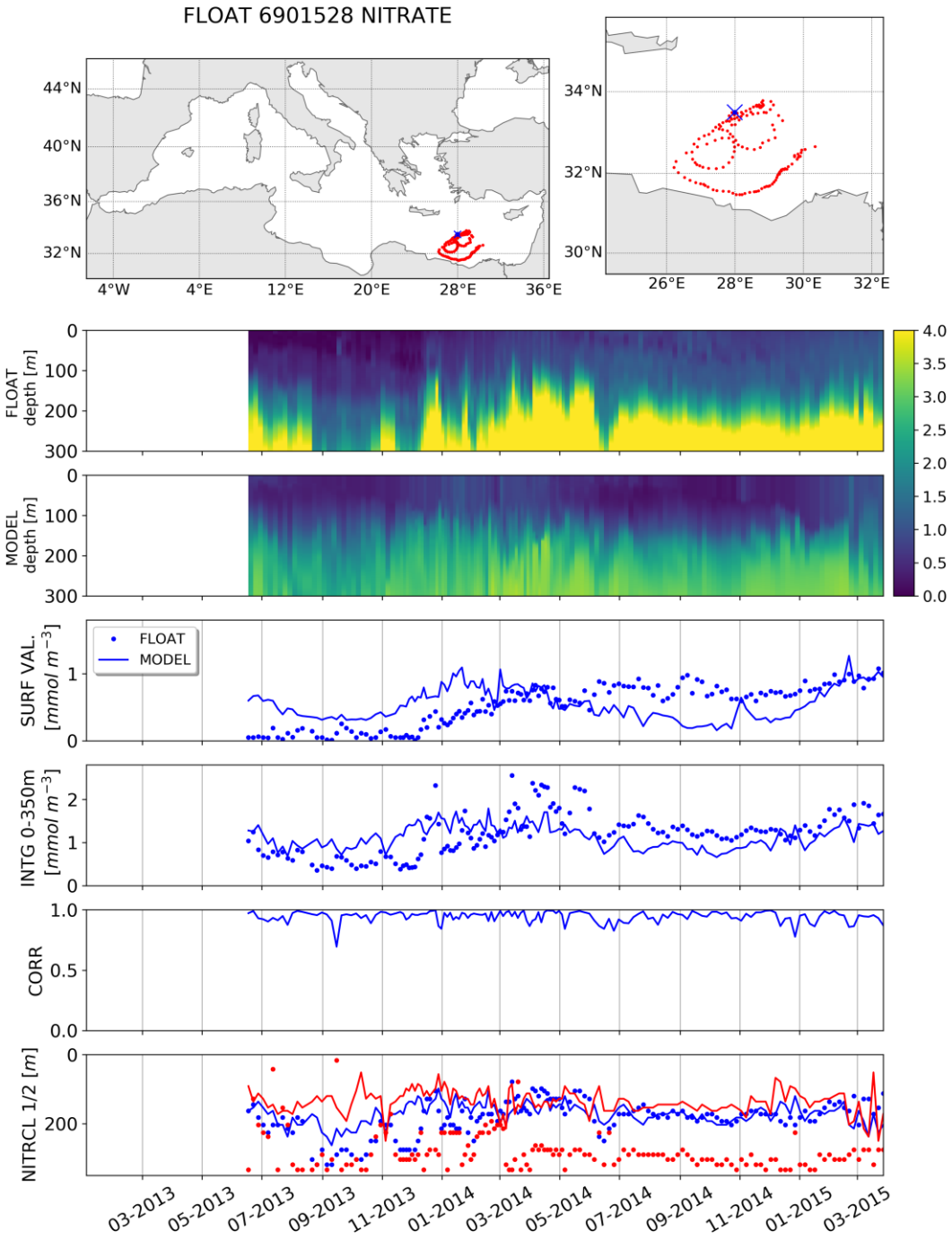

Fig. IV.5.3. Comparison between BGC-Argo floats and model (examples for two selected floats). Panels are: Trajectory of the BGC-Argo float (red dots) with deployment position (blue cross); Hovmöller diagrams of nitrate concentration (mg/m^3) from float data (2nd row) and model outputs (3rd row) matched-up with float position for the period of float life; selected skill indexes for model (solid line) and float data (dots): surface nitrate (SURF, 4th row), 0–350m vertically averaged nitrate (INTG, 5th row), correlation between vertical profiles (CORR, 6th row) and depth of the nitracline (NITRCL 1/2, 7th row).

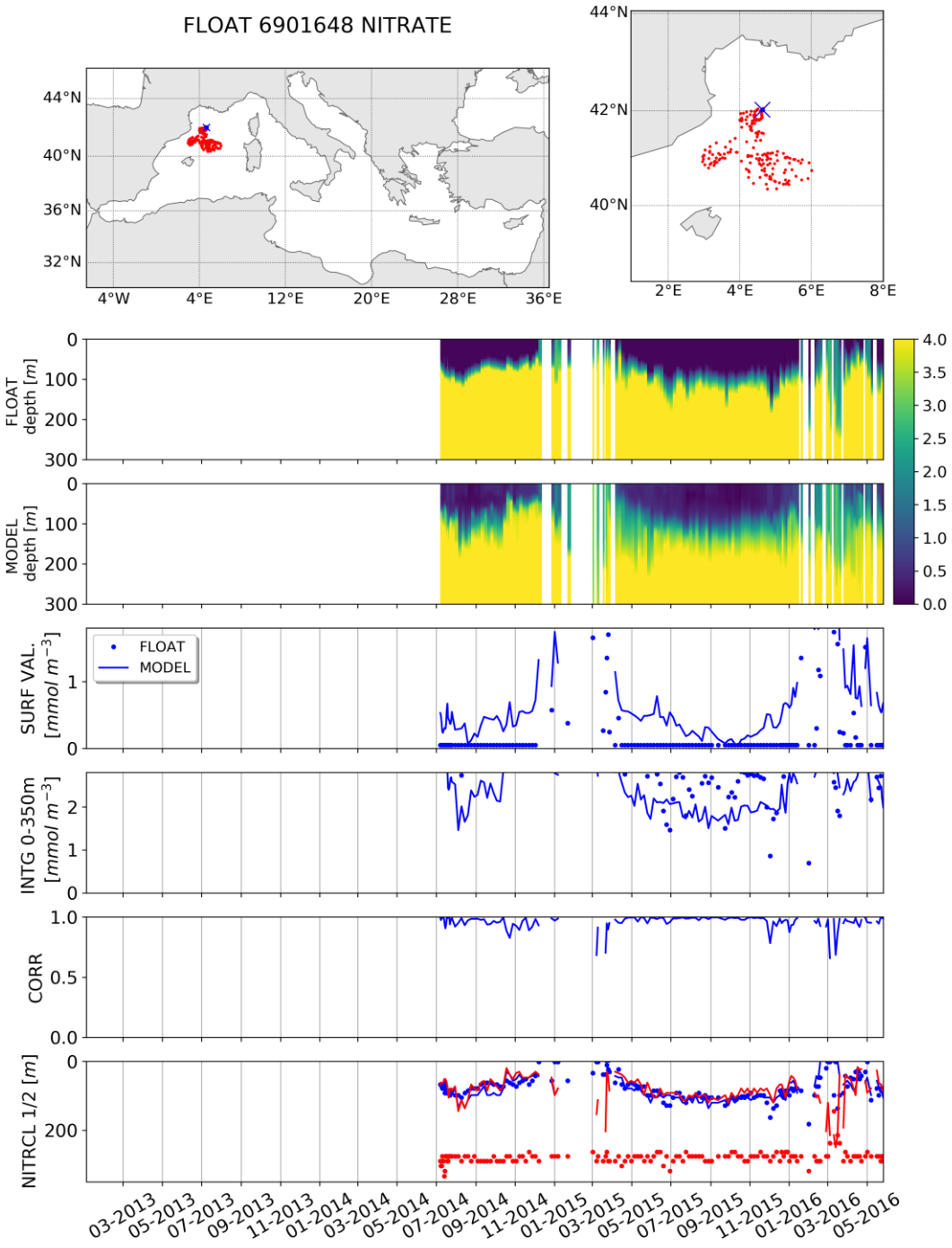

Fig. IV.5.3. Same as above.

Layer depth (m)	0-10		10-30		30-60		60-100		100-150		150-300		300-600		600-1000	
	BIAS															
	R24	INT	R24	INT	R24	INT	R24	INT	R24	INT	R24	INT	R24	INT	R24	INT
alb	-	-	-	-	-	-	-	-	-	-	-	-	-	-	-	-
swm	0.57	-	0.52	-	0.22	-	-0.11	-	-0.73	-	-0.77	-	-1.11	-	-1.66	-
nwm	0.59	0.28	0.51	0.23	0.19	0.06	-0.46	-0.72	-1.09	-1.66	-1.83	-0.88	-1.76	-1.77	-2.32	-2.53
tyr	0.08	0.92	0.03	0.92	-0.12	0.92	-0.48	1.14	-1.09	1.36	-1.70	0.33	-1.50	-1.57	-1.33	-1.48
adr	-0.53	-0.77	-0.31	-0.76	-0.30	-0.88	-0.58	-1.20	-0.96	-1.60	-1.40	-1.93	-1.86	-2.08	-3.05	-2.23
ion	0.23	0.26	0.23	0.27	0.26	0.30	0.39	0.38	0.39	0.30	-0.11	-0.50	-0.92	-1.63	-2.37	-2.39
lev	0.59	0.03	0.56	-0.02	0.47	-0.15	0.50	-0.29	0.68	-0.73	0.23	-1.12	-0.61	-1.09	-1.92	-1.46
	RMSD															
	R24	INT	R24	INT	R24	INT	R24	INT	R24	INT	R24	INT	R24	INT	R24	INT
alb	-	-	-	-	-	-	-	-	-	-	-	-	-	-	-	-
swm	0.57	-	0.52	-	0.37	-	0.84	-	1.71	-	1.05	-	1.11	-	1.66	-
nwm	0.63	0.37	0.58	0.31	0.54	0.32	0.98	1.01	1.53	1.78	1.85	0.88	1.76	1.77	2.32	2.53
tyr	0.50	0.93	0.46	0.92	0.46	0.92	0.81	1.15	1.30	1.37	1.73	0.40	1.50	1.57	1.33	1.48
adr	0.60	0.77	0.45	0.76	0.47	0.88	0.71	1.20	1.06	1.60	1.41	1.93	1.86	2.08	3.05	2.23
ion	0.49	0.39	0.45	0.36	0.41	0.37	0.55	0.49	0.78	0.70	0.84	0.76	1.05	1.65	2.37	2.40
lev	0.63	0.43	0.61	0.46	0.53	0.55	0.59	0.77	0.90	1.24	1.00	1.49	1.21	1.10	1.92	1.46

Table IV.5.3 Averaged BIAS and RMSD of nitrate w.r.t. BGC-Argo floats for the layers of Tab. III.1, aggregated sub-basins (nwm, swm = swm1+sm2, tyr = tyr1+tyr2, ion = ion1+ion2+ion3, lev = lev1+lev2+lev3+lev4). INTERIM product (green cells) has been evaluated between 1 January – 31 December 2020 using the same metrics.

	CORR	mean nitrate concentration 0-350m [mmol/m^3]		Depth of the nitracline [m]		Average number of profiles per month
		BIAS	RMSD	BIAS	RMSD	
alb	-	-	-	-	-	< 1
swm	0.94	0	0.92	-3	43	< 1
nwm	0.97	-0.63	1.06	-7	32	7
tyr	0.95	-0.81	1.17	12	31	6
adr	0.82	-0.8	0.93	91	108	1
ion	0.92	0.25	0.76	9	45	9
lev	0.88	0.71	0.85	-10	32	15

Table IV.5.4. Averages of the monthly nitrate indicators plotted in Figure IV.5.2 during the period January 2013- December 2019. The indicators are the correlation between model and BGC-Argo float data, the BIAS and RMSD of the vertically 0-350 m averaged nitrate concentration, the BIAS and RMSD of the depth of the nitracline (depth of nitrate concentration reaching 2 mmol/m^3). Statistics are computed for selected aggregated sub-basins.

IV.6 Dissolved Oxygen

Dissolved Oxygen accuracy is assessed by three validation levels. Basin scale (Level 1) validation is shown in Figures IV.13.1-16 (Appendix A; comparison between model average vertical profiles and the reference climatological profiles) and summarized in statistics of Table IV.6.1. Figures IV.6.1 and IV.6.2 (density and profile plots) report the point-to-point class4 comparison that is summarized in statistics of Table IV.6.2. Additionally, the level 3 validation (i.e., process-based metrics based on BGC-Argo float comparison; Fig. IV.6.3) shows, for selected floats, the comparison of observations and model daily output and the computation of the specific metrics (i.e., mean surface, mean 0-200 m and depth of maximum Dissolved Oxygen in the layer 0-200m) along the float trajectory. Considering all available BGC-Argo floats in the period 2013-2019, model-observation RMSD statistics are reported in Table IV.6.3 for selected aggregated sub-basins and layers; while specific Dissolved Oxygen metrics are reported in Table IV.6.4.

The MedBFM reanalysis reproduces very well spatial and temporal evolution of surface values at both basin-wide scale (level 1 validation) and mesoscale and daily temporal scale (level 2 and 3 validation), with errors close to 10 mmol/m^3. Higher uncertainties are depicted for mesopelagic layers (i.e., below 300 m) than at surface by the two class 4 metrics (level2 validation): Table IV.6.2 for model vs in situ observations and Table IV.6.3 for model vs BGC-Argo observations.

Accuracy in coastal areas is basically as high as that one of the off-shore areas (Table IV.6.2).

The model accuracy in reproducing vertical oxygen processes is pretty high (Fig. IV.6.3 and Table IV.6.4): correlation between model and BGC-Argo profiles is always higher than 0.62; the oxygen values in the euphotic layer (i.e., 0-200 m) have an error of less than 19 mmol/m^3 and the depth of the maximum oxygen concentration has an error of less than 30 m, except for LEV. The ADR value is not considered because of the very small number of available floats. For the INTERIM product (year 2020), skill performance metrics are generally improved in all layers of the western Mediterranean area and in the surface layers (above 60m depth) in the eastern regions.

	Oxygen		
Layer depth	**BIAS**	**RMSD**	**CORR**
0-10 m	3.6	5.8	0.80
10-30 m	0.7	4.8	0.82
30-60 m	-3.0	4.9	0.86
60-100 m	3.8	7.3	0.52
100-150 m	6.6	8.7	0.62
150-300 m	8.5	10.7	0.77
300-600 m	20.5	21.4	0.87
600-1000 m	17.4	18.9	0.71

Table IV.6.1 Skill metrics for the comparison of oxygen with respect to climatology in open sea. Model average and climatology refers to the period covered by observations (i.e., 1999-2016).

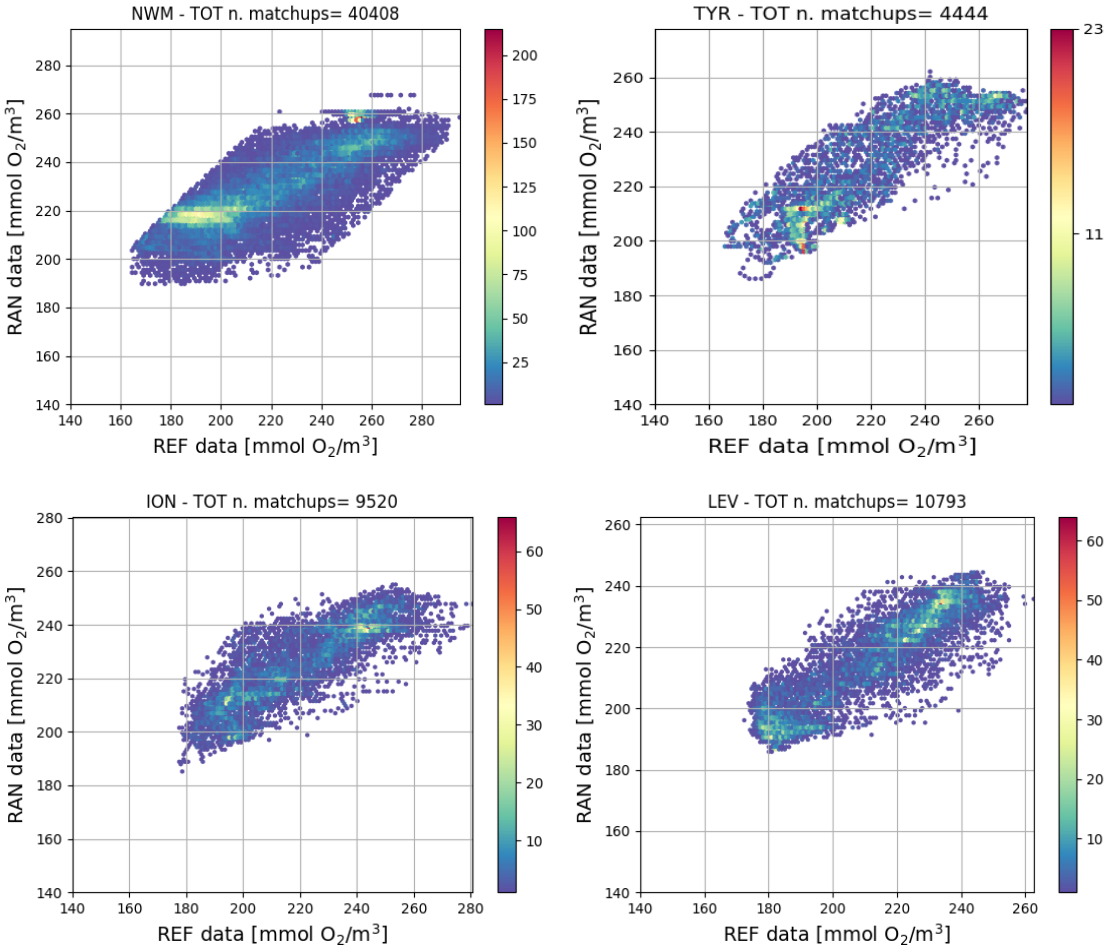

Figure IV.6.1. Density plots of model (RAN, y-axis) and reference (REF, x-axis) matchups of oxygen (mmol O_2/m^3) for NWM, TYR, ION and LEV.

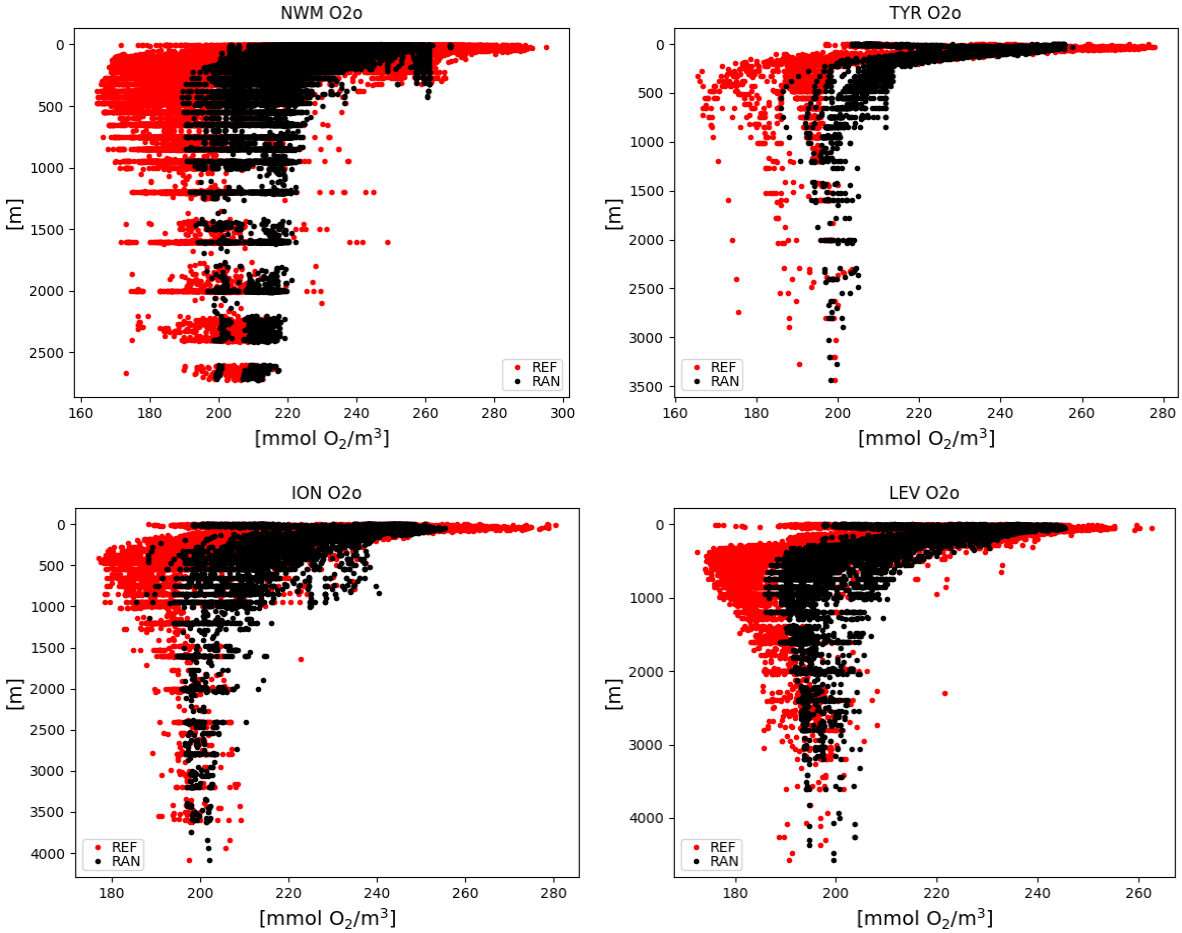

Figure IV.6.2 Vertical profiles of oxygen (mmol O_2/m^3) for reanalysis (RAN; black) and reference dataset (REF; red) for NWM, ION and LEV in open sea.

	Open Sea									Coast		
	RMSD							CORR	n. profiles/ matchups	RMSD		n. profiles/ matchups
Layer [m]	0-30	30-60	60-100	100-150	150-300	300-600	600-1000			0-60	60-200	
ALB	8.9	14.1	nan	22.0	25.5	33.8	30.5	0.94	6/57	-	-	0/0
SWM1	5.4	24.3	21.7	21.2	27.6	28.8	25.0	0.46	7/89	-	-	0/0
SWM2	16.6	12.2	13.8	15.4	14.1	26.8	21.2	0.87	27/904	-	-	0/0
NWM	14.3	15.2	16.2	18.0	22.7	28.2	24.9	0.83	1327/37877	13.5	8.8	489/5097
TYR1	11.3	17.3	20.1	22.2	24.0	33.2	32.3	0.82	35/948	18.5	22.5	33/283
TYR2	11.6	13.8	13.5	14.5	17.1	18.6	12.9	0.90	112/3342	12.0	18.1	52/571
ADR1	4.9	8.8	11.9	14.1	16.2	-	-	0.87	1/26	13.3	13.8	81/759
ADR2	11.4	13.1	9.4	14.8	16.1	25.0	30.0	0.29	13/359	13.0	15.5	9/118
AEG	15.3	14.9	16.4	19.7	20.8	19.0	17.2	0.61	232/6028	13.5	18.3	175/2321
ION1	8.4	8.4	16.1	19.2	15.6	17.0	15.3	0.84	39/1211	6.6	9.0	3/47
ION2	8.5	9.4	9.3	12.9	14.7	17.5	17.4	0.89	107/3287	7.7	9.1	12/199
ION3	9.4	12.6	10.3	11.5	13.4	18.4	18.1	0.82	169/4462	10.9	14.0	68/757
LEV1	8.0	12.8	10.0	11.7	11.5	13.9	13.4	0.84	65/1971	-	-	0/0
LEV2	5.6	8.5	7.5	8.7	9.7	12.9	12.9	0.89	71/1979	-	-	0/0
LEV3	8.6	8.3	6.5	5.5	8.2	15.4	16.9	0.88	49/1468	-	-	0/0
LEV4	8.1	8.9	6.3	5.6	10.5	18.8	14.4	0.93	153/4410	8.8	5.8	44/571
MED average	10.1	12.9	12.7	14.9	16.8	21.8	20.2					

Table IV.6.2. Mean RMSD between oxygen model outputs and EMODnet2018_int dataset computed at the in situ observation locations. The metric is calculated for selected layers (0-30 m, 30-60 m, 60-100 m, 100-150 m, 150-300 m, 300-600 m, 600-1000 m for open sea and 0-60 m and 60-200 m for coastal areas), and averaged over the whole reanalysis period (1999-2019). The overall correlation between observations and model output is also reported (for open sea) with references of n. of profiles and matchups available for open sea and coastal areas. MED average is obtained as the mean od RMSD of all the subbasins with more than 5 profiles in open sea.

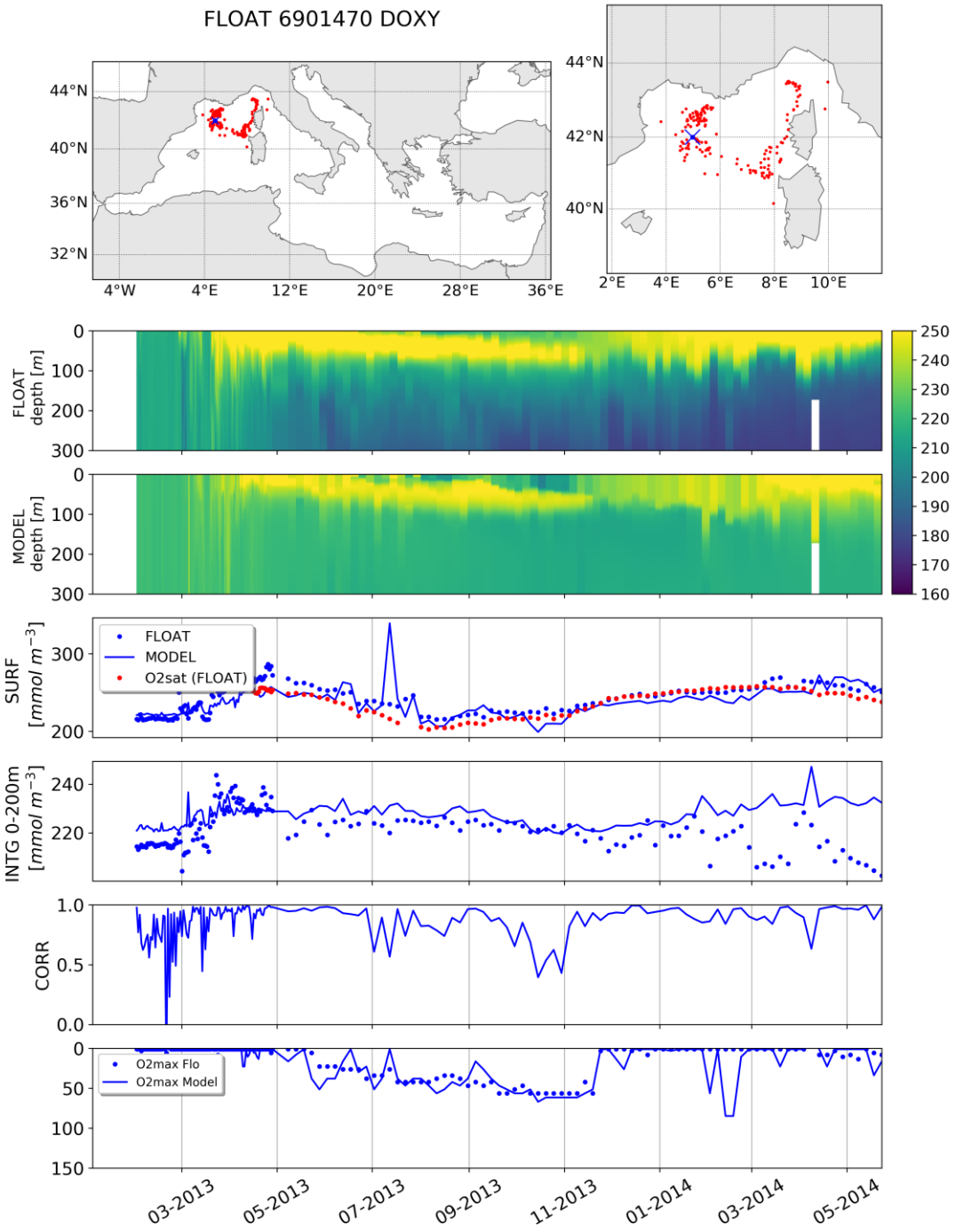

Figure IV.6.3. Comparison between BGC-Argo floats and (example for two selected floats). Panels are: Trajectory of the BGC-Argo float (red dots) with deployment position (blue cross); Hovmöller diagrams of dissolved oxygen concentration (mmol/m^3) from float data (2nd row) and model outputs (3rd row) matched-up with float position for the period of float life; selected skill indexes for model (solid line) and float data (dots): surface dissolved oxygen (SURF, 4th row), 0–200m vertically averaged dissolved oxygen (INTG, 5th row), correlation between vertical profiles (CORR, 6th row) and depth of the oxygen maximum between 0-200m (model in solid line and float data in dots, 7th row).

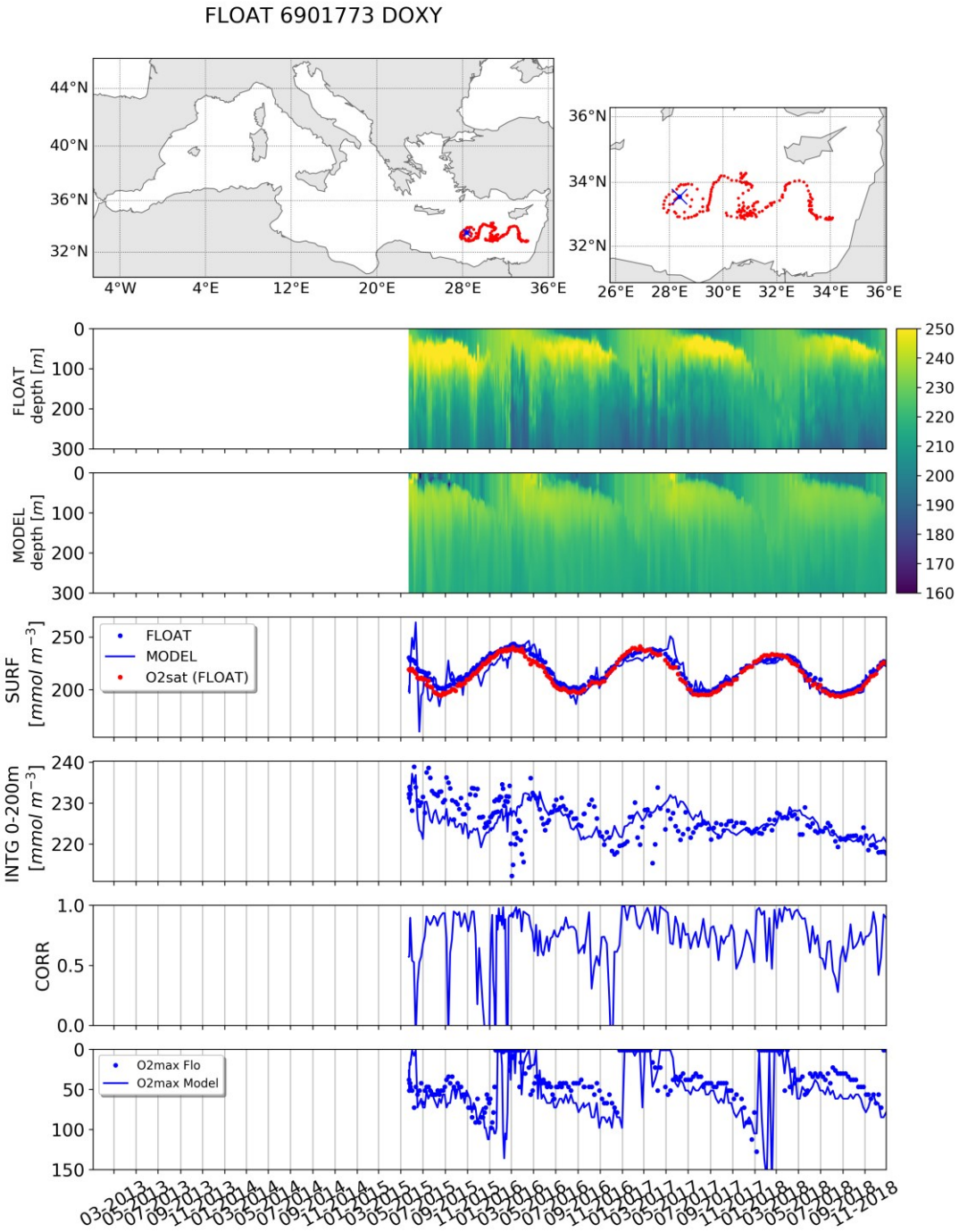

Figure IV.6.3. Same as above.

Layer depth (m)	0-10		10-30		30-60		60-100		100-150		150-300		300-600		600-1000	
	BIAS															
	R24	INT	R24	INT	R24	INT	R24	INT	R24	INT	R24	INT	R24	INT	R24	INT
alb	-	-3.1	-	-1.3	-	6.4	-	15.9	-	26.5	-	39.5	-	43.1	-	32.5
swm	6.7	1.6	6.7	-1.9	10.1	0.9	18.9	15.4	22.8	18.3	36.0	32.1	48.7	47.1	41.4	39.1
nwm	0.9	4.4	0.6	4.1	6.8	5.6	17.3	18.6	23.4	23.8	33.5	36.9	41.2	48.1	36.3	43.5
tyr	-2.9	-3.4	-6.2	-6.4	-5.2	-5.3	9.0	6.9	17.0	13.6	26.1	20.6	31.6	26.4	25.9	23.6
adr	0.2	0.9	-3.7	-1.0	3.9	6.1	14.3	15.8	17.0	19.6	19.4	26.5	27.2	18.9	31.8	22.0
ion	-2.4	0.9	-4.9	-1.0	-8.5	-3.8	-2.4	2.7	4.1	9.5	8.7	13.8	18.9	21.2	26.9	29.9
lev	-6.6	2.4	-9.7	0.0	-9.0	-0.9	-1.5	7.9	5.8	13.4	12.4	19.6	27.1	32.5	28.3	35.5
	RMSD															
	R24	INT	R24	INT	R24	INT	R24	INT	R24	INT	R24	INT	R24	INT	R24	INT
alb	-	6.7	-	5.3	-	7.9	-	16.1	-	26.7	-	39.5	-	43.1	-	32.5
swm	12.1	3.7	13.7	5.4	17.9	8.7	21.2	18.0	24.8	20.2	37.0	32.8	48.9	47.1	41.6	39.1
nwm	8.4	6.1	9.3	6.8	13.9	11.4	20.8	21.1	26.0	26.1	34.8	37.9	41.7	48.2	36.7	43.6
tyr	5.5	3.9	8.7	7.8	11.9	8.7	16.1	10.6	20.4	15.3	26.3	21.3	31.6	26.5	25.9	23.6
adr	4.6	4.0	7.5	6.8	6.5	9.8	14.5	16.5	17.1	20.3	19.4	28.7	27.2	19.0	31.8	22.1
ion	3.4	3.9	5.7	4.8	9.4	7.2	6.1	7.6	6.7	12.0	9.8	15.2	19.2	22.6	26.9	30.3
lev	7.7	4.4	10.9	4.9	10.5	6.3	7.3	11.4	9.0	15.7	13.5	21.1	27.2	33.3	28.4	35.6

Table IV.6.3 Averaged BIAS and RMSD of nitrate w.r.t. BGC-Argo floats for the layers of Tab. III.1, aggregated sub-basins (nwm, swm = swm1+sm2, tyr = tyr1+tyr2, ion = ion1+ion2+ion3, lev = lev1+lev2+lev3+lev4). INTERIM product (green cells) has been evaluated between 1 January – 31 December 2020 using the same metrics.

	CORR	mean oxygen concentration 0-200 m [mmol/m^3]		Oxygen maximum depth [m] in the layer 0-200 m		Average number of profiles per month
		BIAS	RMSD	BIAS	RMSD	
alb	-	-	-	-	-	0
swm	0.79	18.98	26.57	6	28	7
nwm	0.82	18.08	21.92	1	14	31
tyr	0.85	8.87	16.58	5	16	7
adr	0.62	12.82	14.44	24	80	2
ion	0.83	0.25	5.54	6	24	11
lev	0.79	0.76	6.6	12	35	11

Table IV.6.4. Averages of the monthly dissolved oxygen indicators plotted in Figure IV.5.2 during the period January 2013- December 2019. The indicators are the correlation between model and BGC-Argo float data, the BIAS and RMSD of the vertically 0-200 m averaged nitrate concentration, the BIAS and RMSD of the depth of the oxygen maximum (depth in the layer 0-200m). Statistics are computed for selected aggregated sub-basins.

IV.7 Ammonium

Ammonium accuracy is assessed by two validation levels. Class1 metrics (level 1) validation consists of the comparison between model average vertical profiles and the reference climatological profiles (Figures IV.13.1-16; appendix A) and the statistics computed using the 16 sub-basins climatological values and the corresponding model annual means (table IV.7.1). Class4 metrics (level 2) validation consists of the density plots (Fig. IV.7.1) and profiles plots (Fig. IV.7.2) built on the space and time matchup of in situ observations and model daily output. Data are not available in all sub-basins for class 4 metrics. Thus, validation statistics of only 7 sub-basins and 8 depths for the open sea and coastal areas are reported in Tab. IV.7.2.

As reported in Table IV.7.2, ammonium concentrations are simulated by the MedBFM model with an uncertainty of less (or only slightly higher) than 0.5 mmol/m^3 in the upper layers while in the deeper layers (i.e., below 100 m) RMSD values can be higher than 0.7 mmol/m^3. While the order of magnitude of ammonium concentration is fairly well simulated by the MedBFM model (Fig. IV.7.1 and IV.7.2), the low correlation values at both class1 and class4 metrics indicate that the model has some deficiencies in reproducing typical vertical profiles and spatial gradient of ammonium, however the low data availability (only 7 subbasins covered) might have affected the accuracy evaluation.

	Ammonium		
Layer depth	**BIAS**	**RMSD**	**CORR**
0-10 m	-0.30	0.36	-0.24
10-30 m	-0.11	0.17	-0.21
30-60 m	-0.03	0.14	-0.09
60-100 m	<0.05	0.23	-0.43
100-150 m	-0.04	0.30	-0.41
150-300 m	-0.21	0.31	-0.28
300-600 m	-0.37	0.44	0.67
600-1000 m	-0.40	0.55	0.40

Table IV.7.1 Skill metrics for the comparison of ammonium with respect to climatology in open sea. Model average and climatology refers to the period covered by observations (i.e., 1999-2016).

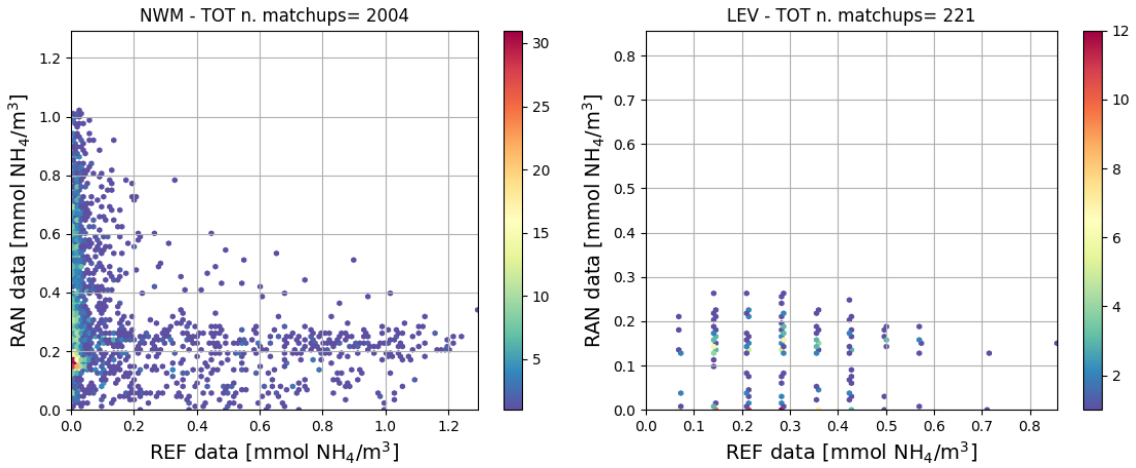

Figure IV.7.1. Density plots of model (RAN, y-axis) and reference (REF, x-axis) matchups of ammonium (mmol /m^3) for NWM and LEV.

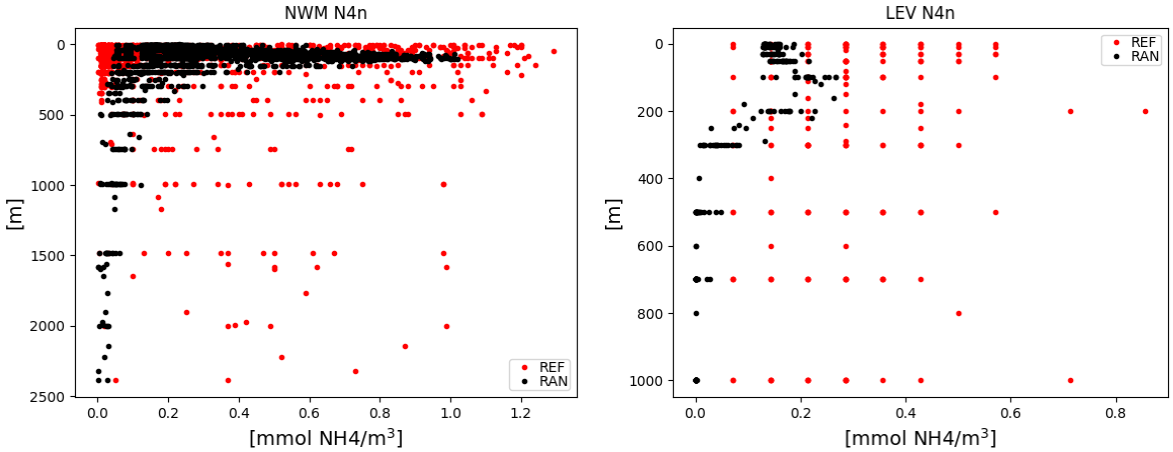

Figure IV.7.2 Vertical profiles of ammonium (mmol/m^3) for reanalysis (RAN; black) and reference dataset (REF; red) for NWM and LEV in open sea.

	Open Sea									Coast		
	RMSD							CORR	n. profiles/ matchups	RMSD		n. profiles /match ups
Layer [m]	0-30	30-60	60-100	100-150	150-300	300-600	600-1000			0-60	60-200	
SWM2	0.35	0.30	0.46	0.43	0.39	0.38	-	-0.14	31/191	0.44	0.46	11/44
NWM	0.29	0.37	0.56	0.56	0.37	0.44	0.40	-0.28	385/2036	0.44	0.41	154/715
TYR1	0.12	0.20	0.41	0.57	0.37	-	-	-0.19	7/41			
TYR2	-	0.10	0.50	0.43	-	-	-	0.19	3/18	0.31	0.34	5/20
LEV2	0.28	0.16	0.09	0.09	0.23	1.03	0.24	0.09	13/110			
LEV3	0.57	0.13			0.22	0.25	0.14	0.19	3/27			
LEV4	0.31	0.22	0.72	0.69	0.95	0.27	0.33	0.08	13/99			
MED (average)	0.24	0.25	0.34	0.36	0.34	0.34	0.32					

Table IV.7.2. Mean RMSD between ammonium model outputs and EMODnet2018_int dataset computed at the in situ observation locations. The metric is calculated for selected layers (0-30 m, 30-60 m, 60-100 m, 100-150 m, 150-300 m, 300-600 m, 600-1000 m for open sea and 0-60 m and 60-200 m for coastal areas), and averaged over the whole reanalysis period (1999-2019). The overall correlation between observations and model output is also reported (for open sea) with references of n. of profiles and matchups available. MED average is obtained as the mean od RMSD of all the subbasins with more than 5 profiles in open sea.

IV.8 pH

The accuracy of pH is evaluated by two quality assessment levels. Level 1 comparison between model annual average vertical profiles and the reference climatological profiles (Class1 metric validation of Figures IV.13.17-32 in appendix A) shows the good skill of the model in representing the basin-wide gradient and sub-basin vertical profiles. The statistics computed using the 16 sub-basins climatological values and the corresponding model annual means (Table IV.9.1) highlight that uncertainty is slightly lower at surface than at the deeper layers.

	pH in total scale		
Layer depth	**BIAS**	**RMSD**	**CORR**
0-30 m	0.002	0.022	0.73
30-60 m	-0.005	0.023	0.45
60-100 m	0.015	0.032	0.51
100-150 m	0.027	0.032	0.67
150-300 m	0.025	0.031	0.86
300-600 m	0.030	0.031	0.94
600-1000 m	0.019	0.023	0.87

Table IV.8.1 Skill metrics for the comparison of alkalinity with respect to sub-basin profiles climatology in open sea. Model average and climatology refers to the period covered by observations (i.e., 1999-2016).

Class4 metrics (level 2) validation consist of the density plots (Fig. IV.8.1) and profiles plots (Fig. IV.8.2) built on the space and time matchup of in situ observations and model daily output. Skill performance statistics of the 16 sub-basins and 8 depths for the open sea and coastal areas are then reported in Tab. IV.8.2. Modelled and observation profiles are characterized by higher variability at surface than in the deeper part where pH has almost constant values around 8.05 in the western sub-basins and 8.10 in the eastern ones (Fig. IV.8.2). Model captures very well the high surface variability (see also density plots of Fig. IV.8.1) but overestimates deep values of about 0.02-0.03 (Table IV.8.1). The mean RMSD (i.e., average of the RMSD computed for the 16 sub-basins, last rows of Tab. IV.8.2) is higher than the values computed on climatology (0.034 vs 0.022 respectively). Thus, we can speculate that half of the uncertainty is due to mesoscale dynamics and high frequency physical-biological dynamics impacting the daily values of pH and half is due to a basin-wide misrepresentation of the DIC and ALK gradients.

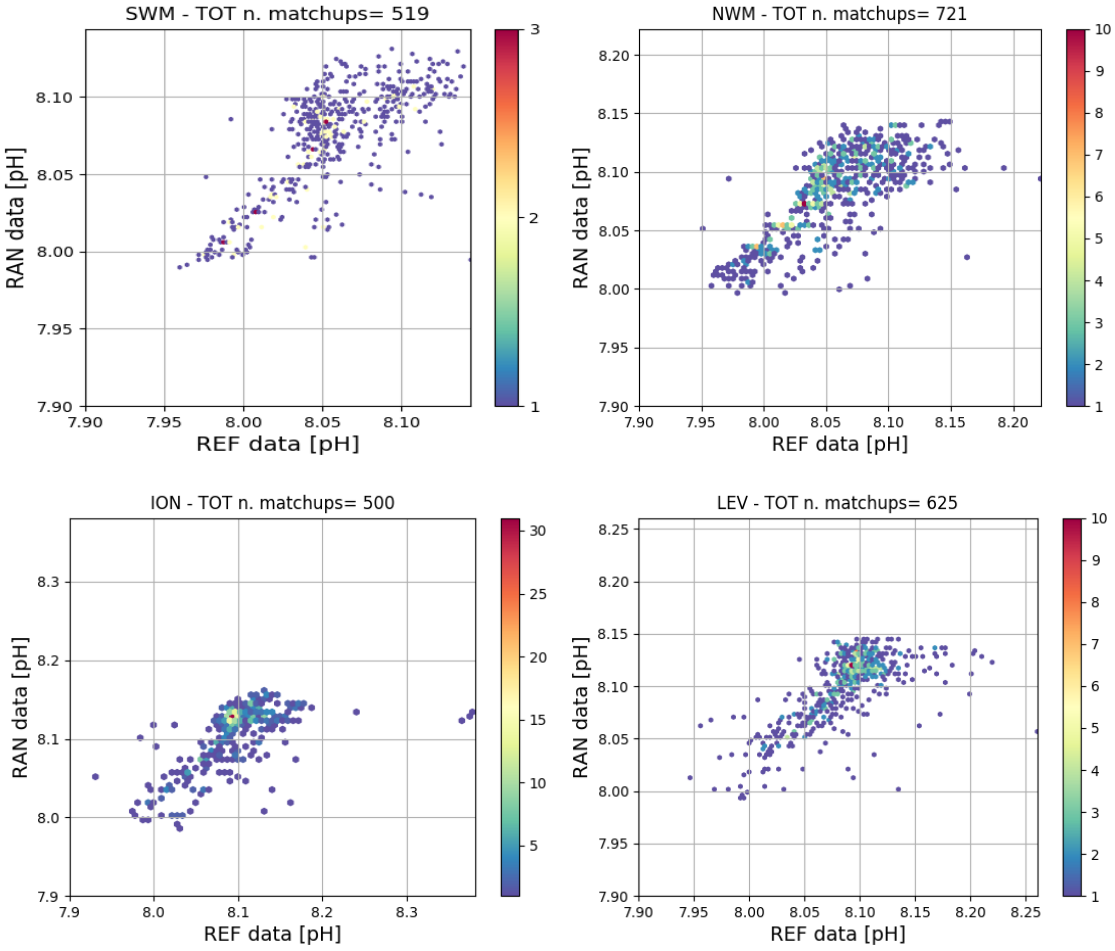

Figure IV.8.1. Density plots of model (Mod, y-axis) and reference (Obs, x-axis) matchups of pH in total scale for SWM, NWM, ION and LEV.

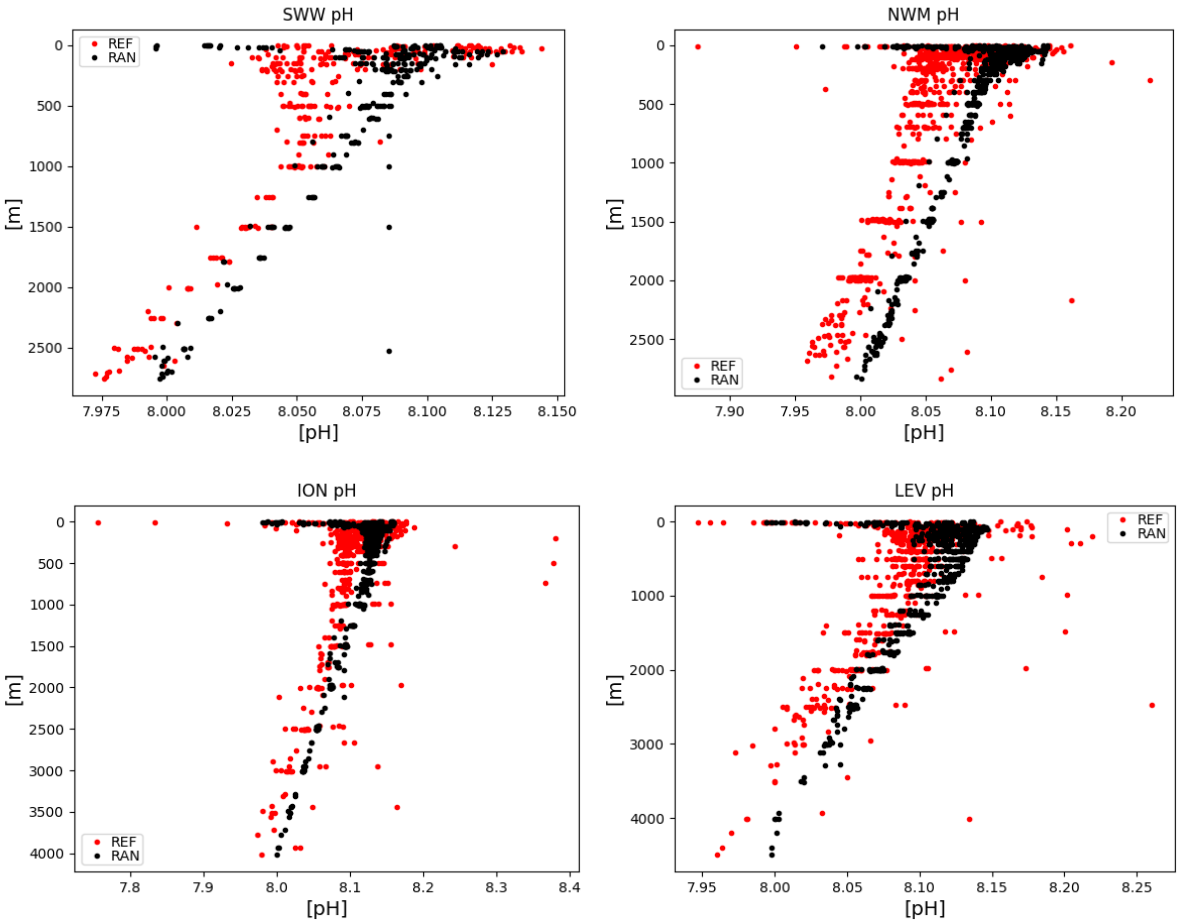

Figure IV.8.2. Vertical profiles of pH in total scale for reanalysis (Mod; black) and reference dataset (Obs; red) for SWM1, NWM, ION and LEV.

	Open Sea									Coast		
	RMSD							CORR	n. profiles/ matchups	RMSD		n. profiles/ matchups
Layer [m]	0-30	30-60	60-100	100-150	150-300	300-600	600-1000			0-60	60-200	
ALB	0.039	0.054	0.069	0.074	0.065	0.057	0.041	0.06	58/460	-	-	2/6
SWM1	0.039	0.023	0.029	0.033	0.036	0.029	0.021	0.36	25/218	-	-	0/0
SWM2	0.018	0.023	0.028	0.038	0.048	0.043	0.025	0.53	21/171		-	0/0
NWM	0.027	0.040	0.047	0.044	0.045	0.039	0.035	0.55	81/548	-	-	1/2
TYR1	0.041	0.021	0.026	0.034	0.045	nan	nan	0.45	2/23	-	-	0/0
TYR2	0.021	0.028	0.037	0.041	0.047	0.041	0.025	0.43	19/177	-	-	0/0
ADR1	0.016	nan	nan	nan	0.110	nan	nan	0.04	2/14	0.057	0.063	21/105
ADR2	0.031	0.044	0.061	0.065	0.048	0.053	0.053	0.27	23/138	0.029	0.064	3/19
AEG	0.058	0.081	0.081	0.011	0.060	0.037	0.037	0.31	18/165	0.036	0.047	4/20
ION1	0.027	nan	0.053	0.046	0.040	0.033	0.029	0.63	4/42	-	-	0/0
ION2	0.061	0.035	0.022	0.024	0.046	0.052	0.055	0.59	22/203	-	-	2/7
ION3	0.020	0.031	0.025	0.039	0.037	0.035	0.029	0.54	22/132	-	-	2/13
LEV1	0.036	0.037	0.036	0.039	0.044	0.033	0.035	0.41	26/171	-	-	0/0
LEV2	0.038	0.009	0.021	0.028	0.030	0.030	0.030	0.71	14/136	-	-	0/0
LEV3	0.016	0.010	0.011	0.020	0.023	0.032	0.027	0.85	10/63	-	-	0/0
LEV4	0.038	0.007	0.014	0.020	0.015	0.022	0.019	0.72	9/95	-	-	0/0
MED average	**0.034**	**0.032**	**0.037**	**0.037**	**0.042**	**0.033**	**0.033**					

Table IV.8.2. RMSD between pH in total scale model outputs and Emodnet2018_int dataset computed at the in situ observation locations. The metric is calculated for selected layers (0-30 m, 30-60 m, 60-100 m, 100-150 m, 150-300 m, 300-600 m, 600-1000 m for open sea and 0-60 m and 60-200 m for coastal areas) and 16 sub-basins. The overall correlation between observations and model output is also reported (for open sea) with references of n. of profiles and matchups available for open sea and coastal areas. MED average is obtained as the mean od RMSD of all the subbasins with more than 5 profiles in open sea.

IV.9 Alkalinity

Alkalinity accuracy is evaluated by two quality assessment levels. Class1 metrics (level 1) validation consists of the comparison between model average vertical profiles and the reference climatological profiles (Figures IV.13.17-32 in appendix A) and of the statistics computed using the 16 sub-basins climatological values and the corresponding model annual means (table IV.9.1). Class4 metrics (level 2) validation consists of the density plots (Fig. IV.9.1) and profiles plots (Fig. IV.5.2) built on the space and time matchup of in situ and model daily output. Validation statistics of the 16 sub-basins and 8 depths for the open sea and coastal areas are reported in Tab. IV.5.2.

Alkalinity basin-wide gradient and mean values are reproduced with an accuracy of around 39 μmol/kg in the upper layers and 12-20 μmol/kg in the deeper layers (Tab. IV.9.1 and Figures in appendix A). Considering the daily and mesoscale variability the errors in upper layers is around 30-60 μmol/kg (Tab. IV.9.2).

An overestimation of around 50 μmol/kg affects the accuracy in Levantine sub-basins in the upper layers (Figure in appendix A and IV.9.2), causing a larger RMSD values. Excess of evaporation effect not

compensated by mixing with low-alkalinity modified Atlantic water can be one of the causes of the positive trend of surface alkalinity in the Levantine sub-basins during the 20 years of simulation.

	Alkalinity		
Layer depth	**BIAS**	**RMSD**	**CORR**
0-30 m	29.8	39.3	0.95
30-60 m	24.8	30.2	0.97
60-100 m	15.6	24.0	0.94
100-150 m	19.4	22.2	0.96
150-300 m	10.5	16.7	0.93
300-600 m	3.8	12.4	0.85
600-1000 m	1.1	12.5	0.83

Table IV.9.1 Skill metrics for the comparison of alkalinity with respect to sub-basin profiles climatology in open sea. Model average and climatology refers to the period covered by observations (i.e., 1999-2016).

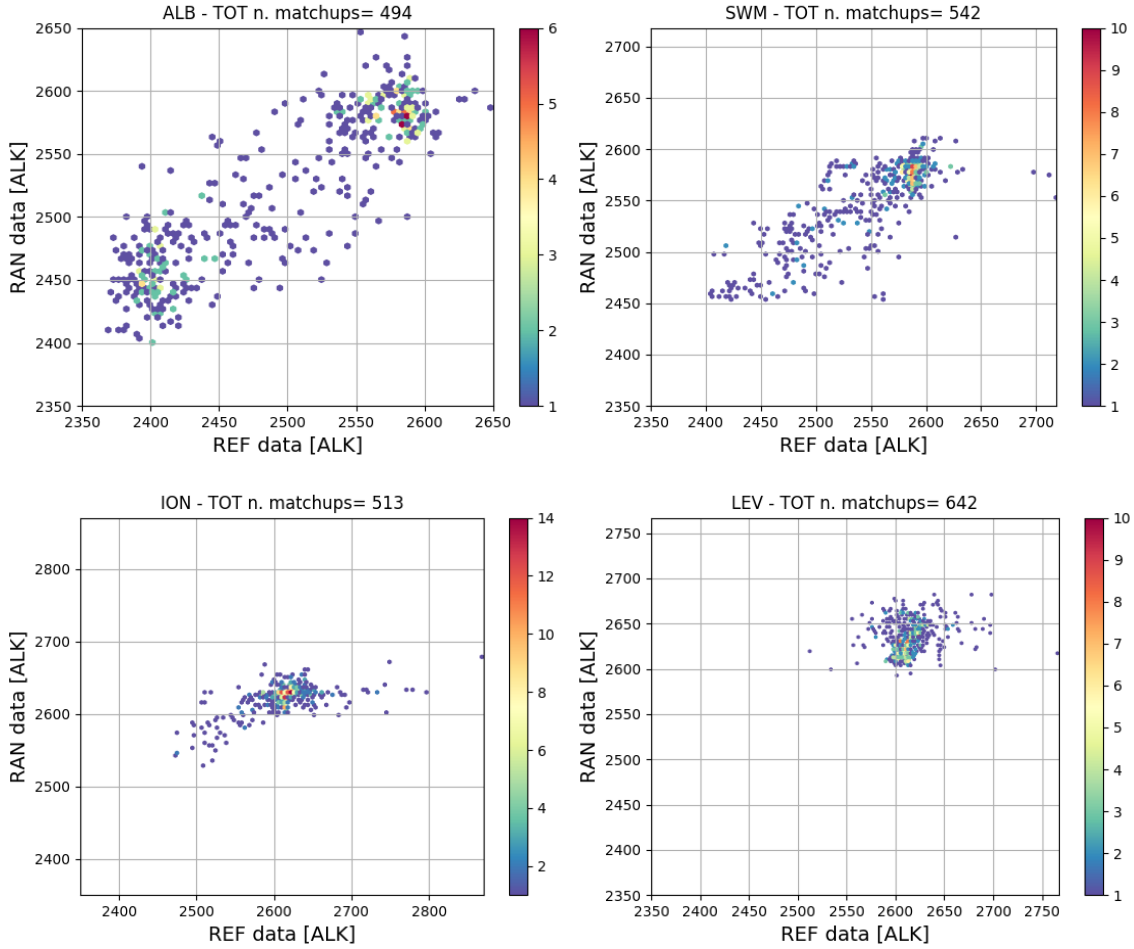

Figure IV.9.1. Density plots of model (RAN, y-axis) and reference (REF, x-axis) matchups of alkalinity (µmol/kg) for ALB, SWM, ION and LEV.

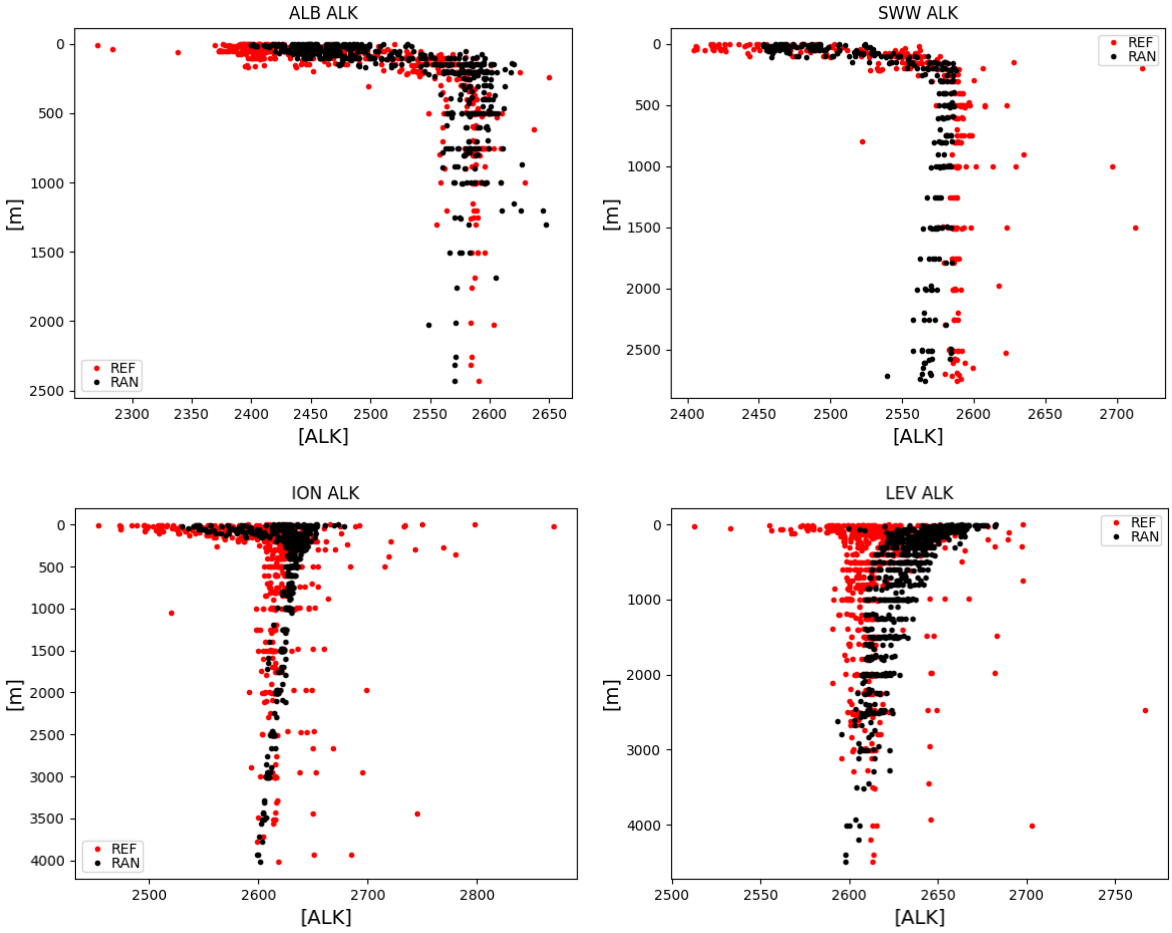

Figure IV.9.2. Vertical profiles of alkalinity (µmol/kg) for reanalysis (RAN; black) and reference dataset (REF; red) for ALB, SWM1, ION and LEV.

	Open Sea									Coast		
	RMSD							CORR	n. prof./ matchups	RMSD		n. profiles/matchups
Layer [m]	0-30	30-60	60-100	100-150	150-300	300-600	600-1000			0-60	60-200	
ALB	54.3	55.7	43.2	53.2	47.0	23.2	21.1	0.89	58/463	-	-	2/6
SWM1	41.6	43.9	26.3	30.5	38.3	13.4	19.9	0.83	25/218	-	-	0/0
SWM2	40.9	36.9	29.1	33.0	31.2	10.3	9.8	0.83	23/190	-	-	0/0
NWM	30.2	27.3	27.9	21.0	25.6	18.3	16.0	0.27	111/1019	-	-	1/2
TYR1	30.0	20.5	18.1	12.5	7.8	-	-	0.77	2/23	-	-	0/0
TYR2	47.8	31.1	23.2	16.0	22.3	28.8	10.6	0.88	19/177	-	-	1/14
ADR1	26.2	-	-	-	30.5	-	-	-0.39	2/14	31.8	20.0	22/108
ADR2	27.5	25.8	24.4	24.9	20.0	15.1	27.3	-0.16	23/138	17.0	12.4	3/19
AEG	48.8	57.9	63.0	19.3	54.4	45.4	40.4	0.56	18/166	63.1	30.9	4/20
ION1	60.0	-	44.7	39.1	17.1	7.9	5.6	0.94	4/42	-	-	0/0
ION2	66.3	45.8	40.0	34.9	28.3	15.8	17.6	0.72	23/214	-	-	2/7
ION3	51.2	22.8	12.6	19.8	36.1	41.3	13.9	0.07	22/130	-	-	2/13
LEV1	60.1	61.4	36.8	25.3	21.8	18.5	25.0	0.30	26/171			0/0
LEV2	46.3	43.3	38.0	31.7	21.4	16.7	16.8	0.36	15/149			0/0
LEV3	45.0	40.8	40.8	39.1	26.5	23.6	24.6	0.36	10/63			0/0
LEV4	48.3	42.0	43.0	36.7	23.0	14.4	11.7	0.38	9/95			0/0
MED average	**47.7**	**41.1**	**35.2**	**30.3**	**29.5**	**20.9**	**18.6**					

Table IV.9.2. RMSD between alkalinity model outputs and Emodnet2018_int dataset computed at the in situ observation locations. The metric is calculated for selected layers (0-30 m, 30-60 m, 60-100 m, 100-150 m, 150-300 m, 300-600 m, 600-1000 m for open sea and 0-60 m and 60-200 m for coastal areas) and 16 sub-basins. The overall correlation between observations and model output is also reported (for open sea) with references of n. of profiles and matchups available for open sea and coastal areas. MED average is obtained as the mean od RMSD of all the subbasins with more than 5 profiles in open sea.

IV.10 Dissolved inorganic carbon

The accuracy of dissolved inorganic carbon (DIC) is evaluated by two quality assessment levels. Class 1 comparison between dissolved inorganic carbon model and the reference climatological profiles (Class1 metric validation of Figures IV.13.17-32 in appendix A) shows the good skill of the model in representing the basin-wide gradient (very high correlation values in the upper layers; Table IV.10.1) and the typical vertical profiles in the Mediterranean sub-basins. The statistics computed using the 16 sub-basins climatological values and the corresponding model annual means (table IV.10.1) highlight that uncertainty is higher at surface where variability is higher.

	Dissolved inorganic carbon		
Layer depth	**BIAS**	**RMSD**	**CORR**
0-30 m	26.09	34.10	0.96
30-60 m	18.80	27.37	0.91
60-100 m	5.21	21.04	0.78
100-150 m	1.50	20.09	0.68
150-300 m	-2.78	11.36	0.38
300-600 m	-12.04	17.58	-0.52
600-1000 m	-8.19	12.28	-0.22

Table IV.10.1 Skill metrics for the comparison of dissolved inorganic carbon with respect to sub-basin profiles climatology in open sea.

The density (Fig. IV.10.1) and profiles (Fig. IV.10.2) plots, which are built on the space and time matchup of in situ observations and model daily output, provide the class 4 metrics comparison whose skill performance statistics are summarized in Tab. IV.10.2 for 16 sub-basins, 7 depths and two areas (i.e., open sea and coastal areas).

Profiles are characterized by high variability in the upper layers (i.e. down to 200m) whereas deeper values remain almost constant for the period of the reanalysis (Fig. IV.10.2). Model captures very well the high surface variability (see also density plots of Fig. IV.10.1) but underestimates values in intermediate and deep layers in some sub-basins (e.g., NWM and SWM) of about 20-30 μmol/kg (Fig. IV.10.2). The mean RMSD (i.e., average of the RMSD computed for the 16 sub-basins, last rows of Tab. IV.8.2) is almost 30% higher than the values computed on climatology (46.7 vs 34.1 μmol/kg respectively). Thus, we can speculate that half of the uncertainty is due to mesoscale dynamics and high frequency physical-biological dynamics and half is due to a basin-wide misrepresentation of the western-to-eastern positive gradient.

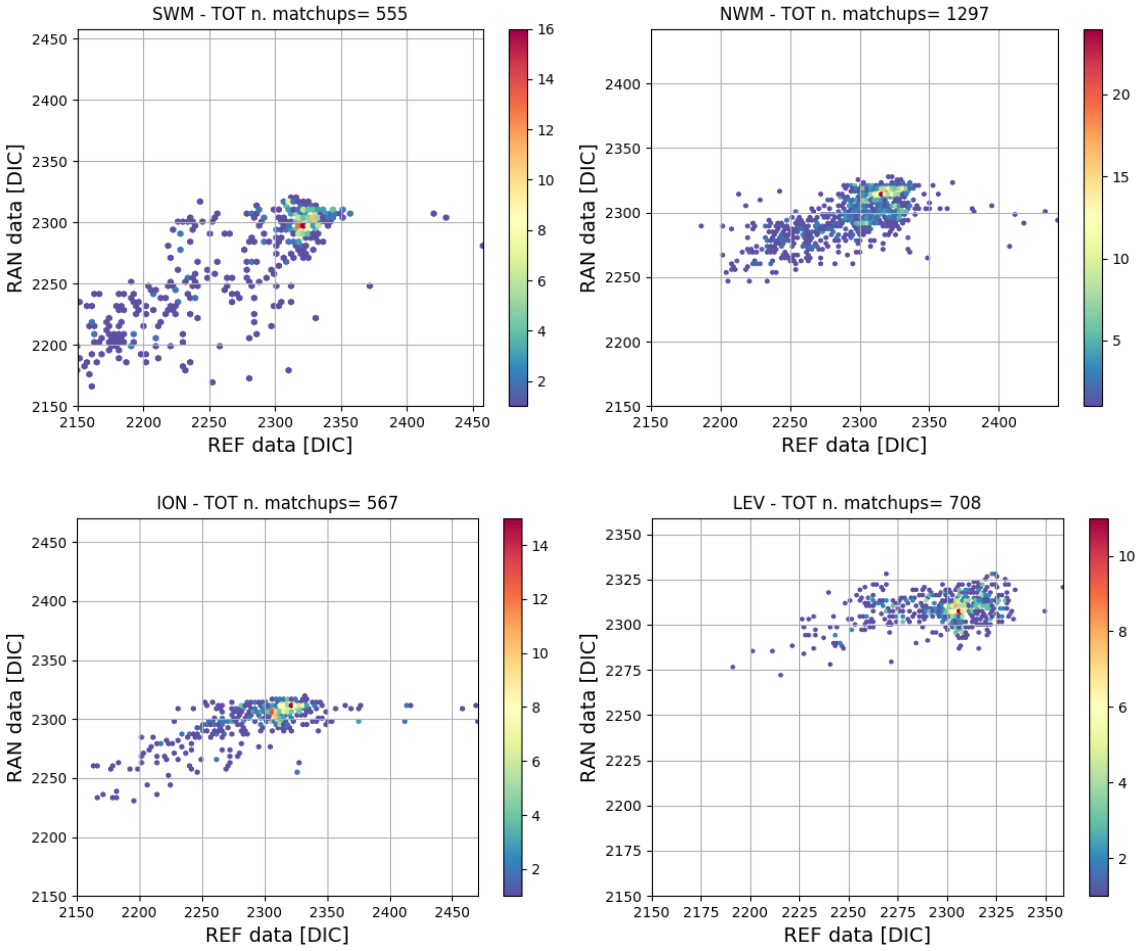

Figure IV.10.1. Density plots of model (RAN, y-axis) and reference (REF, x-axis) matchups of dissolved inorganic carbon (DIC, µmol/kg) for ALB, SWM, ION and LEV.

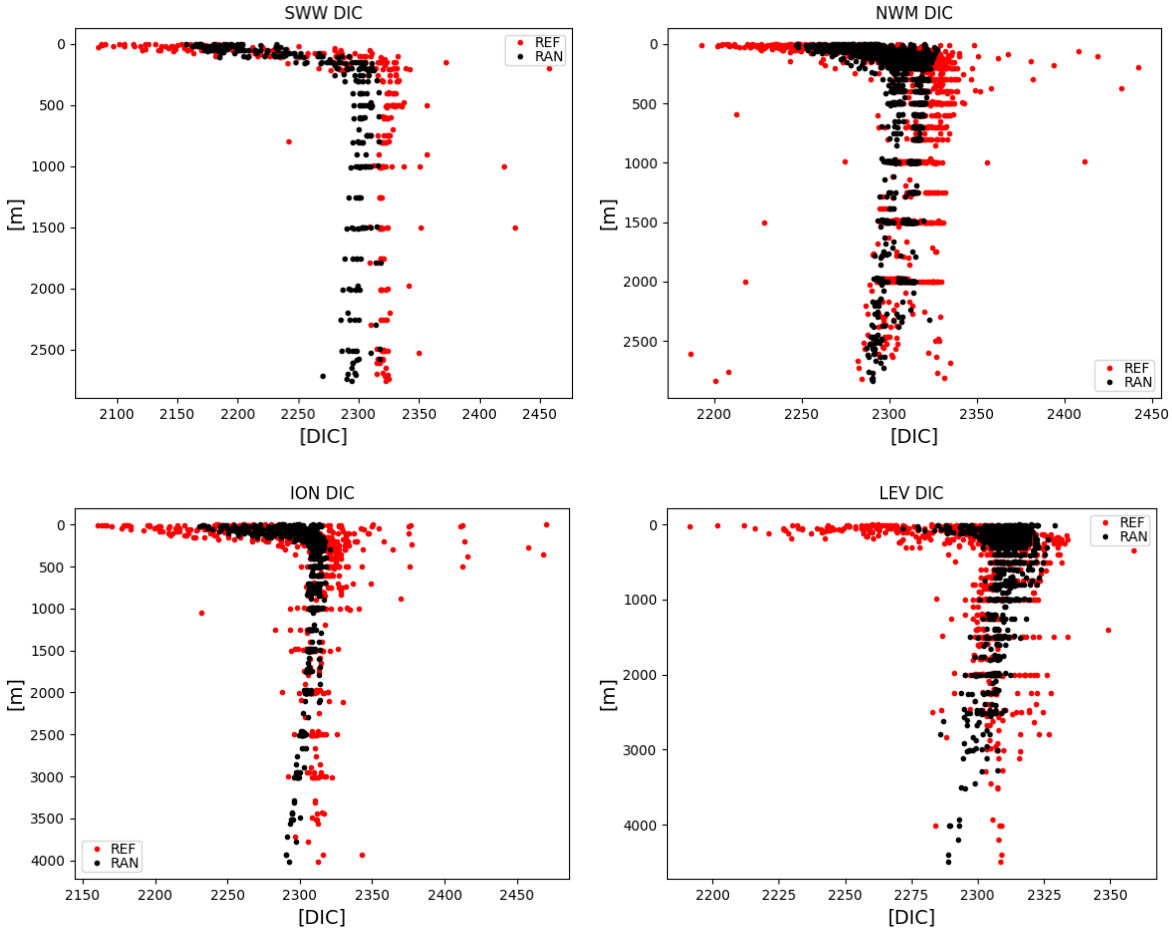

Figure IV.10.2. Vertical profiles of dissolved inorganic carbon (DIC, µmol/kg) for reanalysis (Mod; black) and reference dataset (Obs; red) for SWM1, NWM, ION and LEV.

	Open Sea									Coast		
	RMSD							CORR	n. prof./ matchups	RMSD		n. profiles/ matchups
Layer [m]	0-30	30-60	60-100	100-150	150-300	300-600	600-1000			0-60	60-200	
ALB	58.2	55.5	56.6	63.1	44.4	31.3	27.5	0.88	58/460	-	-	2/6
SWM1	49.5	48.7	36.0	44.2	41.0	24.5	26.0	0.87	25/218	-	-	0/0
SWM2	43.9	38.4	29.6	42.7	39.8	26.7	18.2	0.85	23/201	-	-	1/11
NWM	34.4	20.5	25.9	17.3	21.4	19.7	14.5	0.71	111/1040	-	-	0/0
TYR1	45.4	22.1	9.0	16.2	26.7	-	-	0.81	2/23	-	-	1/14
TYR2	52.0	34.8	21.9	15.6	12.7	25.0	10.9	0.89	19/177	46.7	43.2	21/105
ADR1	24.5	-	-	-	96.5	-	-	0.69	2/14	24.2	33.3	3/19
ADR2	32.2	34.0	30.6	37.2	29.7	30.8	41.2	-0.37	23/137	40.8	13.8	4/20
AEG	48.7	29.3	16.8	18.9	13.1	30.3	25.7	0.50	18/167	-	-	0/0
ION1	64.1	-	21.2	22.8	26.8	14.4	20.3	0.92	4/44	-	-	2/7
ION2	50.8	42.8	34.6	36.4	22.2	11.3	9.8	0.73	23/243	-	-	2/12
ION3	53.3	28.7	22.9	30.9	40.8	45.6	19.1	0.31	23/142	-	-	0/0
LEV1	50.1	52.3	29.9	18.2	17.0	9.3	9.6	0.60	26/174	-	-	0/0
LEV2	33.0	36.9	31.0	22.5	20.2	10.0	8.1	0.52	16/185	-	-	0/0
LEV3	45.3	35.1	28.0	20.8	13.8	12.4	11.9	0.25	10/88	-	-	0/0
LEV4	38.3	40.5	39.5	36.4	21.4	6.9	3.8	0.53	9/95	-	-	0/0
MED average	46.7	38.3	30.3	30.5	26.0	21.3	17.6					

Table IV.10.2. RMSD between dissolved inorganic carbon model outputs and Emodnet2018_int dataset computed at the in situ observation locations. The metric is calculated for selected layers (0-30 m, 30-60 m, 60-100 m, 100-150 m, 150-300 m, 300-600 m, 600-1000 m for open sea and 0-60 m and 60-200 m for coastal areas) and 16 sub-basins. The overall correlation between observations and model output is also reported (for open sea) with references of n. of profiles and matchups available for open sea and coastal areas. Statistics are not computes for less than 3 profiles. MED average is obtained as the mean od RMSD of all the subbasins with more than 5 profiles in open sea.

IV.11 Surface partial pressure of CO2

Two reference datasets are used for the validation of surface pCO2: 1) from in situ or recalculated pCO2 values derived from the Emodnet2018_int dataset (about 360 measurements) and 2) from the dedicated global dataset SOCAT v2 of pCO2 measurements (more than 6600 measurements). Given the larger data availability of the SOCAT v2 dataset, skill performance metrics of SOCAT v2 are ultimately used for the validation of surface pCO2. Then, skill statistics of pCO2 together with those of DIC, alkalinity and pH, provide a comprehensive outlook of the carbonate system functioning.

Class 1 comparison between surface pCO2 model and the reference climatological surface values from Emodnet2018_int (Class1 metric validation of Figures IV.13.17-32 in appendix A) and SOCAT v2 shows the good skill of the model in representing the basin-wide gradient (very high correlation values in the upper layers; Table IV.11.1) and average error of 21.8 and 32.5 ppm.

The class 4 comparison highlights a higher error (average of 38.5 and 38.7 ppm in the Med) when also daily and spatial variability is considering in the model-observation comparison. Model tends to overestimate summer observations possibly due to the model bias on DIC.

Dataset	Surface pCO2 [ppm]		
	BIAS	RMSD	CORR
EMODnet2018_int; pCO2 at 0-30m	5.2	21.8	0.7
SOCAT v2; surface pCO2	31.8	32.5	0.97

Table IV.11.1 Skill metrics for the comparison of surface pCO2 with respect to sub-basin climatology in open sea.

Surface pCO2 [ppm]	Emodnet2018				SOCAT v2 dataset		
	Open Sea		Coastal				
	RMSD	n. obs	RMSD	n. obs	RMSD	CORR	n. obs
ALB	48.1	58	-	2	39.0	0.78	878
SWM1	48.9	25	-	0	39.6	0.92	859
SWM2	25.9	21	-	0	41.3	0.87	302
NWM	33.0	81	-	1	38.4	0.92	1661
TYR1	-	2	-	0	41.6	0.94	342
TYR2	26.4	19	-	0	41.8	0.94	654
ADR1	-	2	37.8	21	41.9	0.80	6
ADR2	31.8	23	28.1	3	42.0	0.86	79
AEG	58.0	18	25.8	4	25.1	0.90	790
ION1	39.3	4	-	0	37.7	0.92	93
ION2	46.9	22	-	2	36.5	0.89	345
ION3	26.8	22	-	2	40.0	0.89	444
LEV1	44.2	26	-	0	42.5	0.82	27
LEV2	43.5	14	-	0	35.3	0.18	5
LEV3	19.4	10	-	0	38.0	-0.19	25
LEV4	46.4	9	-	0	-	-	0
MED (average)	38.5	354	-	-	38.7	0.8	6510

Table IV.11.2. RMSD between surface pCO2 model outputs and Emodnet2018_int dataset (left columns) and SOCAT v2 dataset (right column) computed at the in situ observation locations. The metrics are computed for 16 sub-basins with references of n. of matchups available (statistics are not computes for less than 3 observations). Emodnet2018_int data refer to the surface layer (0-30 m, for open sea and 0-60 m for coastal areas); SOCAT v2 data refer to surface layer (surface model layer). MED average is obtained as the mean od RMSD of all the subbasins with more than 5 profiles in open sea.

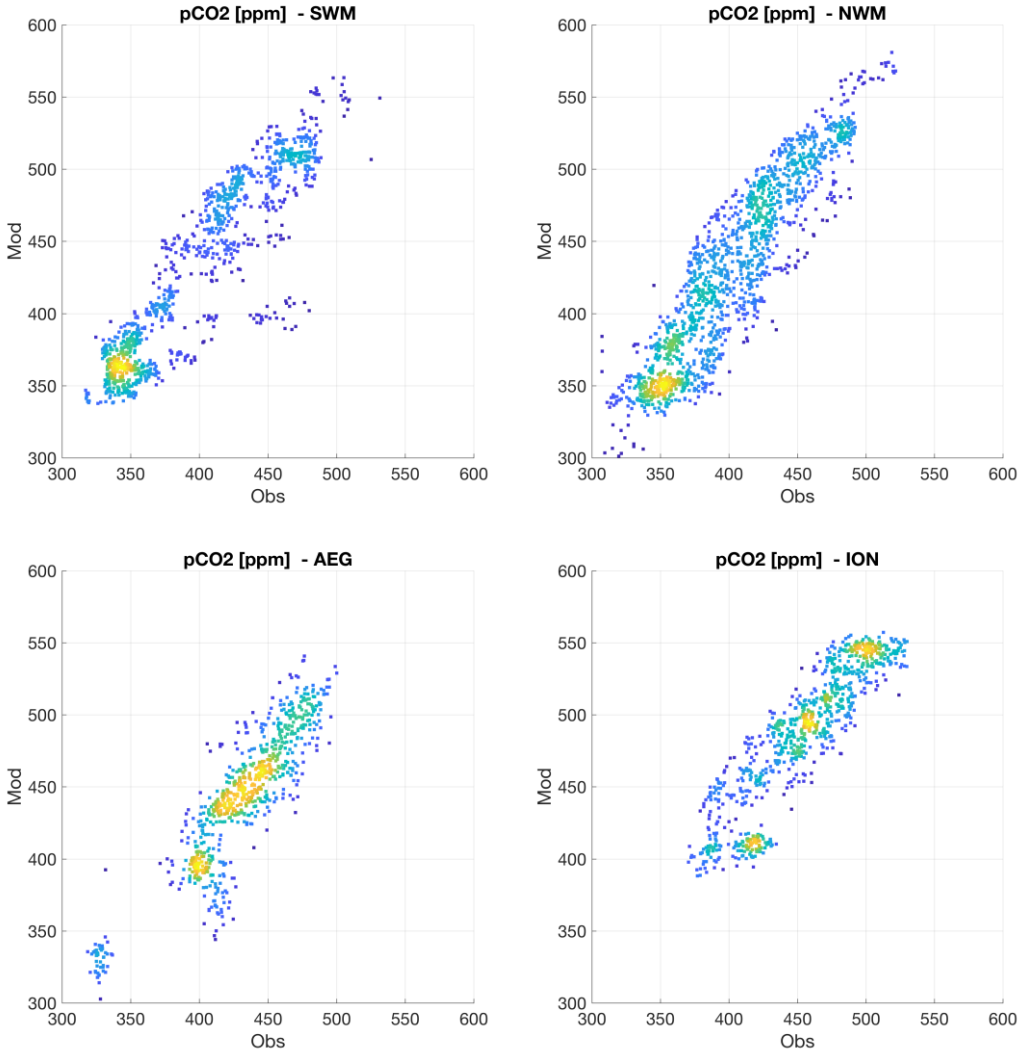

Figure IV.11.1. Density plots of model (RAN, y-axis) and SOCAT v2 observations (REF, x-axis) matchups of surface pCO2 (ppm) for SWM, NWM, AEG and ION. The warmth of the colors indicate the density of the observations.

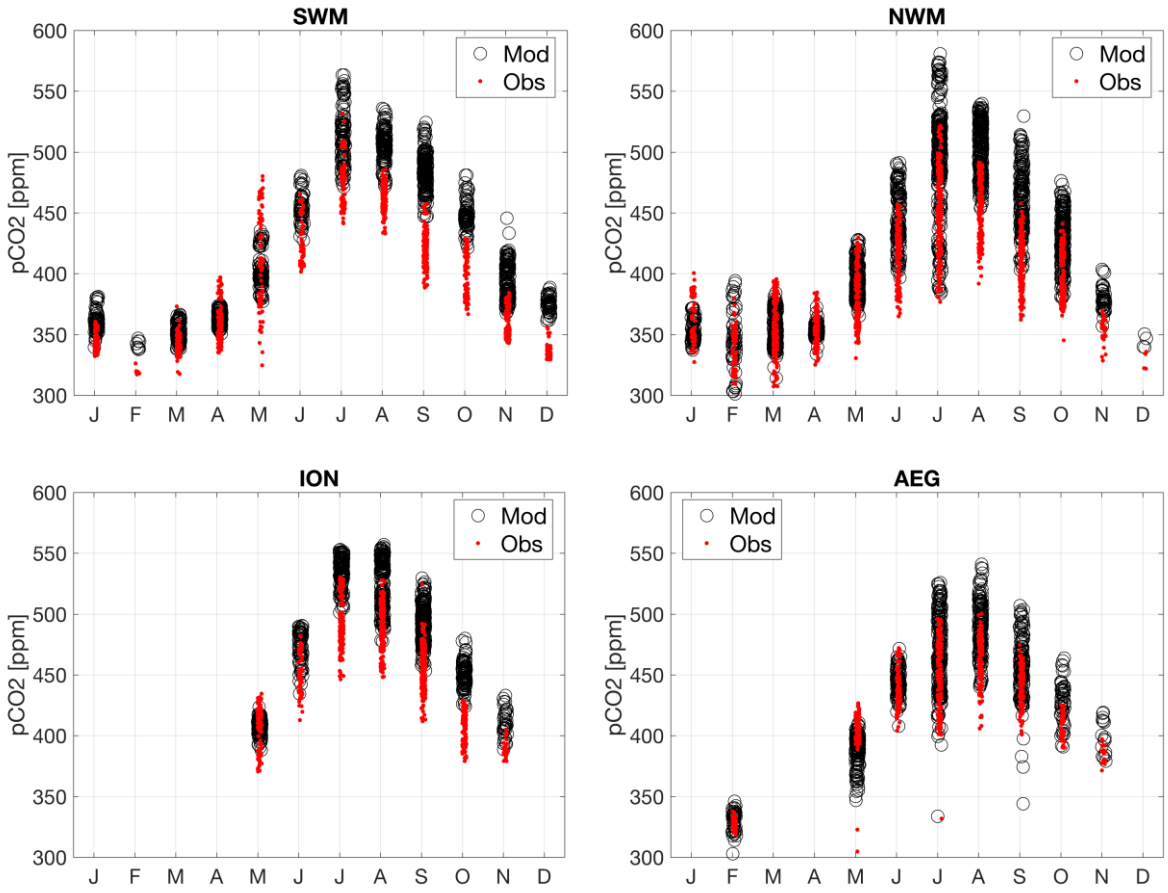

Figure IV.11.2. Annual cycle of surface pCO2 (ppm) for reanalysis (Mod; black) and SOCAT v2 reference dataset (Obs; red) for SWM, NWM, AEG and ION.

IV.12 Surface flux of CO2

The modelled mean annual surface flux of CO2 (Fig. IV.12.1) can be qualitatively compared with previous published estimations (section 1.7 of the Ocean State Report in Schuckmann et al., 2018; D'Ortenzio et al., 2008; Melaku Canu et al., 2015). The mean annual patterns, i.e. western-to-eastern and northern-to-southern decreasing gradients and the almost neutral condition, are consistently in agreement with the previous estimations.

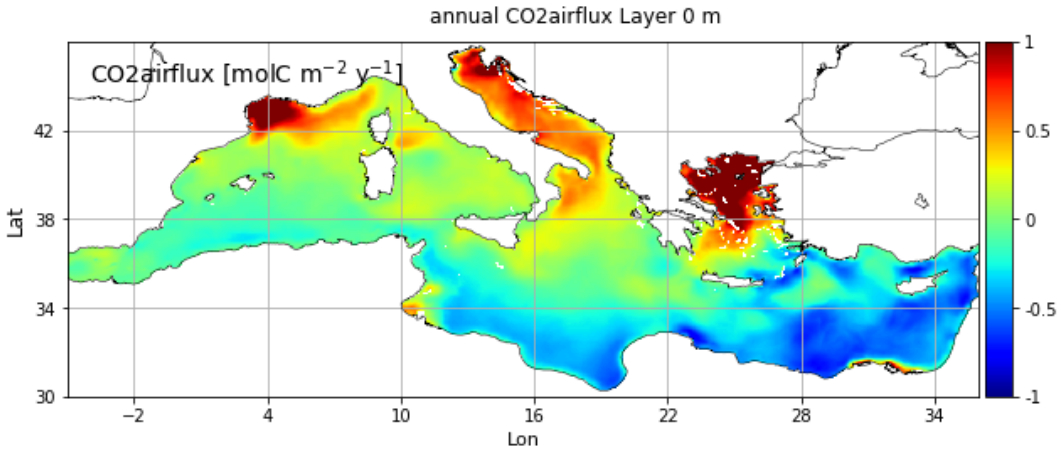

Figure IV.12.1. Mean annual map of surface flux of CO2.

IV.13 Appendix A: class 1 climatological comparison

This section reports the class 1 visual comparison for all the model variables. Weekly (grey lines) and overall average (black lines) profiles for the model reanalysis are compared with climatological vertical profiles (red dots for means and dashed lines for standard deviations) for the 16 sub-basins of Fig. III.1. Model averages refer to the period covered by observations (i.e. 1999-2016). Two sets of figures are present: one for chlorophyll, nutrients (nitrate, phosphate, silicate, ammonium) and oxygen variables (Figure IV.13.1-16), and one for carbonate system variables (pCO2, DIC, ALK, pH; Figures IV.13.17-32).

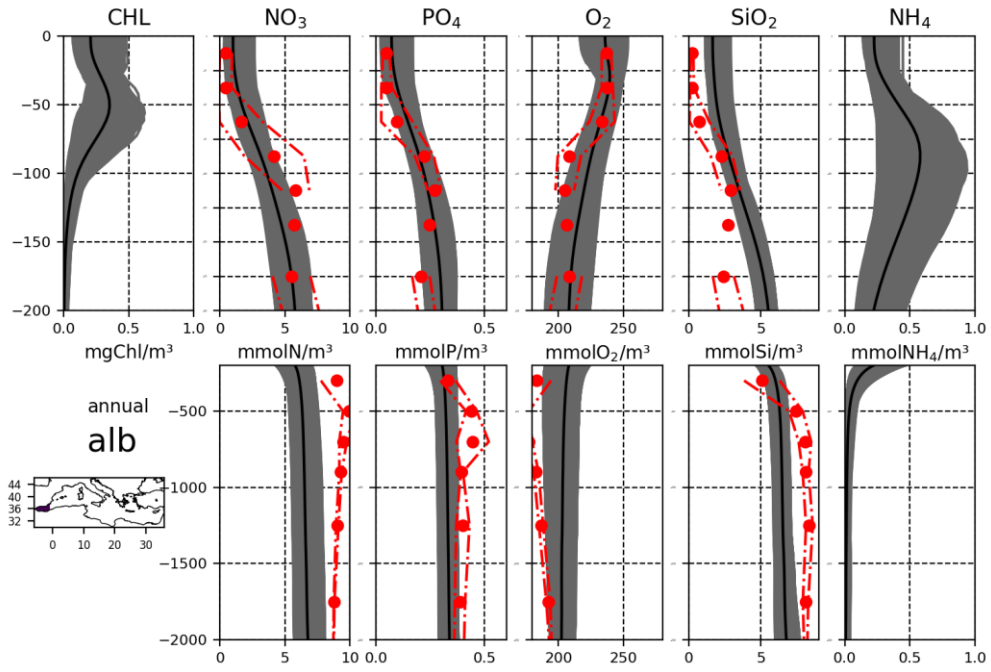

Fig. IV.13.1.

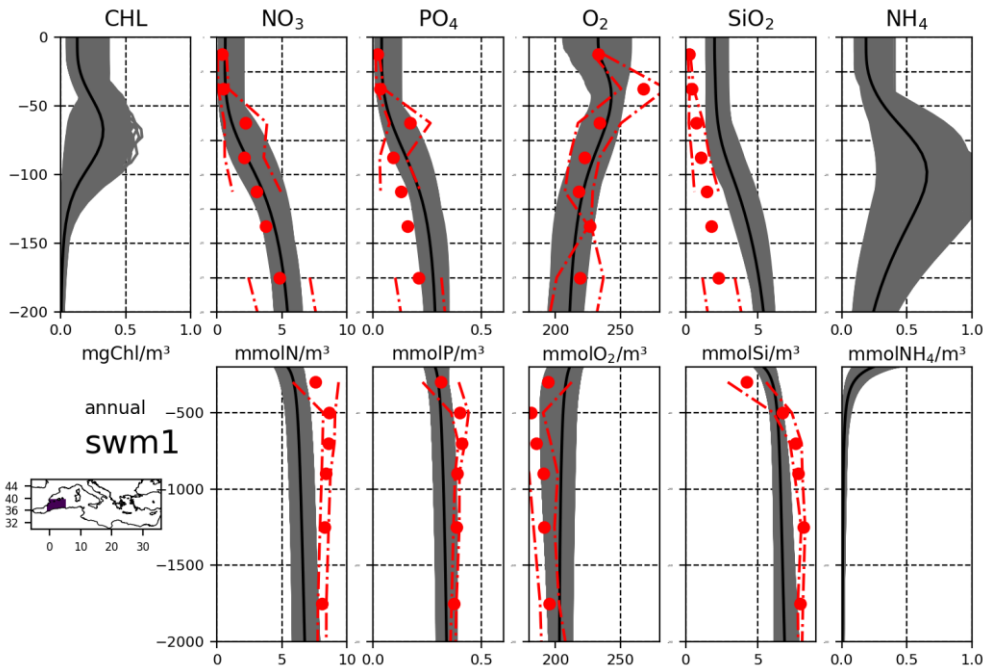

Fig. IV.13.2.

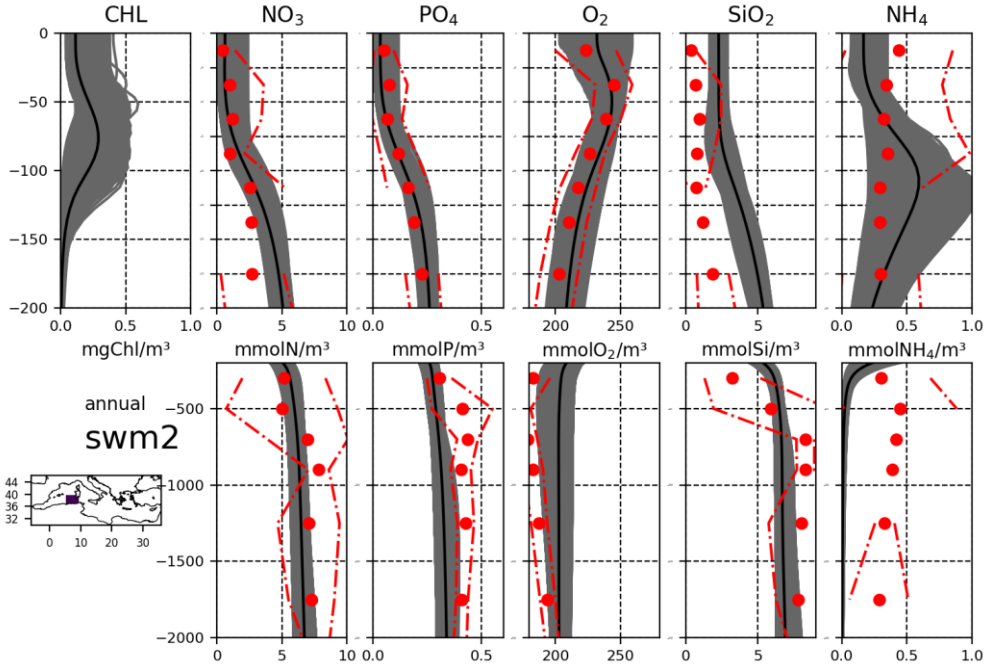

Fig. IV.13.3.

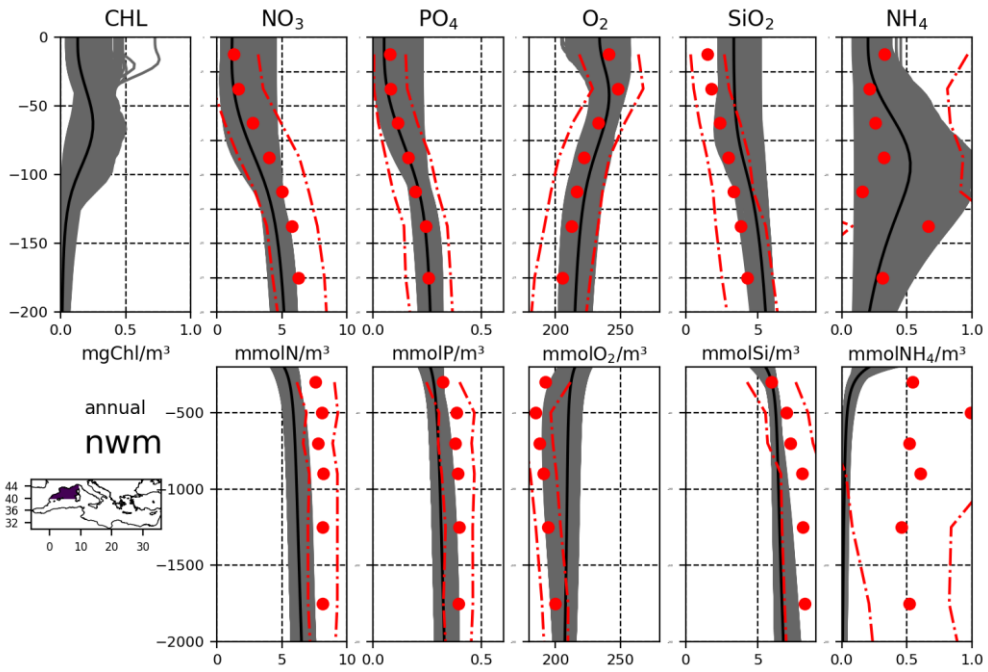

Fig. IV.13.4.

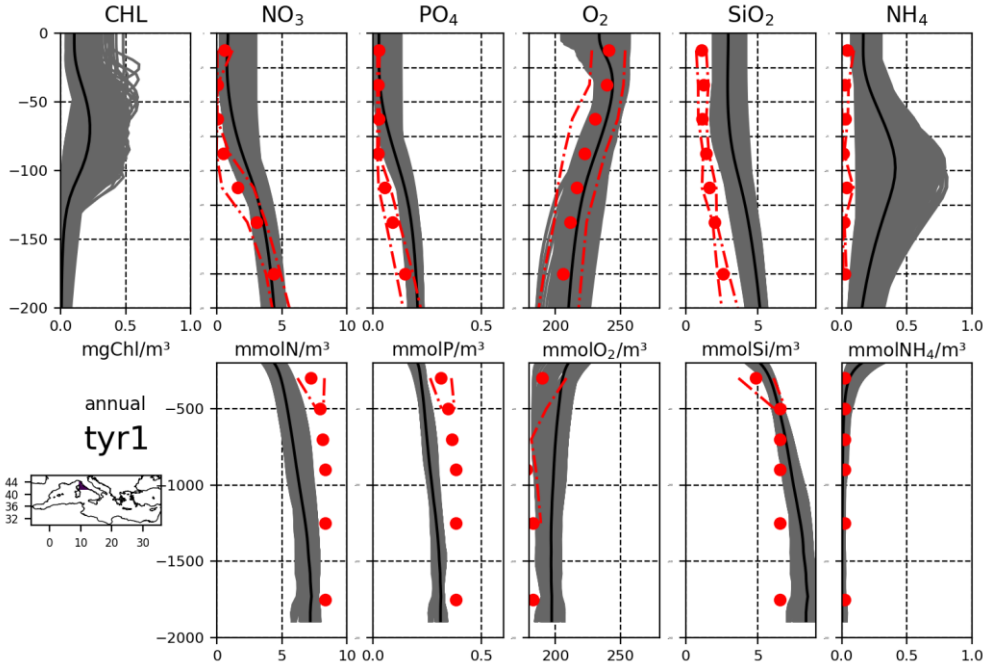

Fig. IV.13.5.

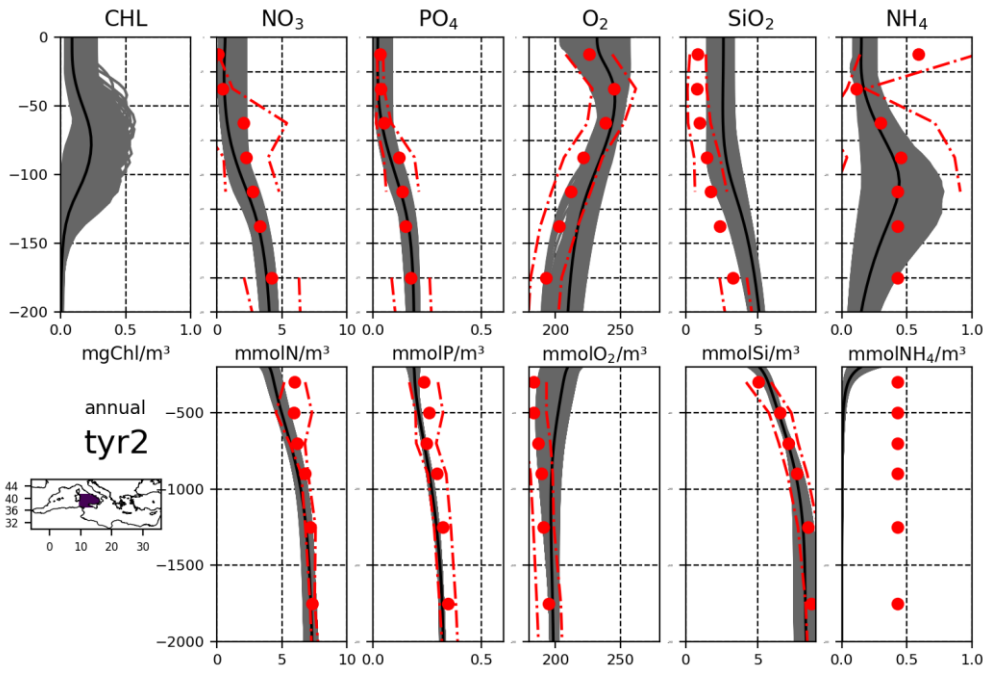

Fig. IV.13.6.

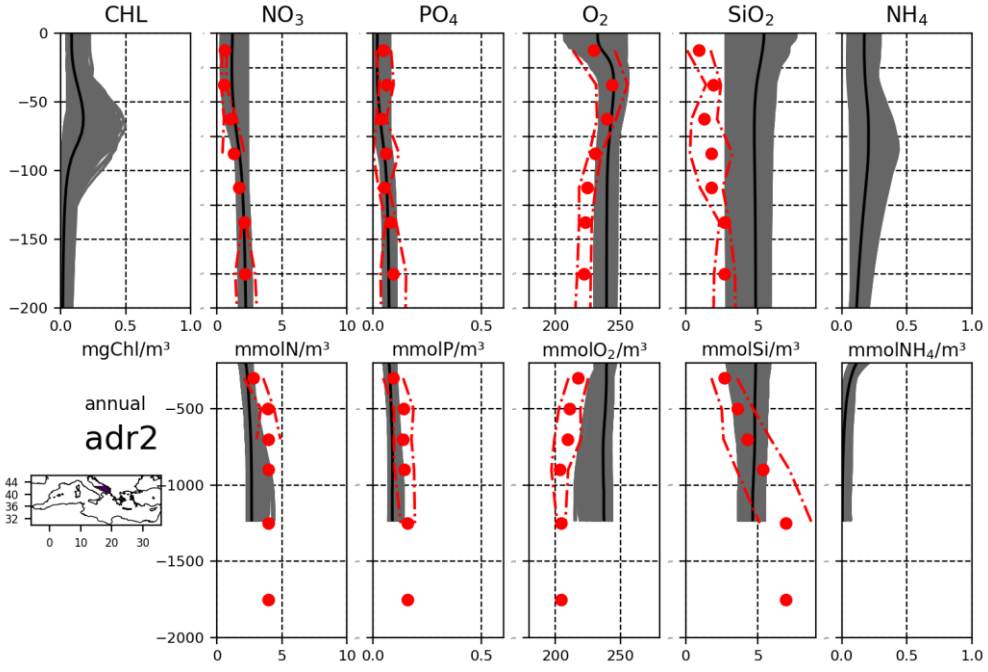

Fig. IV.13.7.

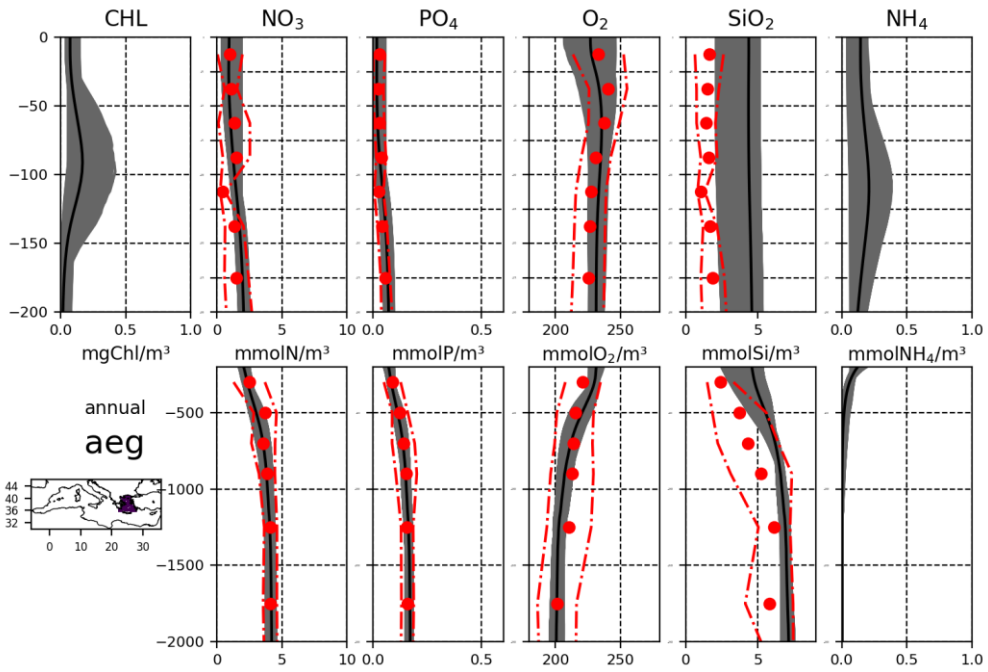

Fig. IV.13.8.

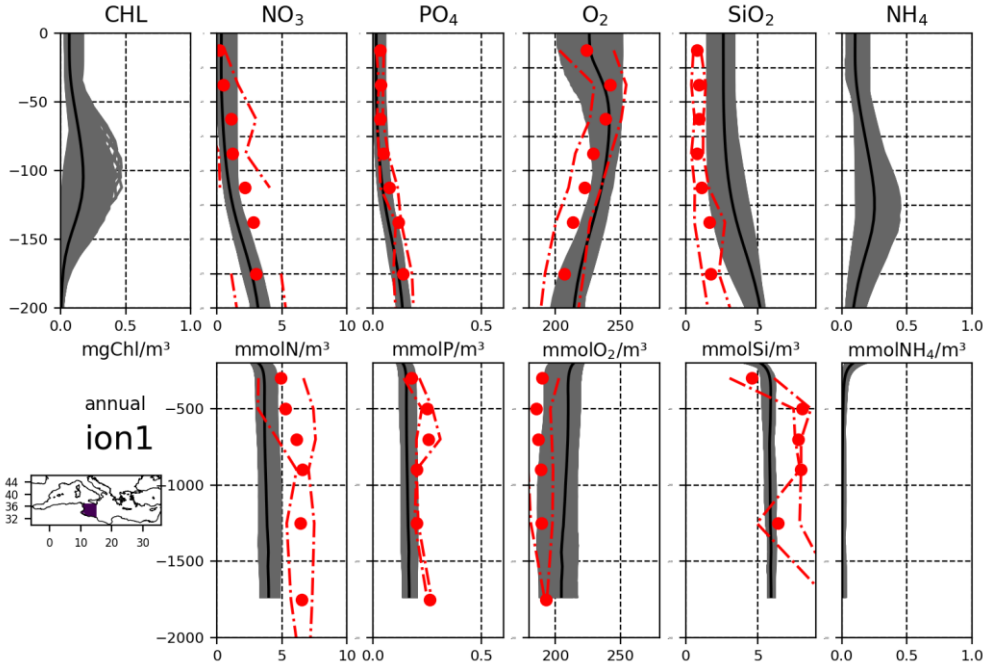

Fig. IV.13.9.

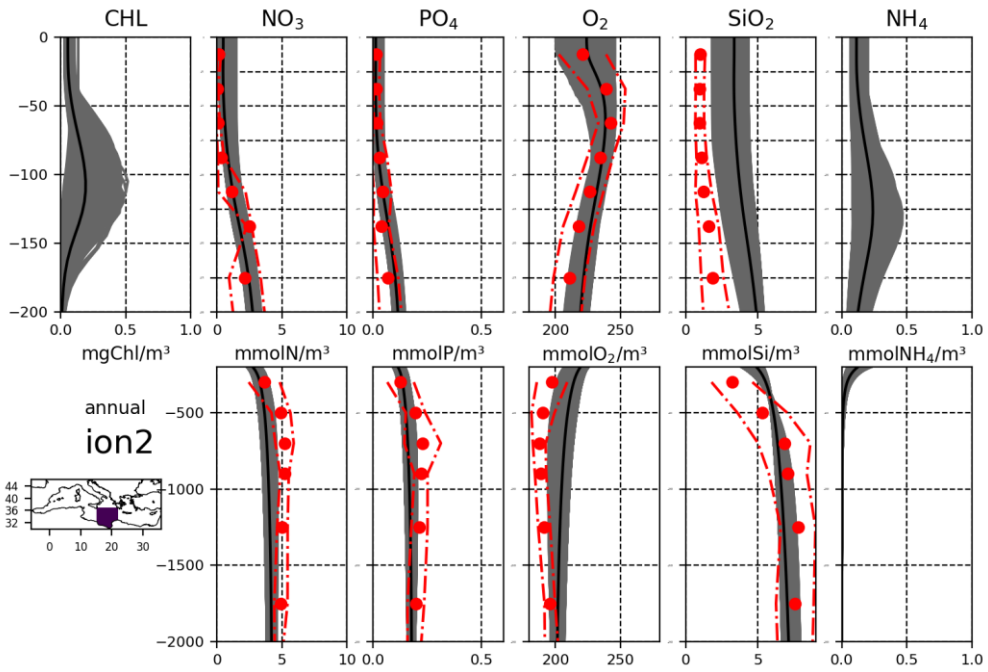

Fig. IV.13.10.

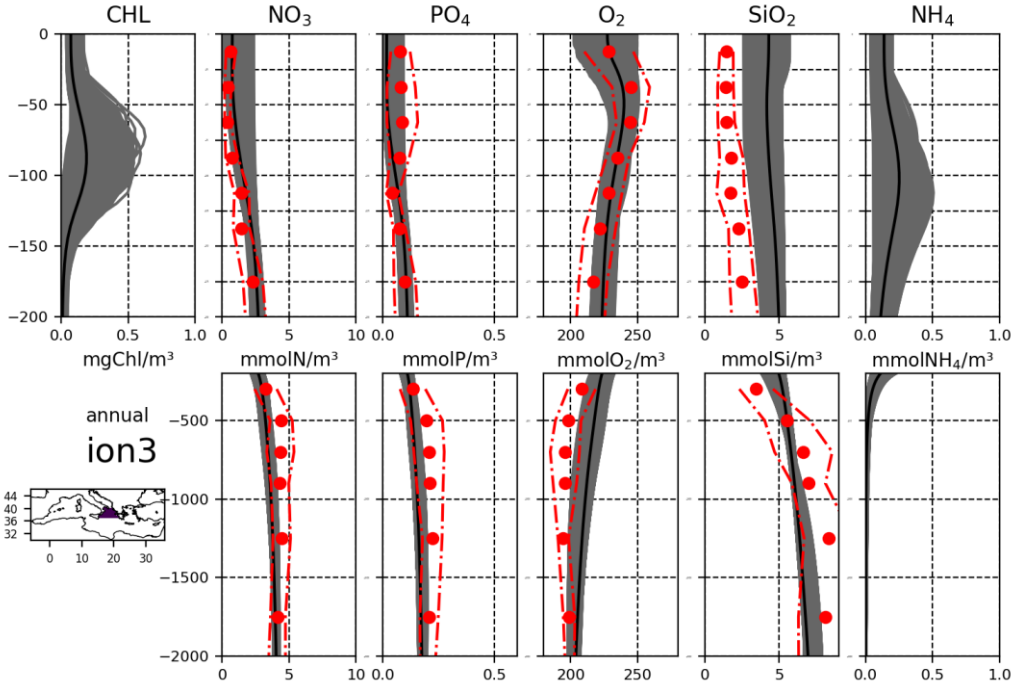

Fig. IV.13.11.

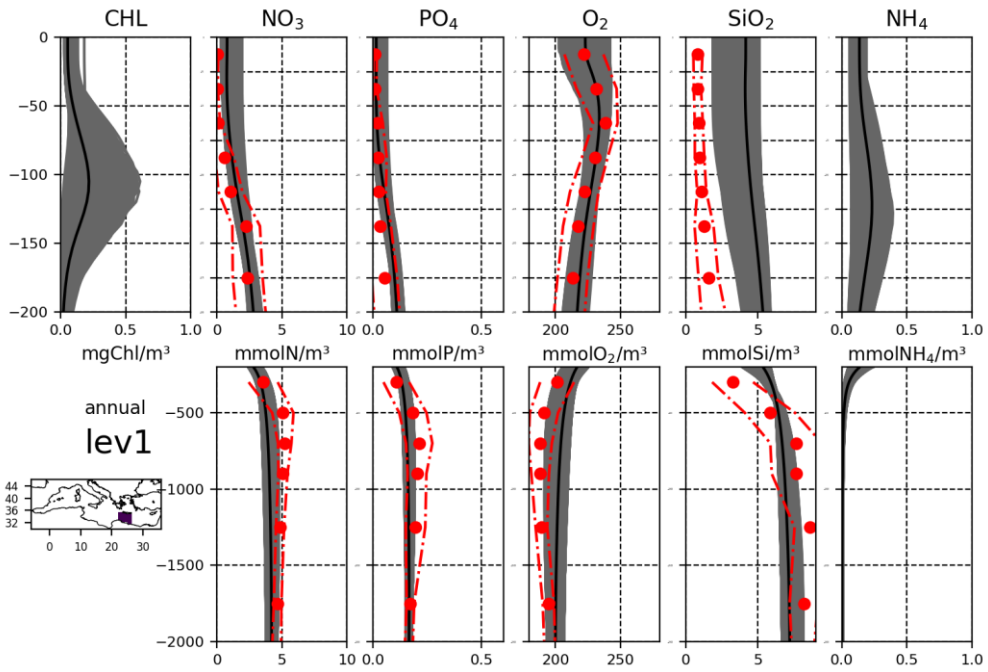

Fig. IV.13.12.

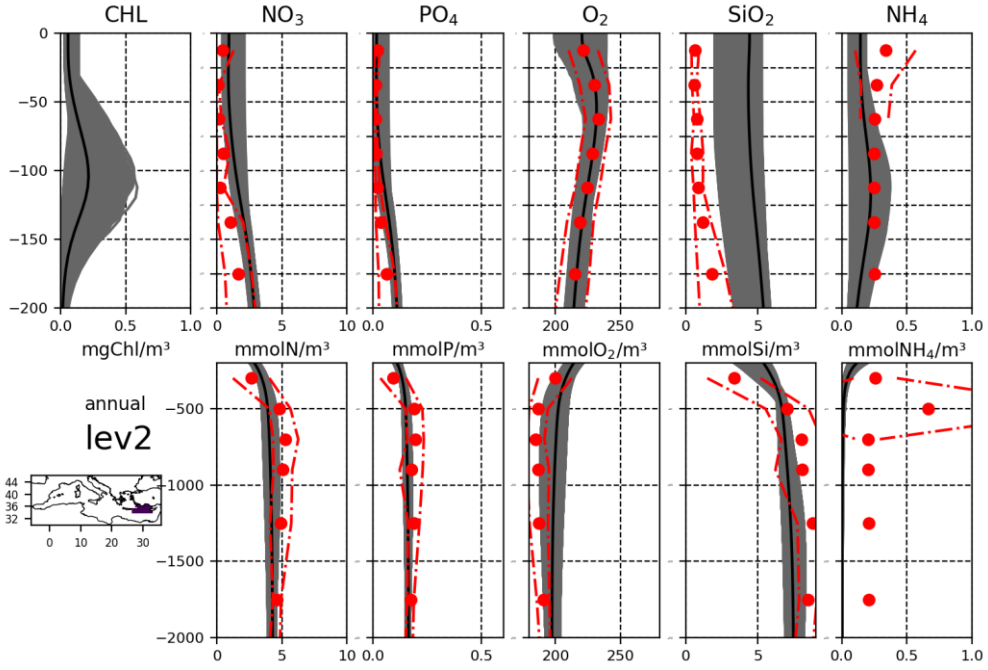

Fig. IV.13.13.

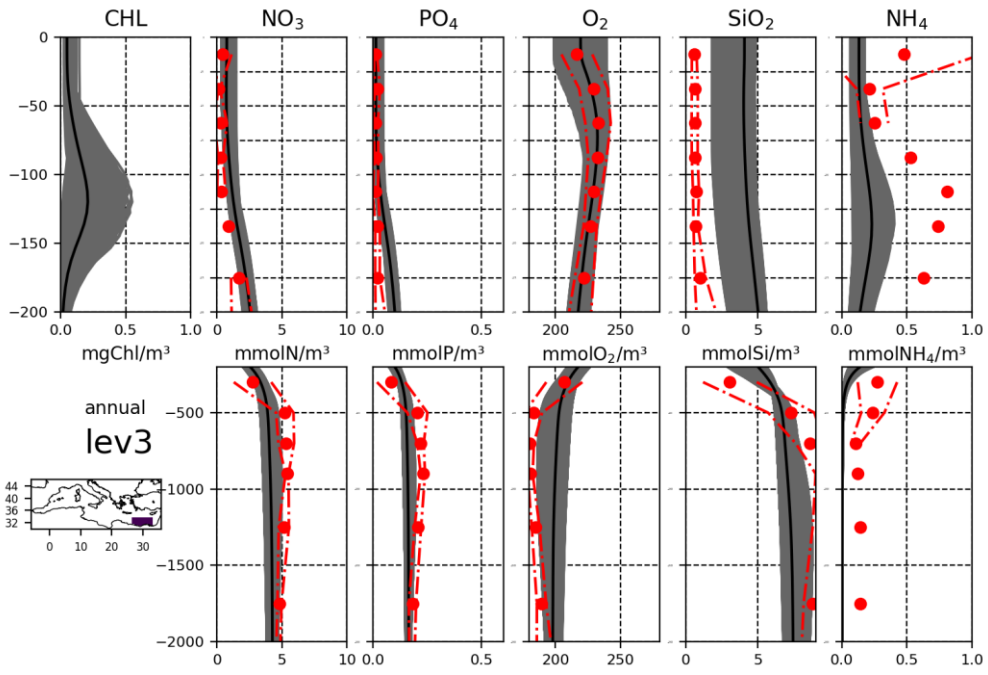

Fig. IV.13.14.

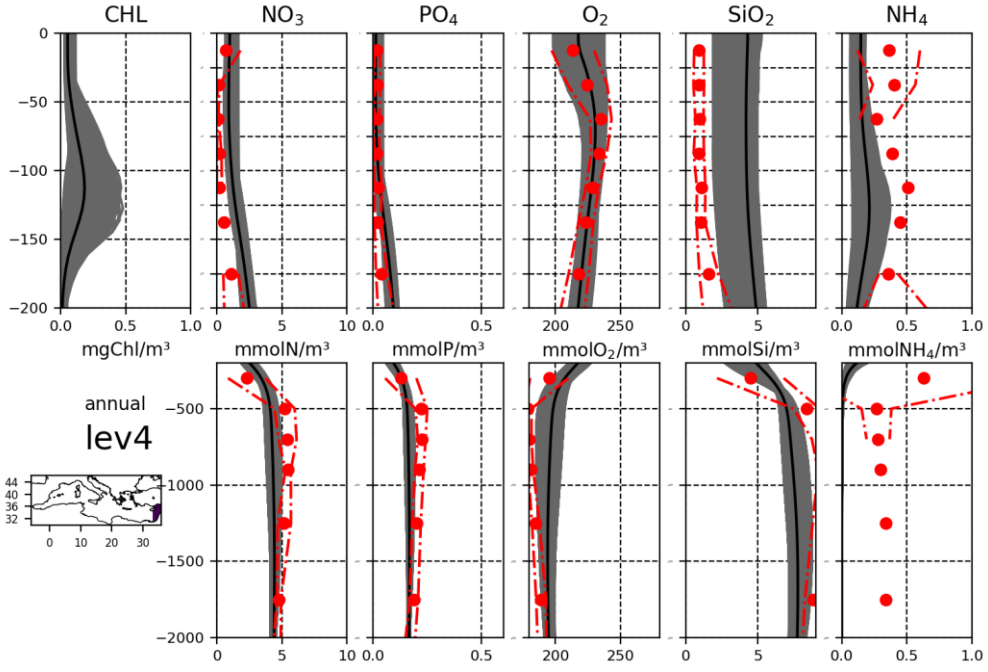

Fig. IV.13.15.

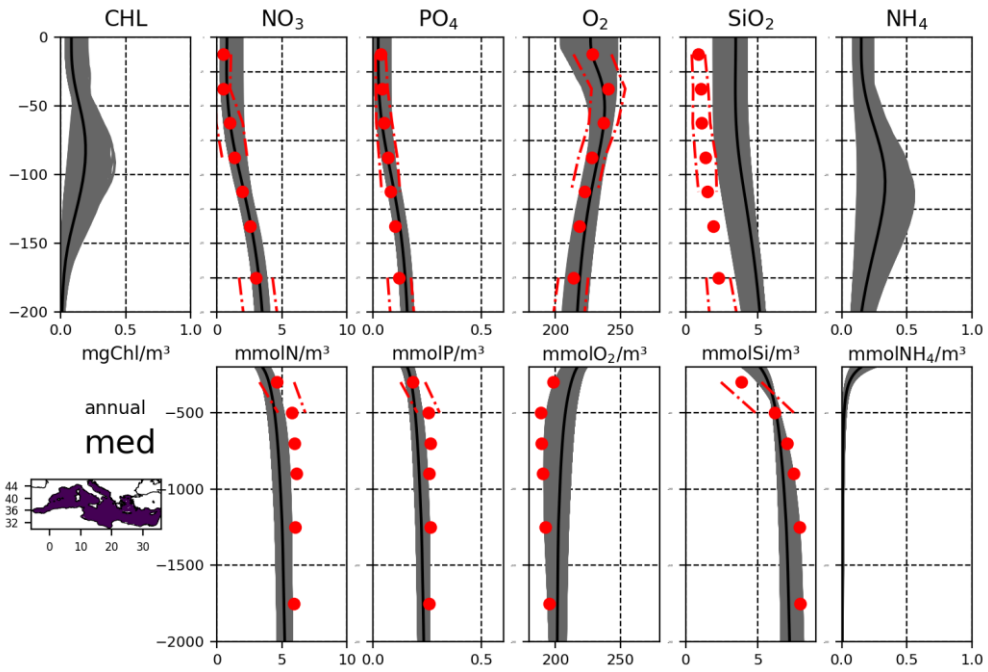
CHL
NO3
PO4
O2
SiO2
NH4
mgChl/m³
mmolN/m³
mmolP/m³
mmolO2/m³
mmolSi/m³
mmolNH4/m³
annual
med

Fig. IV.13.16.

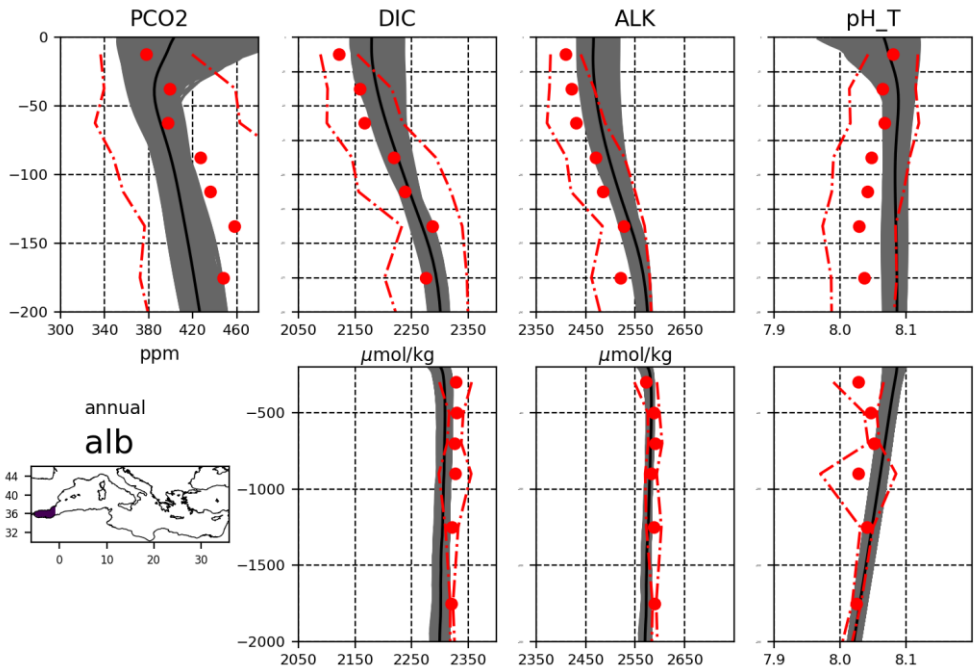

Fig. IV.13.17.

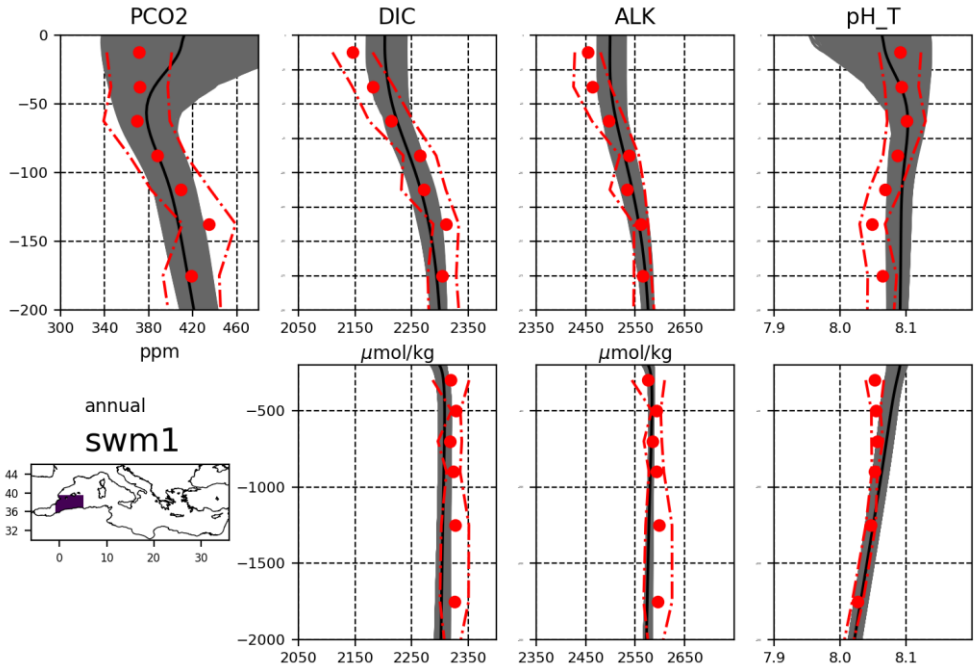

Fig. IV.13.18.

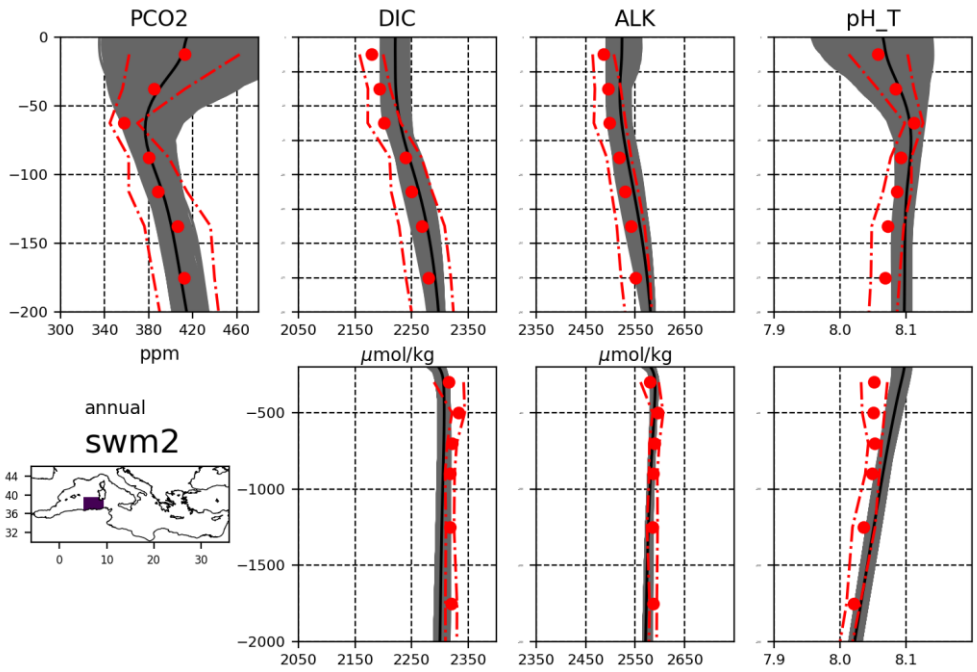

Fig. IV.13.19.

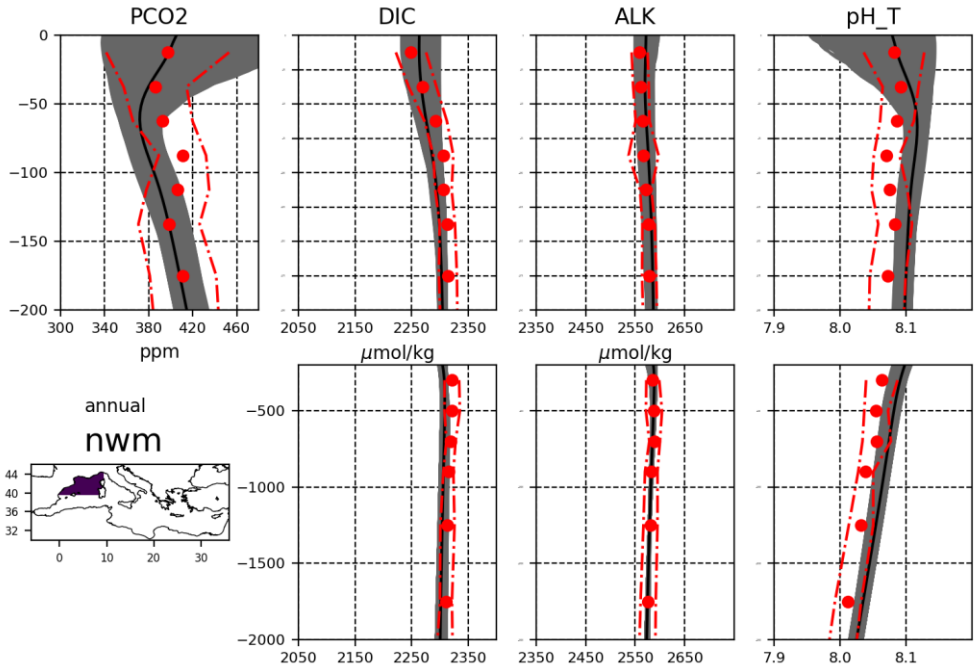

Fig. IV.13.20.

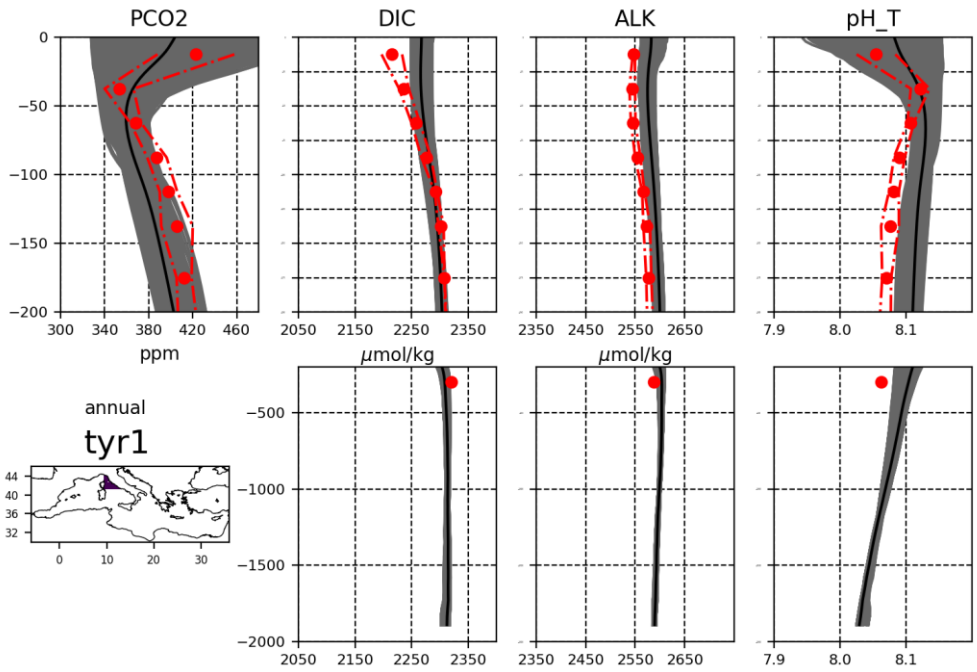

Fig. IV.13.21.

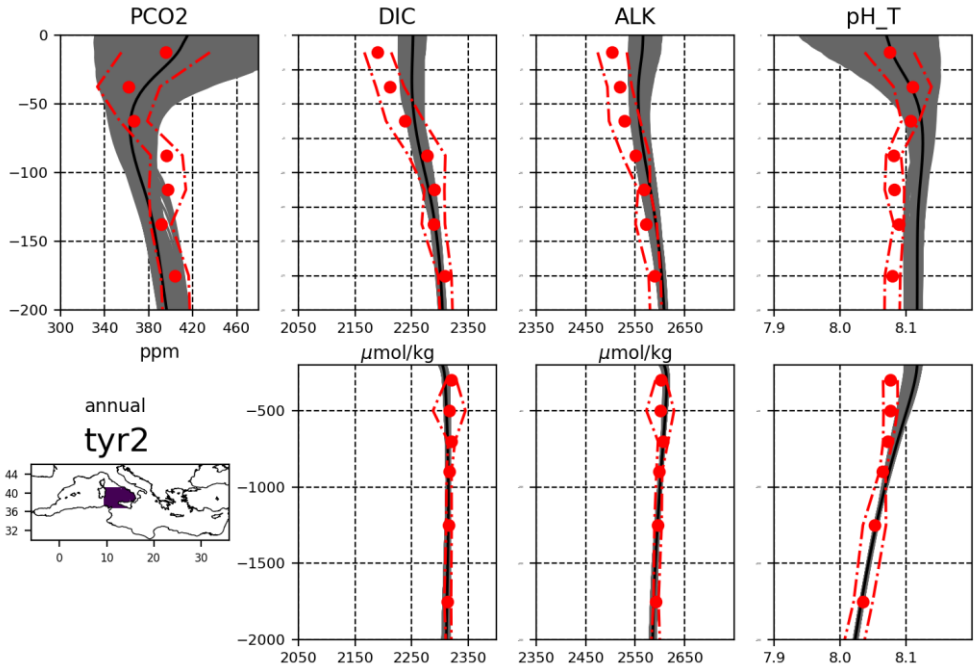

Fig. IV.13.22.

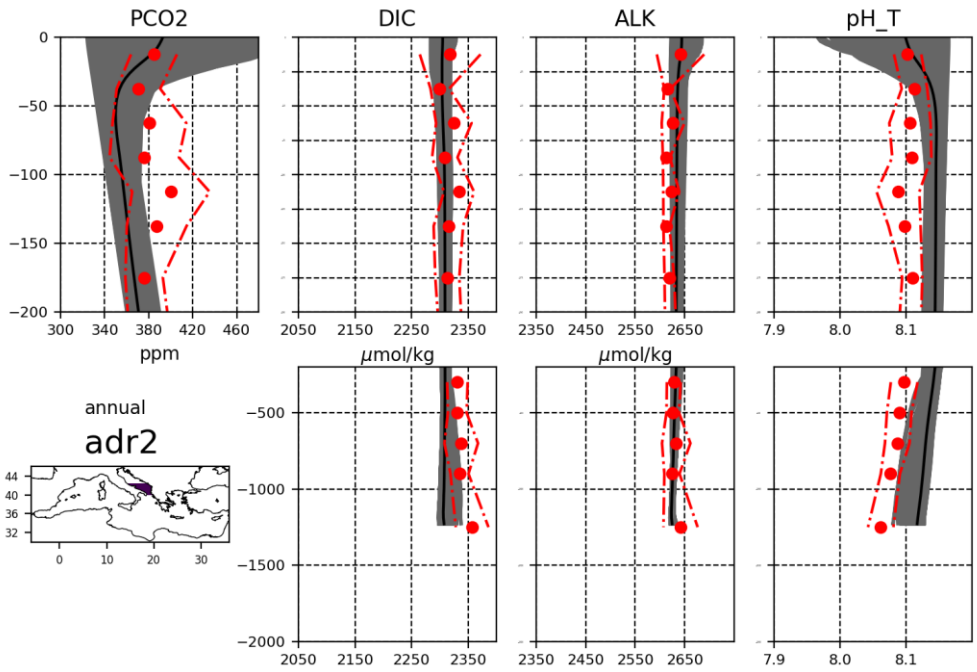

Fig. IV.13.23.

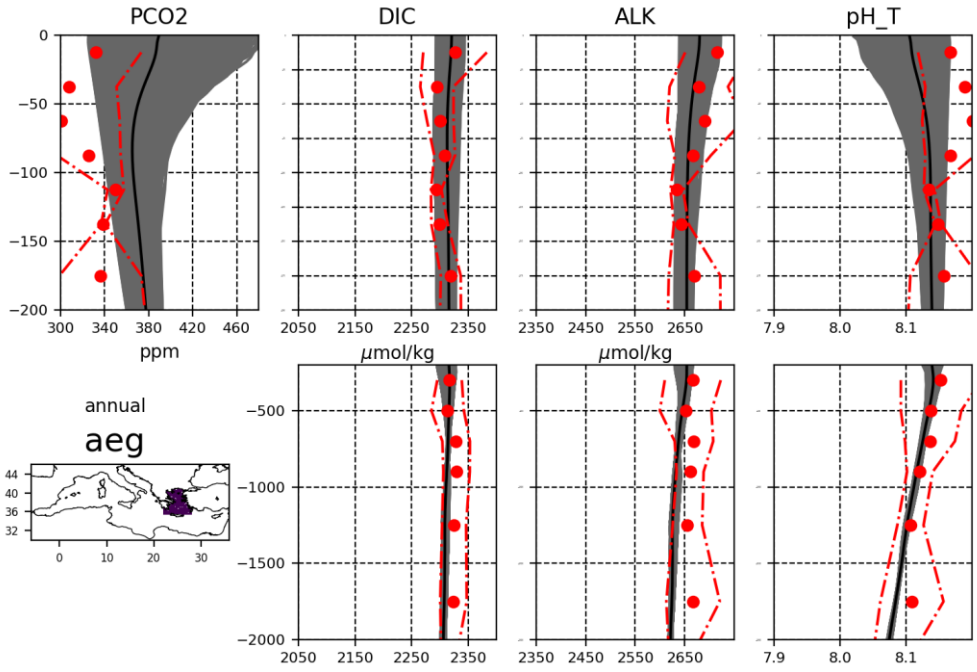

Fig. IV.13.24.

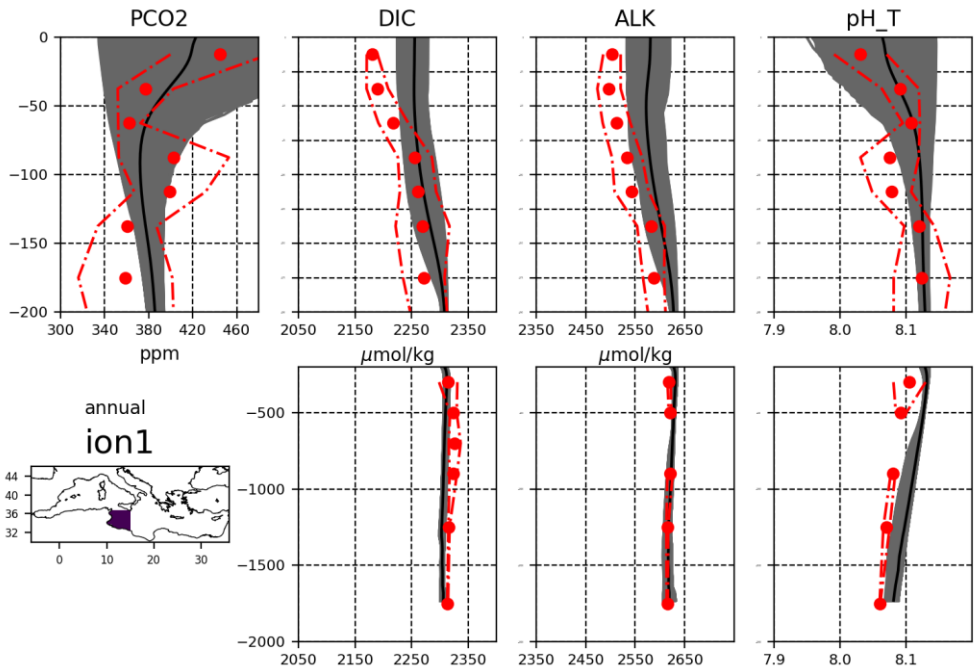

Fig. IV.13.25.

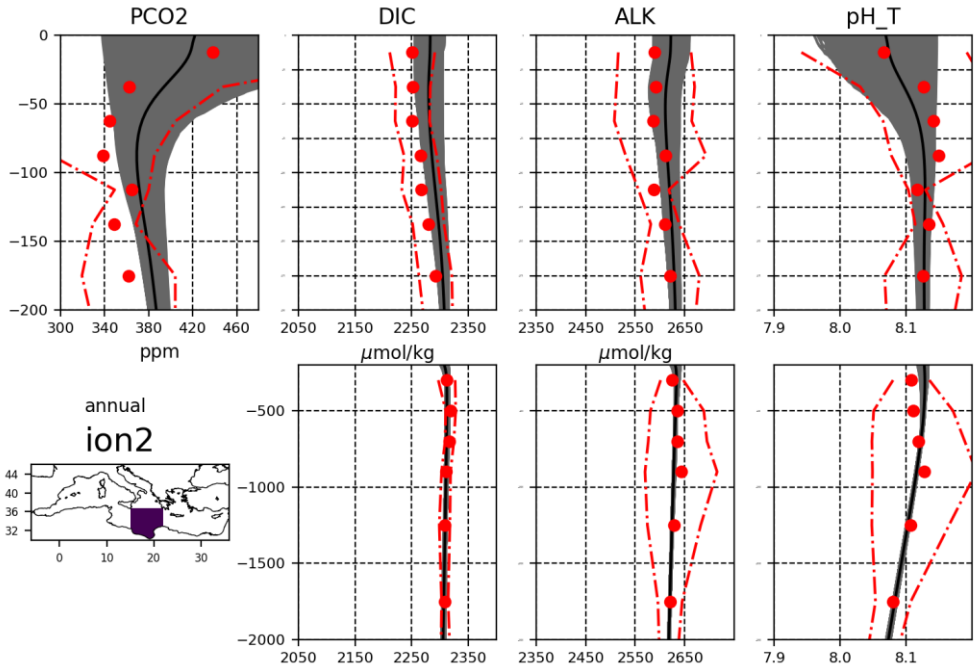

Fig. IV.13.26.

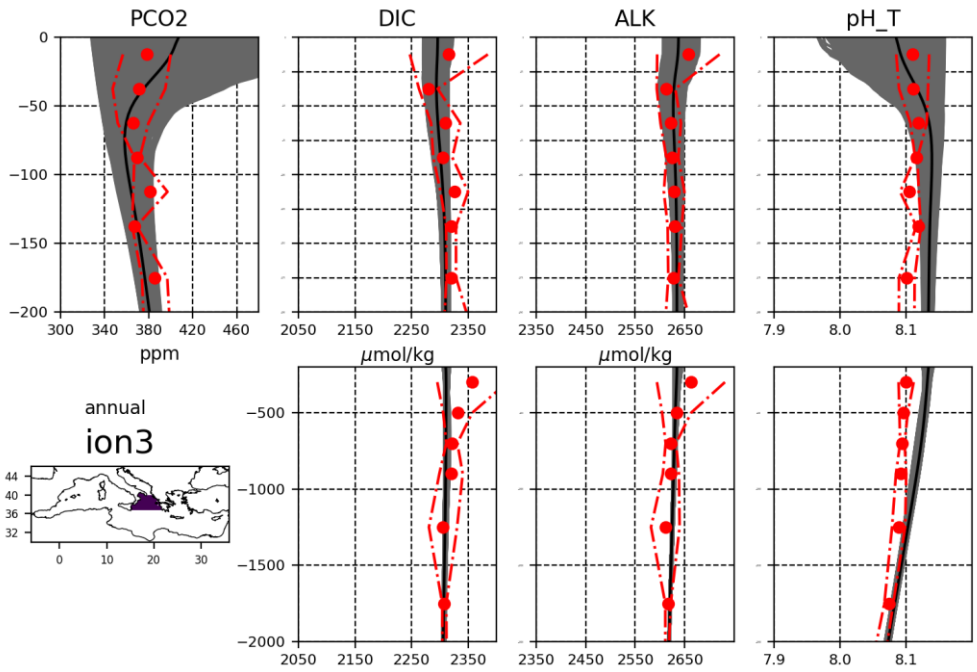

Fig. IV.13.27.

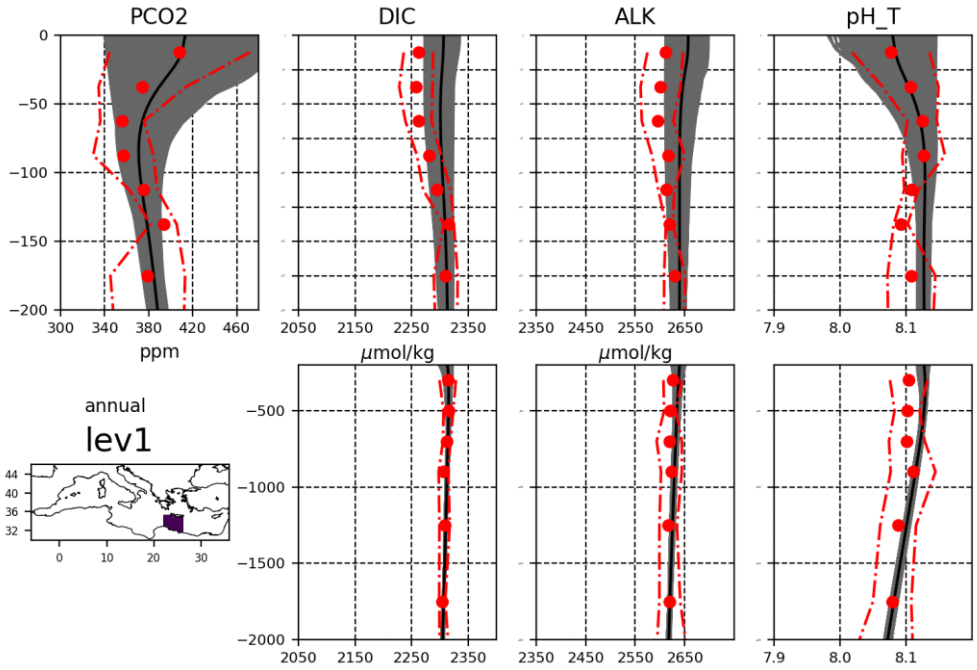

Fig. IV.13.28.

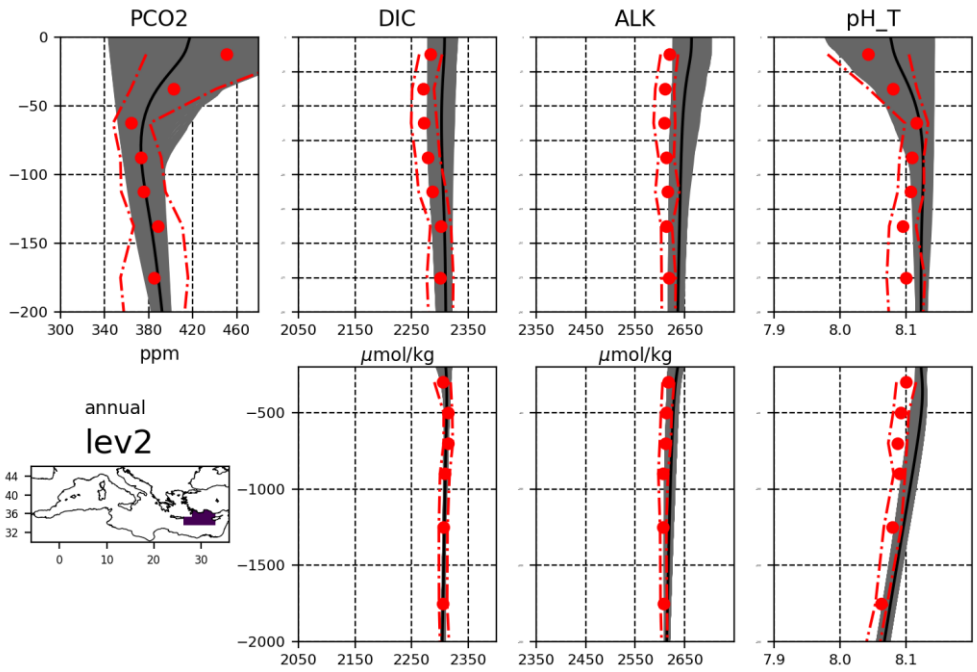

Fig. IV.13.29.

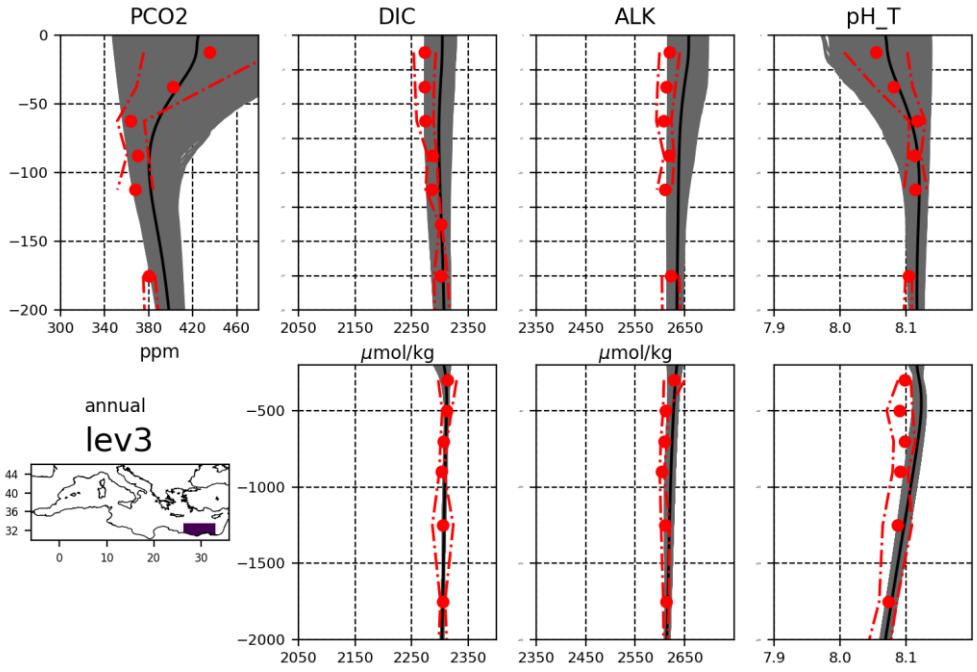

Fig. IV.13.30.

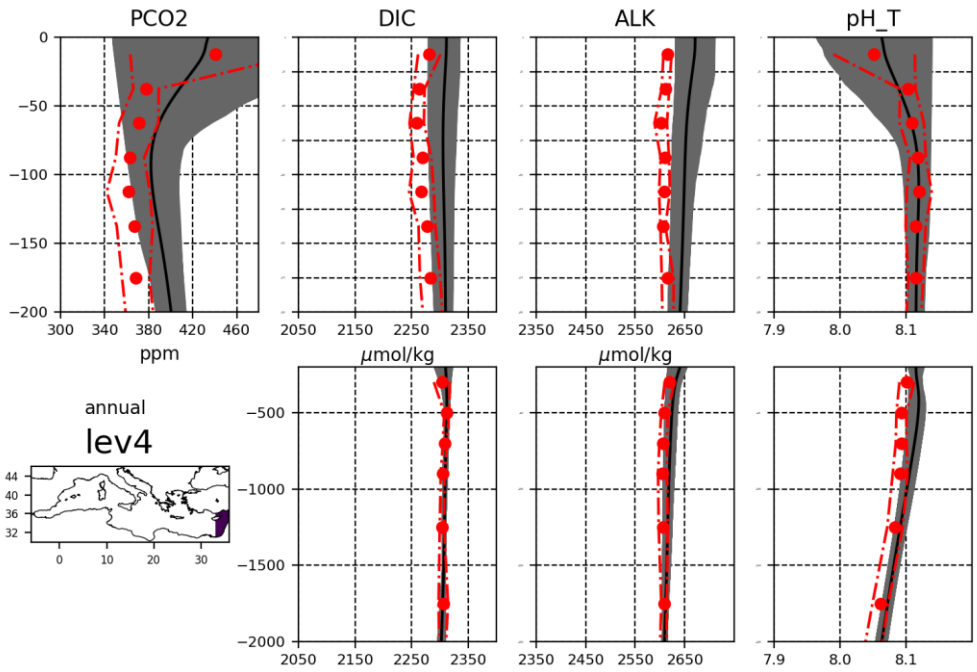

Fig. IV.13.31.

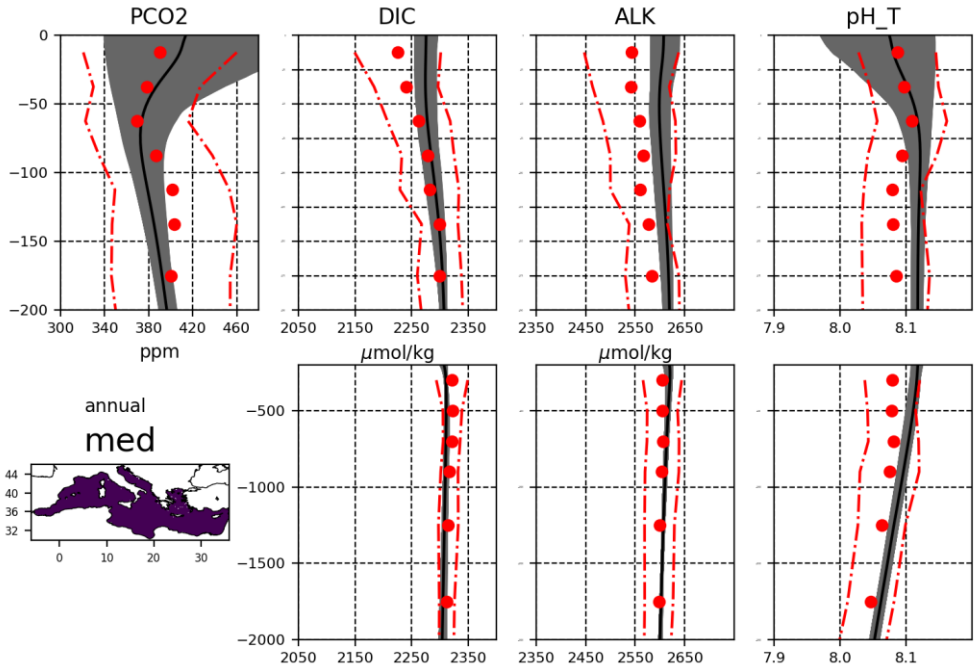

Fig. IV.13.32.

V SYSTEM'S NOTICEABLE EVENTS, OUTAGES OR CHANGES

Date	Change/Event description	System version	other
05/03/2016	First release of Mediterrean Sea biogeochemical reanalysis at 1/16 including carbonate system variables for the period 1999-2014	MedBFM0	V2 version
16/04/2017	Upgrade of data assimilation scheme including satellite chlorophyll over the entire domain (both coastal and open sea areas), re-run of the whole period 1999-2014 and extension of one year (2015)	MedBFM1	V3 version
18/04/2018	Extension of one year (2016)	MedBFM1	V4 version
16/04/2019	Extension of one year (2017)	MedBFM1	Q2 2019
03/09/2019	Extension of one year (2018)	MedBFM1	Q4 2019
15/01/2021	New reanalysis of the Mediterranena Sea at 1/24° horizontal resolution forced with ERA 5 atmospheric forcing. New offline phy-bio coupled model featuring vvl version of NEMO3.6 and new version of the Biogeochemical Flux Model version 5.2.	MedBFM3.2	Q2 2021
03/09/2021	Inclusion of INTERIM	MedBFM3.2	Q4 2021
14/06/2022	Substitution of the January 2016 – May 2020 timeseries due to change of dependency (update of the Med-PHY reanalysis). Extension of the reanalysis timeseries from June 2020 to June 2021.	MedBFM3.2	Q4 2022

VI QUALITY CHANGES SINCE PREVIOUS VERSION

The present report covers the new biogeochemical reanalysis of the Mediterranena Sea at 1/24° horizontal resolution forced with ERA 5 atmospheric forcing. The new offline phy-bio coupling integrates the vvl version of NEMO3.6 for the free surface formulation and the vertical dynamics of model layers (Salon et al., 2019). New version of the Biogeochemcial Flux Model version 5.2 includes new features of the nutrient formulation (Lazzari et al., 2016) and the carbonate system (Cossarini et al., 2105; Salon et al., 2019). Data assimilation includes the new ESA-CCI ocean color observations and novel coastal data assimilation formulation (Teruzzi et al., 2018). The validation framework has been greatly improved by including new observational datasets (EMODnet, 2018, SOCAT v2 2019, BGC-Argo float) and by building a 3-level validation (i.e., basin wide class1 metrics, mesoscale class 4 metrics and process-based metrics; Salon et al., 2019). Twelve variables are validated using the 3-level validation framework providing a different “degree of confirmation” for each variable with respect to the different scales of variability derived from the available observations.

No change in the quality of the reanalysis product is observed after the substitution of the 2016-2020 timeseries and the extension till June 2021 (i.e., evaluation done with metrics based on satellite observations)

The INTERIM product is validated using a test simulation that covers the period January – December 2020 and using observations of chlorophyll, nitrate and oxygen (available from CMEMS satellite and BGC-Argo) and the EAN scores are listed in Section I.3. The INTERIM product has generally the same accuracy of the reanalysis.

VII REFERENCES

Álvarez, M., Sanleón-Bartolomé, H., Tanhua, T., Mintrop, L., Luchetta, A., Cantoni, C., Schroeder, K., Civitarese, G., 2014. The CO2 system in the Mediterranean Sea: a basin wide perspective. Ocean Sci. 10, 69–92. https://doi.org/10.5194/os-10-69-2014

Artuso, F., Chamard, P., Piacentino, S., Sferlazzo, D.M., De Silvestri, L., di Sarra, A., Meloni, D., Monteleone, F., 2009. Influence of transport and trends in atmospheric CO2 at Lampedusa. Atmos. Environ. 43, 3044–3051. https://doi.org/10.1016/j.atmosenv.2009.03.027

Bakker, D.C.E., Pfeil, B., Landa, C.S., Metzl, N., O'Brien, K.M., Olsen, A., Smith, K., Cosca, C., Harasawa, S., Jones, S.D., Nakaoka, S., Nojiri, Y., Schuster, U., Steinhoff, T., Sweeney, C., Takahashi, T., Tilbrook, B., Wada, C., Wanninkhof, R., Alin, S.R., Balestrini, C.F., Barbero, L., Bates, N.R., Bianchi, A.A., Bonou, F., Boutin, J., Bozec, Y., Burger, E.F., Cai, W.-J., Castle, R.D., Chen, L., Chierici, M., Currie, K., Evans, W., Featherstone, C., Feely, R.A., Fransson, A., Goyet, C., Greenwood, N., Gregor, L., Hankin, S., Hardman-Mountford, N.J., Harlay, J., Hauck, J., Hoppema, M., Humphreys, M.P., Hunt, C.W., Huss, B., Ibánhez, J.S.P., Johannessen, T., Keeling, R., Kitidis, V., Körtzinger, A., Kozyr, A., Krasakopoulou, E., Kuwata, A., Landschützer, P., Lauvset, S.K., Lefèvre, N., Lo Monaco, C., Manke, A., Mathis, J.T., Merlivat, L., Millero, F.J., Monteiro, P.M.S., Munro, D.R., Murata, A., Newberger, T., Omar, A.M., Ono, T., Paterson, K., Pearce, D., Pierrot, D., Robbins, L.L., Saito, S., Salisbury, J., Schlitzer, R., Schneider, B., Schweitzer, R., Sieger, R., Skjelvan, I., Sullivan, K.F., Sutherland, S.C., Sutton, A.J., Tadokoro, K., Telszewski, M., Tuma, M., van Heuven, S.M.A.C., Vandemark, D., Ward, B., Watson, A.J., Xu, S., 2016. A multi-decade record of high-quality fCO2 data in version 3 of the Surface Ocean CO2 Atlas (SOCAT). Earth Syst. Sci. Data 8, 383–413. https://doi.org/10.5194/essd-8-383-2016

Bellacicco, M., Vellucci, V., Scardi, M., Barbieux, M., Marullo, S., D'Ortenzio, F., 2019. Quantifying the Impact of Linear Regression Model in Deriving Bio-Optical Relationships: The Implications on Ocean Carbon Estimations. Sensors 19, 3032. https://doi.org/10.3390/s19133032

Bergametti, G., Remoudaki, E., Losno, R., Steiner, E., Chatenet, B., Buat-Menard, P., 1992. Source, transport and deposition of atmospheric phosphorus over the Northwestern Mediterranean. J. Atmospheric Chem. 14, 501–513. https://doi.org/10.1007/BF00115254

Berner, R.A., Morse, J.W., 1974. Dissolution kinetics of calcium carbonate in sea water; IV, Theory of calcite dissolution. Am. J. Sci. 274, 108–134. https://doi.org/10.2475/ajs.274.2.108

Béthoux, J.P., Morin, P., Chaumery, C., Connan, O., Gentili, B., Ruiz-Pino, D., 1998. Nutrients in the Mediterranean Sea, mass balance and statistical analysis of concentrations with respect to environmental change. Mar. Chem. 63, 155–169. https://doi.org/10.1016/S0304-4203(98)00059-0

Bosc, E., Bricaud, A., Antoine, D., 2004. Seasonal and interannual variability in algal biomass and primary production in the Mediterranean Sea, as derived from 4 years of SeaWiFS observations. Glob. Biogeochem. Cycles 18, GB1005. https://doi.org/10.1029/2003GB002034

Buga, L., Sarbu, G., Fryberg, L., Magnus, W., Wesslander, K., Gatti, J., Leroy, D., Iona, S., Larsen, M., Koefoed Rømer, J., Østrem, A.K., Lipizer, M., Giorgietti, A., 2018. EMODnet Chemistry Eutrophication and Acidity aggregated datasets v2018. https://doi.org/10.6092/EC8207EF-ED81-4EE5-BF48-E26FF16BF02E

Colella, S. 2006. La produzione primaria nel Mar Mediterraneo da satellite: sviluppo di un modello regionale e sua applicazione affidati SeaWiFS, MODIS e MERIS, PhD Thesis, Università degli studi di Napoli "Federico II".

Copin-Montégut, C., 1993. Alkalinity and carbon budgets in the Mediterranean Sea. Glob. Biogeochem. Cycles 7, 915–925. https://doi.org/10.1029/93GB01826

Cornell, S., Randell, A., Jickells, T., 1995. Atmospheric inputs of dissolved organic nitrogen to the oceans. Nature 376, 243–246. https://doi.org/10.1038/376243a0

Cossarini, G., Lazzari, P., Solidoro, C., 2015. Spatiotemporal variability of alkalinity in the Mediterranean Sea. Biogeosciences 12, 1647–1658. https://doi.org/10.5194/bg-12-1647-2015

D'Ortenzio, F., Antoine, D., Marullo, S., 2008. Satellite-driven modeling of the upper ocean mixed layer and air–sea CO2 flux in the Mediterranean Sea. Deep Sea Res. Part Oceanogr. Res. Pap. 55, 405–434. https://doi.org/10.1016/j.dsr.2007.12.008

Garcia, H., Weathers, K., Paver, C., Smolyar, I., Boyer, T., Locarnini, M., Zweng, M., Mishonov, A., Baranova, O., Seidov, D., Reagan, J., 2019. World Ocean Atlas 2018. Vol. 4: Dissolved Inorganic Nutrients (phosphate, nitrate and nitrate+nitrite, silicate).

Guerzoni, S., Chester, R., Dulac, F., Herut, B., Loÿe-Pilot, M.-D., Measures, C., Migon, C., Molinaroli, E., Moulin, C., Rossini, P., Saydam, C., Soudine, A., Ziveri, P., 1999. The role of atmospheric deposition in the biogeochemistry of the Mediterranean Sea. Prog. Oceanogr. 44, 147–190. https://doi.org/10.1016/S0079-6611(99)00024-5

Hernandez, F., Smith, G., Baetens, K., Cossarini, G., Garcia-Hermosa, I., Drevillon, M., Maksymczuk, J., Melet, A., Regnier, C., von Schuckman, K., 2018. Measuring Performances, Skill and Accuracy in Operational Oceanography: New Challenges and Approaches, in: Chassignet, E.P., Pascual, A., Tintoré, J., Verron, J. (Eds.), New Frontiers in Operational Oceanography. CreateSpace Independent Publishing Platform, pp. 759–795.

Herut, B., Krom, M., 1996. Atmospheric Input of Nutrients and Dust to the SE Mediterranean, in: Guerzoni, S., Chester, R. (Eds.), The Impact of Desert Dust Across the Mediterranean, Environmental Science and Technology Library. Springer Netherlands, Dordrecht, pp. 349–358. https://doi.org/10.1007/978-94-017-3354-0_35

Johnson, K., Pasqueron De Fommervault, O., Serra, R., D'Ortenzio, F., Schmechtig, C., Claustre, H., Poteau, A., 2018. Processing Bio-Argo nitrate concentration at the DAC Level.

Kempe, S., Pettine, M., Cauwet, G., 1991. Biogeochemistry of European rivers, in: Degens, E.T., Kempe, S., Richey, J.E. (Eds.), Biogeochemistry of Major World Rivers, Scope 42, Aquatic Conserv: Mar. Freshw. Ecosyst. John Wiley, Chichester, pp. 169–211.

Krom, M.D., Kress, N., Brenner, S., Gordon, L.I., 1991. Phosphorus limitation of primary productivity in the eastern Mediterranean Sea. Limnol. Oceanogr. 36, 424–432. https://doi.org/10.4319/lo.1991.36.3.0424

Lazzari, P., Solidoro, C., Ibello, V., Salon, S., Teruzzi, A., Béranger, K., Colella, S., Crise, A., 2012. Seasonal and inter-annual variability of plankton chlorophyll and primary production in the Mediterranean Sea: a modelling approach. Biogeosciences 9, 217–233. https://doi.org/10.5194/bg-9-217-2012

Lazzari, P., Solidoro, C., Salon, S., Bolzon, G., 2016. Spatial variability of phosphate and nitrate in the Mediterranean Sea: A modeling approach. Deep Sea Res. Part Oceanogr. Res. Pap. 108, 39–52. https://doi.org/10.1016/j.dsr.2015.12.006

Lewis, E.R., Wallace, D.W.R., 1998. Program Developed for CO2 System Calculations (No. cdiac:CDIAC-105). Environmental System Science Data Infrastructure for a Virtual Ecosystem. https://doi.org/10.15485/1464255

Loÿe-Pilot, M.D., Martin, J.M., Morelli, J., 1990. Atmospheric input of inorganic nitrogen to the Western Mediterranean. Biogeochemistry 9, 117–134. https://doi.org/10.1007/BF00692168

Lueker, T.J., Dickson, A.G., Keeling, C.D., 2000. Ocean pCO2 calculated from dissolved inorganic carbon, alkalinity, and equations for K1 and K2: validation based on laboratory measurements of CO2 in gas and seawater at equilibrium. Mar. Chem. 70, 105–119. https://doi.org/10.1016/S0304-4203(00)00022-0

Mehrbach, C., Culberson, C.H., Hawley, J.E., Pytkowicx, R.M., 1973. Measurement of the Apparent Dissociation Constants of Carbonic Acid in Seawater at Atmospheric Pressure1. Limnol. Oceanogr. 18, 897–907. https://doi.org/10.4319/lo.1973.18.6.0897

Melaku Canu, D., Ghermandi, A., Nunes, P.A.L.D., Lazzari, P., Cossarini, G., Solidoro, C., 2015. Estimating the value of carbon sequestration ecosystem services in the Mediterranean Sea: An ecological economics approach. Glob. Environ. Change 32, 87–95. https://doi.org/10.1016/j.gloenvcha.2015.02.008

Meybeck, M. (Michel), Ragu, A., 1997. River discharges to the oceans :

Olsen, A., Key, R.M., van Heuven, S., Lauvset, S.K., Velo, A., Lin, X., Schirnick, C., Kozyr, A., Tanhua, T., Hoppema, M., Jutterström, S., Steinfeldt, R., Jeansson, E., Ishii, M., Pérez, F.F., Suzuki, T., 2016. The Global Ocean Data Analysis Project version 2 (GLODAPv2) – an internally consistent data product for the world ocean. Earth Syst. Sci. Data 8, 297–323. https://doi.org/10.5194/essd-8-297-2016

Olsen, A., Lange, N., Key, R.M., Tanhua, T., Álvarez, M., Becker, S., Bittig, H.C., Carter, B.R., Cotrim da Cunha, L., Feely, R.A., van Heuven, S., Hoppema, M., Ishii, M., Jeansson, E., Jones, S.D., Jutterström, S., Karlsen, M.K., Kozyr, A., Lauvset, S.K., Lo Monaco, C., Murata, A., Pérez, F.F., Pfeil, B., Schirnick, C., Steinfeldt, R., Suzuki, T., Telszewski, M., Tilbrook, B., Velo, A., Wanninkhof, R., 2019. GLODAPv2.2019 – an update of GLODAPv2. Earth Syst. Sci. Data 11, 1437–1461. https://doi.org/10.5194/essd-11-1437-2019

Oreskes, N., Shrader-Frechette, K., Belitz, K., 1994. Verification, Validation, and Confirmation of Numerical Models in the Earth Sciences. Science 263, 641–646. https://doi.org/10.1126/science.263.5147.641

Orr, J.C., Epitalon, J.-M., 2015. Improved routines to model the ocean carbonate system: mocsy 2.0. Geosci. Model Dev. 8, 485–499. https://doi.org/10.5194/gmd-8-485-2015

Ribera d'Alcalà, M., Civitarese, G., Conversano, F., Lavezza, R., 2003. Nutrient ratios and fluxes hint at overlooked processes in the Mediterranean Sea. J. Geophys. Res. Oceans 108, 8106. https://doi.org/10.1029/2002JC001650

Salon, S., Cossarini, G., Bolzon, G., Feudale, L., Lazzari, P., Teruzzi, A., Solidoro, C., Crise, A., 2019. Novel metrics based on Biogeochemical Argo data to improve the model uncertainty evaluation of the CMEMS Mediterranean marine ecosystem forecasts. Ocean Sci. 15, 997–1022. https://doi.org/10.5194/os-15-997-2019

Schmechtig, C., Poteau, A., Claustre, H., D'Ortenzio, F., Dall'Olmo, G., Boss, E., 2018. Processing Bio-Argo particle backscattering at the DAC level.

Schuckmann, K. von, Traon, P.-Y.L., Smith, N., Pascual, A., Brasseur, P., Fennel, K., Djavidnia, S., Aaboe, S., Fanjul, E.A., Autret, E., Axell, L., Aznar, R., Benincasa, M., Bentamy, A., Boberg, F., Bourdallé-Badie, R., Nardelli, B.B., Brando, V.E., Bricaud, C., Breivik, L.-A., Brewin, R.J.W., Capet, A., Ceschin, A., Ciliberti, S., Cossarini, G., Alfonso, M. de, Collar, A. de P., Kloe, J. de, Deshayes, J., Desportes, C., Drévillon, M., Drillet, Y., Droghei, R., Dubois, C., Embury, O., Etienne, H., Fratianni, C., Lafuente, J.G., Sotillo, M.G.,

Garric, G., Gasparin, F., Gerin, R., Good, S., Gourrion, J., Grégoire, M., Greiner, E., Guinehut, S., Gutknecht, E., Hernandez, F., Hernandez, O., Høyer, J., Jackson, L., Jandt, S., Josey, S., Juza, M., Kennedy, J., Kokkini, Z., Korres, G., Kõuts, M., Lagemaa, P., Lavergne, T., Cann, B. le, Legeais, J.-F., Lemieux-Dudon, B., Levier, B., Lien, V., Maljutenko, I., Manzano, F., Marcos, M., Marinova, V., Masina, S., Mauri, E., Mayer, M., Melet, A., Mélin, F., Meyssignac, B., Monier, M., Müller, M., Mulet, S., Naranjo, C., Notarstefano, G., Paulmier, A., Gomez, B.P., Gonzalez, I.P., Peneva, E., Perruche, C., Peterson, K.A., Pinardi, N., Pisano, A., Pardo, S., Poulain, P.-M., Raj, R.P., Raudsepp, U., Ravdas, M., Reid, R., Rio, M.-H., Salon, S., Samuelsen, A., Sammartino, M., Sammartino, S., Sandø, A.B., Santoleri, R., Sathyendranath, S., She, J., Simoncelli, S., Solidoro, C., Stoffelen, A., Storto, A., Szerkely, T., Tamm, S., Tietsche, S., Tinker, J., Tintore, J., Trindade, A., Zanten, D. van, Vandenbulcke, L., Verhoef, A., Verbrugge, N., Viktorsson, L., Schuckmann, K. von, Wakelin, S.L., Zacharioudaki, A., Zuo, H., 2018. Copernicus Marine Service Ocean State Report. J. Oper. Oceanogr. 11, S1–S142. https://doi.org/10.1080/1755876X.2018.1489208

Siokou-Frangou, I., Christaki, U., Mazzocchi, M.G., Montresor, M., Ribera d'Alcalá, M., Vaqué, D., Zingone, A., 2010. Plankton in the open Mediterranean Sea: a review. Biogeosciences 7, 1543–1586. https://doi.org/10.5194/bg-7-1543-2010

Teruzzi, A., Bolzon, G., Salon, S., Lazzari, P., Solidoro, C., Cossarini, G., 2018. Assimilation of coastal and open sea biogeochemical data to improve phytoplankton simulation in the Mediterranean Sea. Ocean Model. 132, 46–60. https://doi.org/10.1016/j.ocemod.2018.09.007

Teruzzi, A., Di Cerbo, P., Cossarini, G., Pascolo, E., Salon, S., 2019. Parallel implementation of a data assimilation scheme for operational oceanography: The case of the MedBFM model system. Comput. Geosci. 124, 103–114. https://doi.org/10.1016/j.cageo.2019.01.003

Teruzzi, A., Dobricic, S., Solidoro, C., Cossarini, G., 2014. A 3-D variational assimilation scheme in coupled transport-biogeochemical models: Forecast of Mediterranean biogeochemical properties. J. Geophys. Res. Oceans 119, 200–217. https://doi.org/10.1002/2013JC009277

Thierry, V., Bittig, H., Gilbert, D., Kobayashi, T., Kanako, S., Schmid, C., 2018. Processing Argo oxygen data at the DAC level.

Thingstad, T.F., Rassoulzadegan, F., 1995. Nutrient limitations, microbial food webs and "biological C-pumps": suggested interactions in a P-limited Mediterranean. Mar. Ecol. Prog. Ser. 117, 299–306.

Wanninkhof, R., 2014. Relationship between wind speed and gas exchange over the ocean revisited. Limnol. Oceanogr. Methods 12, 351–362. https://doi.org/10.4319/lom.2014.12.351